"RECONSTRUCTION OF HIGH RESOLUTION IMAGE USING LOW RESOLUTION COLOR IMAGE(S) FOR QUALITY IMPROVEMENT"

Thesis submitted for the award of the degree of

Doctor of Philosophy (Ph.D.)

in

Electronics Engineering

in the faculty of

Engineering and Technology

by

Dighe Devidas Dnyaneshwar

Under the supervision of

Prof. (Dr.) Gajanan K. Kharate

Research Centre,

Department of Applied Electronics,

Sant Gadge Baba Amravati University, Amravati

to

Sant Gadge Baba Amravati University, Amravati

July, 2020

Approval Sheet

Thesis entitled: **Reconstruction of High Resolution Image Using Low Resolution Color Image(s) for Quality Improvement**

by Devidas Dnyaneshwar Dighe is approved for the award of degree of DOCTOR OF PHILOSOPHY in Electronics Engineering, under the faculty Engineering and Technology, Sant Gadge Baba Amravati University, Amravati.

[Signature]
Prof. Dr. Gajanan K. Kharate
Supervisor

[Signature]
Examiner(s)

Date: / /2020
Place: **Amravati**

Sant Gadge Baba Amravati University

Department of Applied Electronics,

Amravati-444602 (MS)

Certificate

This is to certify that **Mr. Devidas Dnyaneshwar Dighe** is the registered scholar whose registration no is **SGBAU/Ph.D./ETC-4526/2011w.e.f. 15/01/2011** has completed the research work entitled, "**Reconstruction of High Resolution Image Using Low Resolution Color Image(s) for Quality Improvement**" in the subject **Electronics Engineering** in the faculty **Engineering and Technology** under the supervision of **Dr. Gajanan K. Kharate**. He has successfully completed the pre-defense of the thesis and the thesis is hereby forwarded to the University for evaluation.

S. V. Dudul

Prof. (Dr.) Snajay V. Dudual

HOD

Department of Applied Electronics

Co-ordinator
Research Laboratory
P. G. Deptt. of Applied Electronics
Sant Gadge Baba Amravati University

SANT GADGE BABA AMRAVATI UNIVERSITY
Department of Applied Electronics
AMRAVATI

5.8.2020

Date: / **07/2020**

Place: **Amravati**

DECLARATION

I, the undersigned, hereby declare that the work presented in this thesis entitled, **"Reconstruction of High Resolution Image Using Low Resolution Color Image(s) for Quality Improvement"** in the subject **Electronics Engineering** in the faculty **Engineering and Technology** is the original contribution carried out by me conforming to research norms under the supervision of **Prof. (Dr.) Gajanan K. Kharate**. This work has not been submitted to any other university / institution for the award of any degree.

I further declare that, this work is free from any kind of plagiarism.

Name of Scholar: **Devidas D. Dighe**

Registration No.: SGBAU/Ph.D./ETC-4526/2011 w.e.f. 15/01/2011

Date of Registration: 15/01/2011

Date: / /**2020**

Place: **Amravati**

CERTIFICATE OF THE SUPERVISOR

This is to certify that the work presented in this thesis entitled, "**Reconstruction of High Resolution Image Using Low Resolution Color Image(s) for Quality Improvement**" is the own and original work of **Mr. Devidas D. Dighe** carried out under my supervision. The work embodied in this thesis has not been submitted earlier to any university/institution for any degree to the best of my knowledge.

I further certify that, this work is free from any kind of plagiarism.

Name of Supervisor: Prof. **(Dr.) Gajanan K. Kharate**

Research Centre

Department of Applied Electronics,

Sant Gadge Baba Amravati University, Amravati

Date: / /**2020**

Place: **Amravati**

ACKNOWLEDGEMENT

My profound gratitude to the Almighty for his wonderful grace and abundant blessings bestowed upon me.

I wish to thank all the people whose assistance was a milestone in the completion of this thesis.

I would like to express my deepest and sincere gratitude to my mentor and guide, ***Dr. Gajanan K. Kharate*** whose unfailing support helped me achieve this endeavor. His strong motivation and guidance helped me in channeling the research in a proper direction. His wit and resourceful demeanor helped me complete this thesis successfully.

I would like to extend my heartfelt gratitude to ***Dr. D. T. Ingole***, Director-Innovation, Incubation & Linkages, Sant Gadge Baba Amravati University, Amravati and ***Dr. Sanjay Dudul***, Head, Department of Applied Electronics, Sant Gadge Baba Amravati University, Amravati for providing me with their unparalleled and timely guidance, key inputs and administrative support and lab facilities. I am also grateful to ***Dr. V. H. Patil,*** Head, Computer Engineering, ***Prof. N. L. Bhale,*** Head, IT department and ***Dr. J. J. Chopade***, Head R&D, of Matoshri College of Engineering and Research Center for their unwavering support, precious guidance and extension of infrastructure and lab facilities whenever required.

I gratefully acknowledge the assistance, help and efforts of management of Matoshri Education Society's Matoshri College of Engineering and Research Center, Nashik. I sincerely appreciate the valuable support and encouragement from all the staff of E&TC department of Matoshri College of Engineering and Research Center, Nashik.

Special thanks and my heartfelt gratitude to ***Lai, Wei-Sheng and Huang, Jia-Bin and Ahuja, Narendra and Yang, Ming-Hsuan*** for giving me access to their dataset for the verification of my algorithms.

I am greatly indebted to my mother ***Mrs. Leela D. Dighe*** and my father Late ***Mr. Dnyaneshwar N. Dighe*** for always showering me with their blessings and best wishes. It is due to their profound belief in my abilities, unconditional and precious

support which has driven me this far. They were, they are and they will always be the reason and key to my success.

My biggest thanks to my family for the enthusiastic moral support they have shown me throughout this research work. I would like to express my deepest gratitude and appreciation to my beloved wife ***Mrs. Anjali Dighe*** who spent sleepless nights with me and was my support in the moments when there was no one to answer my queries. I thank with love, my daughter ***Miss Apurva Dighe*** and son ***Master Vihaan Dighe*** who are the pride and joy of my life. I would like to thank my children for being with me through thick and thin during this entire period of time.

Devidas Dnyaneshwar Dighe

Abstract

The image capturing devices have their hardware limitations to reach to the perfection. The applications demand more and more details for accurate analysis; therefore there is a need to develop a technique for improving the resolution.

Super resolution image reconstruction can overcome the inherent resolution limitation of the imaging system and provide a high resolution image to improve the performance of image processing applications. Consequently, there is a need to develop the novel technique that improves the resolution of an image.

There are different techniques proposed to reconstruct the super resolved image such as reconstruction based, learning based and wavelet based. Each of these techniques has few limitations. A new Cost effective, fast, real time, web based and reliable approach is needed, that avoids the existing systems drawbacks and exploits natural image features in a better way to reconstruct a high resolution Image with better quality.

The aim of this research work is to develop a novel algorithm to reconstruct a high resolution image which overcomes the limitations of current techniques in use and satisfies the needs of different applications. The leading outcome of the research work is a novel technique for reconstructing super-resolution image from low-resolution natural color images.

The research work reported, focuses on the techniques for reconstructing super resolution image from low resolution natural color image(s). Image Registration is an essential and must require step to obtain the information from a combination of a large number LR images captured by the source. Various registration techniques are discussed which are implemented, analyzed and utilized for the reconstruction process. These techniques also compared for their potential benefit for the result of super-resolution. The performance of hybrid approach using log-polar (L-P) Fast Fourier Transform (FFT), an iterative planar motion estimation algorithm based on Taylor series expansions is found better. It is an iterative algorithm to find the rotation angle, shift in x and shift in y direction.

The registration results are used in reconstruction phase of SR, here various reconstruction techniques are discussed which are implemented and analyzed. The Structure Adaptive Normalized Convolution Super Resolution (SANC SR) Reconstruction approach is found better that all other implemented techniques.

The results of the Super Resolution reconstruction are further improved by an innovative state-of-the-art super resolution technique of reconstruction of super resolution image using Particle Swarm Optimization (PSO) with multiple low resolution images is presented. The technique uses PSO to optimize the parameters for selection of best particle in the super resolution image from multiple low resolution images. The images used in this work include many popular images as well as own generated dataset.

TABLE OF CONTENTS

LIST OF FIGURES

LIST OF TABLES

LIST OF ABBREVIATIONS

HR	High Resolution
CCD	Charge Coupled Devices
CMOS	Complementary Metal Oxide Semiconductor
DDV	Distance Of Distinct Vision
RMDS	Remote Medical Diagnosis System
HDTV	High Definition Television
SR	Super Resolution
LR	Low Resolution
MOS	Mean Option Score
DSCQS	Double Stimulus Continuous Quality Scene
MSE	Mean Square Error
RMSE	Root Mean Square Error
SNR	Signal To Noise Ratio
PSNR	Peak Signal To Noise Ratio
MTF	Modulation Transfer Function
ppi	Pixels Per Inch
dpi	Dots Per Inch
FPS	Frames Captured Per Second
HR	High Resolution
STFT	Short-Time Fourier Transform
NK	Normalized Cross-Correlation
AD	Average Difference
MD	Maximum Difference
SC	Structural Content
NAE	Normalized Absolute Error
IBP	Iterative Back Propagation
POCS	Projection Onto Convex Sets
CFT	Continuous Fourier Transform
DFT	Discrete Fourier Transform
MAE	Maximum Posteriori Estimation

CLS	Constrained Least Squares
MAP	Maximum A Posteriori
ML-POCS	Maximum Likelihood -Projection Onto Convex Sets
DFD	Depth From Focus
SFS	Shape From Shading
DT-CWT	Dual-Tree Complex Wavelet Transform
IGMRF	Inhomogeneous Gaussian Markov Random field
SWT	Stationary Wavelet Transform
NEDI	New Edge-Directed Interpolation
HMM	Hidden Markov Model
AWGN	Additive White Gaussian Noise
AM	Alternating Minimization
HMRF	Huber-Markov Random field
NC	Normalized Convolution
NN	Nearest Neighbor
KRR	Kernel Ridge Regression
DL	Dictionary Learning
CSNE	Clustering And Supervised Neighbor Embedding
SVR	Support Vector Regression
MMSE	Minimum Mean Square Error
MCMC	Markov Chain Monte Carlo
SAVD	Sum Of Absolute Value Of The Differences
TES	Total Squared Error
FFT	Fast Fourier Transform
MRI	Magnetic Resonance Imaging
OC	Orientation Correlation
PET	Positron Emission Tomography
SPECT	Single Photon Emission Computed Tomography
MRS	Magnetic Resonance Spectroscopy
L-P FFT	Log-Polar Fft
PC	Phase-Only Correlation

GC	Gradient Correlation
NGC	Normalized Gradient Correlation
FBP	Filtered Back Projection
PG	Popoulis-Gerchberg
SANC	Structure-Adaptive Normalized Convolution
GST	Gradient Structure Tensor
RD	Redundant Dictionary
PCA	Principal Component Analysis
OMP	Orthogonal Marching Pursuit
PSO	Particle Swarm Optimization
VQ	Vector Quantization
MAD	Minimum Absolute Difference

LIST OF SYMBOLS

P(i)	grade probability
$f(r,c)$	original image
$\hat{f}(r, c)$	result of processing
W_k	Warp matrix
n_k	Lexicographically Ordered Noise Vector
y_k	Low resolution image
Δx , Δy	Horizontal and vertical shifts
φ	planar rotation angle
f(x,y)	Image in special domain
F(u,v)	Fourier Transform of image
|F(u,v)|	Magnitude of Fourier Transform of image
$f_{LR,m}$	Low resolution images
(r, θ)	polar coordinates
$h_m(\alpha)$	Fourier coefficients
t_x and t_y	Translations along the x- and y-axis
θ_0 , s	Rotation and uniform scale factor
$\hat{\theta}_0$, $\hat{s}$	estimated of rotation and scale factor
σ	Normalized cut off frequency
$\overrightarrow{E_k}$	Normality distributed additive noise recorded in vector.
$\overrightarrow{F_k}$	Geometric warp function.
$\overrightarrow{C_k}$	Blurring matrix
$\overrightarrow{D_k}$	Decimation function.
$(\overrightarrow{B_k})$	Gradient of image
∇L	Sum of the gradient
λ	Scale Factor
h^{BP}	Back Projection Kernel
$(f-\hat{f})$	Residual error in intensity estimation
{u, v}	Eigenvectors
(λ_u , λ_v)	Eigenvalues
∇I	gradient structure tensor (GST)
σ_r	Photometric Spread

σ_u , σ_v	Directional Scales Of The Anisotropic Gaussian Kernel
A	anisotropy
P Best	Particle Best Solution
G Best	Global Best Solution
$X_{i,d}$	Position of the particle i in dimensions d
$v_{i,d}$	Velocity of the particle i in dimensions d
$Pb_{i,d}$	location in the dimension d with the best fitness of all the visited
x_t^q	Patch in an image
g^n	Estimate Of The SR Image At The Nth Iteration

Chapter 1

Introduction

The chapter consists of brief discussion on the super resolution imaging which includes need for super resolution imaging, study of existing techniques in use with their merits and demerits, motivation and objectives of research work. The application areas of super resolution imaging are also conferred. The chapter ends with organization of the thesis.

1.1 Overview

Image processing is quite a mature field and has its applications in assorted areas. The most significant and one of the desired features of all image processing applications is quality of the image. The quality of an image can be more properly evaluated by its spatial resolution. High resolution (HR) image provides more details to the user, which is crucial for the analysis in numerous applications like medical image analysis and diagnosis. High resolution is nothing but higher pixel density within the image. Principally, the resolution of image depends on the resolution of image acquisition device. It is desirable to have the High Resolution level close to that of an analog 35mm film that has no visible artifacts when an image is magnified. In conventional cameras, the resolution depends on CCD or CMOS sensor density, which may not be sufficiently high [1]. For Super resolution, hardware solution is possible by reducing the pixel size by sensor technology. However, the reduction in pixel size leads to less availability of light to individual sensor, this results in generation of shot noise that degrades the quality and decreases the shutter speed. This ultimately reduces the frames per second (fps) rate. Another approach is by increasing the chip size, which leads to an increase in the capacitance provided by sensors, which limits the charge transfer rate and response time [02]. In addition to this, the cost for high-precision optics and sensors is large and may not be reasonable for general-purpose applications. Thus there is scope to improve the resolution of the captured image using software approach. So, signal processing approach is

preferred for super-resolution. The goal of super resolution, as its name suggests, is to increase the resolution of an image.

A resolution fortification using signal processing technique needs concern in many areas, called as super resolution (SR) (or HR) image reconstruction [3,38,44]. The process of super resolution consist of up sampling the image, thereby increasing the pixel density, and processing one or more low-resolution (LR) image(s) contribute for enriching the information for up sampling. Methods for digital image resolution enhancement have been the subject of research over the past two decades. Today, super resolution image reconstruction is one of the most lime lighted research areas, as it can overcome the inherent resolution limitation of the imaging hardware. It improves the performance of digital image processing applications, while existing low cost imaging systems can still be used. The research is intended at improving the spatial resolution of an image and overcome the drawbacks of the existing techniques in use.

1.2 Motivation

The super resolution means, to have quality of the image to the extent of the maximum capability of the technology referring to it. Human visual system has the limitation in capturing the details of an image, but artificial eye can see beyond it to capture the miniature details. The naked human eye cannot see the matter in detail beyond 0.1 mm with object at Distance of Distinct Vision (DDV). For example, naked human eye cannot see molecular or atomic structure of the matter, but with the help of intelligent computational and analytical power it is possible. The image capturing devices have their hardware limitations to increase the resolution [38]. But the applications demand more and more details for accurate analysis. So, there is a need to develop a technique for improving the resolution.

Super resolution image reconstruction can overcome the resolution limitation of the imaging system and provide a high resolution image to improve the conclusion drawn from image processing applications. The high resolution image in medical imaging improves the precision in the diagnosis process, which may be significant [1,65, 66]. Therefore there is need to develop the novel technique to improves the resolution of image.

Recently the wireless sensor networks are being used to collect

information from remote sites. To collect the pictorial information, low cost and low power consumption are the prime constraints. So, low resolution image capturing devices are preferred to limit the data. Researchers are working towards improving the life span of such devices by reducing the power consumption. Low cost and low power devices have imitated resolution which obviously affects the quality of the image. Thus there is need to develop a cost effective technique that obtain an image equivalent to high cost sensor network devices.

In the process of Remote Medical Diagnosis system (RMDS), digital medical images from remote patients are used. The resolution of medical images decides diagnosis efficiency and accuracy. The resolution of transmitted medical image has limitations due to digital camera, integrated circuit technology used, bandwidth availability, and cost. Due to these limitations, it is difficult to obtain the desired high resolution images. In order to improve resolution of an image, the low resolution image(S) can be collected and used to reconstruct the desired high resolution image using super resolution imaging technique.

The high resolution image is requisite for a range of applications. The objective of research work is to develop the novel algorithm to reconstruct the super resolution image which overcomes the limitations of current techniques in use and satisfies the need of different applications as discussed.

1.3 Applications

High resolution images are likely to increase the ability of detection and identification of details in the image which in turn will improve performance of pattern recognition as well as automatic classification algorithms in computerized systems. Super resolution imaging has wide set of applications such as face recognition, Iris recognition, Network aware applications [91], High Definition Television (HDTV), reproduction of photographs, biomedical Imaging, telemedicine, medical imaging, military, space research, and satellite imaging among many others.

1.4 Current Techniques in Use

One of the ways to increase resolution of image is to use a high end camera which is often not a sensible option for every system. The smoothing and interpolation are the renowned software approaches for enhancing the visual

quality of the still image. Smoothing is generally achieved by applying different spatial filters such as Gaussian, Wiener, and median. The filtering of an image results in addition of low frequency components and the loss of the focus from high frequency components. As human eye is more sensitive to low frequency components than high frequency components, the results of the filtering appears as enhancement in the visual quality of the image, but at the cost of loss of information.

Interpolation is a technique used for increasing the number of pixels in a digital image. The high resolution image is obtained by estimating the pixel value at a location in between existing pixels. Interpolation technique converts the discrete data into a continuous function. For two dimensional data such as an image, the interpolation converts the discrete matrix into continuous function of two variables. The high resolution image is obtained by estimating the pixels in between original data based on the continuous function constructed.

It is one of the techniques used in digital camera to increase (or decrease) the number of pixels in a digital image and to produce a higher (or lower) resolution image than the one captured by the sensor. Generally all image editing software support one or more interpolation techniques. Commonly used interpolation methods are nearest neighbour, bilinear, and bicubic interpolation [87,88,89].

Investigators have alleged that these methods suffer from a number of most noticeable visual degradations and the zigzagging artifact [5,87,99]. Zigzag type of artifact is a main dilemma of Bilinear and Bicubic interpolation and are normally detected in edges as a stair case pattern or as moiré patterns in areas having fine textures. But edges are crucial to image perception; therefore zigzagging is the most exasperating visual artifacts.

Nearest neighbour interpolation method makes the number of pixels larger. The value of a new pixel in the image is considered as the value of the nearest pixel of the original image [99]. It is not appropriate to super resolve the images as it increases the width of edges, which is undesirable. The bilinear interpolation method estimates the value of a new pixel using a weighted average of the pixels in the nearest 2 x 2 neighborhood of the pixel in the original image [99]. The averaging produces comparatively smooth edges than the nearest neighbor interpolation. In Bicubic interpolation method the value of a new pixel is

decided based on a weighted average of the 16 pixels in the nearest 4 x 4 neighborhood of the pixel in the original image [99], Which results in even further smoother edges than bilinear interpolation.

Performance of interpolation methods is better than simple smoothing methods. However, both methods are based on generic smoothness priors and are indiscriminate as the smooth edges as well as regions with little variations. It results in blurring and checkerboard effect [67]. In short, currently used interpolation and smoothing techniques are not enough to reconstruct high resolution image from low resolution image [87]. So the recent research trend is confined to reconstruct high resolution image from low resolution image(s). Super resolution often implies bandwidth extrapolation beyond the pass band of the imaging system. An additional spatio-temporal information is available in the sequence of low resolution (LR) images enables reconstruction at resolutions higher than LR images. Hence, there is a need to find a technique to enhance the current resolution level.

1.5 Objectives of Research Work

Super Resolution (SR) is a technique to enhance the resolution of an image using multiple Low Resolution (LR) image(s), which extracts significant information from the images. Efficient representation of visual information is the heart of several image processing applications. Efficient representation is nothing but the ability to capture significantly correct information from available information. In super resolution imaging, the significant information calculation from available information is the estimation of the intermediate pixels values based on available data set.

The leading objective of the research work is to develop novel technique for reconstructing super-resolution image from low-resolution natural color image(s). The thesis presents an innovative state-of-the-art super resolution technique. The images used in this work include many popular images as well as own generated dataset. Additionally real images have been captured with camera and few synthetic images are used for testing the technique. Objectives of the research work are:

1. Carry out a survey in the area of low resolution, high resolution, quality improvement and reconstruction of quality image.

2. Propose a new technique for Reconstruction of high resolution image using low resolution color image(s) for quality improvement.
3. Implement the proposed technique and test the same over vast set of images.
4. Compare the performance, analyze and conclude.

1.6 Organization of Thesis

The work reported in this thesis has been organized into seven chapters. The content discussed in each chapter are presented in brief in the following paragraphs.

Chapter one includes brief discussion on super resolution imaging, motivation behind the work and the objectives of the research work. Application areas of super resolution imaging are listed as well. The chapter ends with organization of the thesis.

Chapter two includes the generalized model of super resolution process and existing techniques in use along with their limitations. Literature survey of current trends and techniques for topic under research.

Chapter three includes survey of classic image quality assessment techniques. The criteria for image quality measurements of super resolution are mentioned in detail. Thereafter discussion on super resolution using multiple low resolution images. Various approaches for registration of low resolution images are discussed and analyzed for their suitability of method to obtain the accurate registration parameters. The finalized approach is further is used for reconstruction of high resolution image. Different reconstruction approaches are presented and compared for betterment of performance. There after finalized approach for registration and reconstruction are combined together for better results. Further PSO based novel algorithm for reconstruction of SR image has been discussed.

Chapter four includes results of the algorithms as super resolved images. The images include a wide variety of natural and synthetic colored and gray images.

Chapter five includes summary of research work with future scope.

Chapter 2

Literature Survey

The chapter includes the digital image acquisition model along with its limitations, image representation. Literature survey of current techniques and approaches for topic under research are acquired. The topic under research is classified by using two different ways i.e. one is domain of processing and other is use of single or multiple low resolution images presented. The insufficiency and contradiction of different methods are identified and brought out. The shortcomings and contradictions of techniques are identified and pointed out.

An ideal capturing system can sense and record all frequency components of input scene so that there would be no be any loss of information. But practically no system is ideal so, there is loss of some information. This is known as optical distortion. The optical distortion is one of the causes for loss of spatial resolution. Resolution of an image is defined as the smallest discernible or measurable details in a visual presentation. Image resolution has three different categories: spatial resolution, brightness resolution and temporal resolution. The digital image is represented as two-dimensional array of picture elements. Different techniques are available to represent the digital image. The color models are to support the color image representation. In terms of digital image processing the models most commonly used in practice are RGB (Red, Green, Blue); the CMY (Cyan, Magenta, Yellow); the CMYK (Cyan, Magenta, Yellow, Black); and the HSI (Hue, Saturation and Intensity) [5,99,100].

2.1 Super Resolution

In the current decade multimedia has made remarkable impact on human lives and now it is an integral part of our day-to-day activities. An Image is one of the most important media contributing to multimedia. The significant feature of all image

processing applications is good quality of image. The resolution of an image is the principal factor in determining the quality of an image. The resolution is nothing but number of pixels per unit area. There is a huge demand for high resolution (HR) images with the advancement and expansion in the area of image processing applications. The high resolution images give users a pleasing picture and also offer minute additional details that may be important for the analysis of an image in various applications. Preliminary technology to obtain high resolution images prominently depends on sensor manufacturing technology; which has its own limitations. The cost for high precision optics and sensors may not be affordable for general purpose commercial applications such as sensor networks. So, recently researchers have started paying attention towards the enhancement of image resolution. Super Resolution is a process to increase the resolution of an image beyond the resolving power of the imaging system. Hence super resolution allows overcoming the limitations of the imaging system without the need for additional hardware.

This thesis presents various algorithms to reconstruct the high resolution image that can take care of low frequency as well as high frequency image with optimum time and cost.

2.1.1 The Super Resolution Process

The aim of super resolution is to increase the resolution of an image. Resolution is a measure of frequency content in an image; high-resolution (HR) images are band limited to a larger frequency range than low-resolution (LR) images. In applications where we need to extract more information from images it is better to have more details in an image. Super Resolution is a process of reconstructing high resolution image from available information. The low frequency components in an image represent smoothness in the image whereas high frequency components provide details in an image. The basic idea is to reconstruct a super resolution image by restoring the appropriate frequency components that are lost by the image capturing process due to an aliasing effect. Super resolution is an approach that attempts to resolve this problem with software rather than hardware. The concept behind this is time (or space)-frequency resolution and the fact that there is always a tradeoff in resolution between the two.

In the context of super resolution for images, it is assumed that several LR images (e.g. from a video sequence) can be combined into a single HR image: we are decreasing

the time resolution, and increasing the spatial frequency content. The LR images should not be identical. Rather, there must be some variation between them, such as translational motion parallel to the image plane (most common), some other type of motion (rotation, moving away or toward the camera), or different viewing angles. In theory, the information contained about the object in multiple frames, and the knowledge of transformations between the frames, can enable us to obtain a much better image of the object. In practice, there are certain limitations: it might sometimes be difficult or impossible to deduce the transformation. For example, the image of a cube viewed from a different angle will appear distorted or deformed in shape as compared to the original one, because the camera is projecting a 3-D object onto a plane, and without a prior knowledge of the transformation, it is impossible to tell whether the object was actually deformed. In general, however, super resolution can be broken down into two broad parts [44]: 1) registration of the changes between the LR images, and 2) restoration, or synthesis, of the LR images into a HR image; this is only a conceptual classification, as sometimes the two steps are performed simultaneously.

Since Tsai and Huang's first work in 1984 [4] a huge number of papers have been published on super resolution and related topics, It would be impossible to mention each one of them. Here, we try to briefly present some of the main developments on the topic. In the special issue of the IEEE Signal Processing Magazine published in May 2003 has a series of super resolution-related articles that provide a good overview of the field.

Super-resolution refers to the reconstruction of an image which is visually superior to the original low resolution observations. This often implies bandwidth extrapolation beyond the pass band of the imaging system as additional spatio-temporal information available in the sequence of low-resolution images enables reconstruction at resolutions higher than that of the original data. The super resolution approaches suggested by researchers in literature reconstruct the high resolution image using low resolution image(s) of same scene or low resolution images of similar scenes or a low resolution image. In the context of super resolution for images, it is assumed that several LR image(s) (e.g. from a video sequence) can be combined into a single HR image: by decreasing the time resolution, and increasing the spatial frequency content. The generalized block diagram of super resolution process is shown in fig 2.1. Most of the multiframe super resolution image reconstruction methods consist of three basic

components [44]: i) motion compensation (registration), ii) interpolation, and iii) blur and noise removal, if any (restoration).

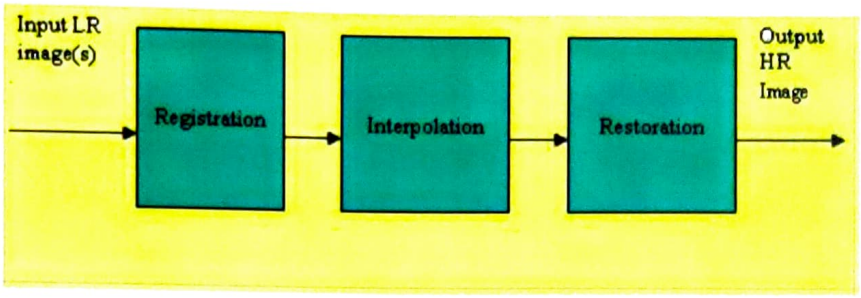

Figure No. 2.1: The Super Resolution Process

Registration is basically preprocessing of the input information. An image registration is to align the different images as precisely as possible by estimating the relative linear and angular motion between them. The LR images should not be identical and there must be some sub pixel variation between them, such as translational motion parallel to the image plane (most common), some other type of motion (rotation, moving away or toward the camera), or different viewing angles. The information contained about the object in multiple frames, and the knowledge of transformations between the frames, can enable us to obtain a much better image of the object. All the frames in the observed low-resolution image sequence are geometrically registered to a fixed reference frame, resulting in a composite HR image grid of non-uniformly-spaced samples. These non-uniformly spaced sample points are then interpolated and resampled on a regularly spaced high resolution sampling lattice. Any noise and blur existing in the resultant image is removed by using Restoration.

2.2 Performance Measure

Performance measure of image SR is image quality assessment. Many efforts have been made towards development of both qualitative and quantitative measures but still the appropriate quality measures for super resolution imaging are not detected. Therefore there is a need to find suitability of conventional performance measures for super resolution imaging.

Imaging and video devices have limitations in spatial and temporal resolution. The spatial resolution indicates the number of pixels per unit area and temporal resolution is the number of frames per second. The spatial resolution relates to the

quality of still image whereas the temporal resolution defines the quality of video. Researchers have developed a range of super resolution algorithms for both spatial as well as temporal resolution. The prime aim of super resolution imaging is to enhance the quality of the image/video. An appropriate performance measure is to be utilized in order to assess the performance of super resolution imaging technique. Most of the researchers have used peak signal to noise ratio (PSNR) as measure for quality assessment of super resolved image. However, they also alleged that PSNR is not suitable for performance measurement as the real reference is not present while estimating PSNR [45-76]. In number of cases it is observed that there is a mismatch between the PSNR and the quality observed by visual inspection. An image which looks better may not always have higher PSNR. Therefore, there is a need to visually inspect the results and show the high frequency images to highlight the difference.

Commonly there are two approaches that are used for image quality assessment; that are subjective and objective measures. Subjective quality measure is based on human visual system and objective measure criteria involving numerical calculations to obtain the computable distortion measures. So, for super resolution imaging there is a need to know the suitability of these performance measures.

Image Quality Measures: Broad set of quality measures are used to assess visual quality of an image. These image quality measures are broadly sort out into:

- Subjective quality measures and
- Objective quality measures

2.2.1 Subjective Quality Measures

The subjective criteria are based on ultimate end user of SR image, mostly human assessing the image quality. In subjective criteria of analysis the group of human experts examine the original image and the reconstructed image. They assign certain grades as per individual perception. On the basis of these assigned grades by number of users, usually, quality of the reconstructed image is evaluated using statistical computations. Mean Opinion Score (MOS) is one of the subjective image quality measure and its values are obtained from an experiment consisting of a group of people. The testing methodology is the double stimulus impairment scale method. The double stimulus

impairment scale method employs references and test conditions, which are arranged in pairs such that the first in the pair is unimpaired reference, the second are the same sequence impaired. The original source image is used as the reference condition. The evaluator has to comment on the second using the first and five-grade impairment scales that are assigned as described in ITU-BT Rec. 500. The method makes use of five grade impairment with proper description: 5-imperceptible, 4-perceptible, 3-slightly annoying, 2-annoying, 1-very annoying. MOS for each test condition and test image are calculated.

$$\text{MOS}= \sum_{i=1}^{5}(p(i)) \qquad 2.1$$

Where 'i' is the grade and P(i) is the grade probability.

Another method for evaluation of the quality is Double Stimulus Continuous Quality Scale (DSCQS) [94], which presents two images to viewers: the original image and the processed image. Viewers evaluate image quality of both images using grading scale of five intervals (1-Excellent, 2-Good, 3-Fair, 4-Poor, 5-Bad). Though subjective evaluation is usually too convenient, it is more expensive, and measurements are to be processed very carefully [94-98]. This method has some difficulties:

- Human judgment vary from time to time and person to person
- Human judgment may be significantly affected by the presence of the system, which introduces errors or artifacts.

As Human Intervention is involved in subjective criteria of image quality assessment, it is sensitive to improper interpretation. Therefore, objective criteria are preferred as compared to the subjective criteria for image quality assessment. Still, their conveniences consider their use in certain applications.

2.2.2 Objective Quality Measures

In the process of super resolution image reconstruction, the noise may get introduced due to erroneous image fusion or inappropriate predictions. The noise is an error in image processing, which leads to the degradation in quality of the image. There are numerous objective quality measures that have been building up for image quality evaluation. These measures involve computations to work out various parameters contributing to quality assessment of an image. These parameters rely on numerical measures of image quality and computable distortion measures [96]. These discrete parameters are establishing some degree of closeness between the digital images. It is

accomplished by exploiting the differences in the statistical distributions of pixels. The common objective quality measures are listed as.

- Mean Square Error (MSE)
- Signal to Noise Ratio (SNR)
- Peak Signal to Noise Ratio (PSNR)
- Normalized Cross-correlation (NK)
- Average Difference (AD)
- Maximum Difference (MD)
- Structural Content (SC)
- Normalized Absolute Error (NAE)

The Mean Square Error (MES) and Peak Signal to Noise Ratio (PSNR) are most commonly used objective quality measures in image quality evaluation. They are simple to calculate, have clear physical meanings and are mathematically suitable in the context of optimization. For color images, the Mean Square Error is calculated for each color and their average is used to generate the Peak Signal to Noise Ratio. If the value of MSE is low, it indicates that noise introduced is low and it is desirable as it signifies the good quality of processed image. If the value of PSNR is high, it indicates that noise introduced due to processing is low and it is desirable as it results in good quality of processed image.

2.3 Performance Measures for Super Resolution Imaging

For super resolution imaging, quality is measure of closeness of resultant image to originality of scene. When image is captured, the originality of scene is lost and distortions are observed in the captured image. The distortions are added due to limitation over point spread function of capturing device. To remove distortions, different algorithms are put forward in digital image processing.

The subjective measures need human factor, but it is not recommended for quality assessments due to variance of results. It requires a set of two images for comparison; the original and the resultant available processing. It is difficult to quantitatively assess the super resolution technique as the true high resolution image is not available for reference. Hence, the subjective measures are not suitable for accessing quality of the super resolved image.

The objective measures are based on numerical computations. These computations also needs two images; the original image *f(r,c)* and the result of processing $\hat{f}(r, c)$. The key requirement for computations is that, the two images must have same spatial resolution in both dimensions i.e. same size. The result of processing is the reconstructed high resolution image whereas the source is/are the low resolution image(s). Variation in the sizes of SR and LR images put constraint on these computations. Still few investigators have suggested use of MSE, SNR and PSNR for quality assessment of super resolution imaging techniques.

Often, to quantify the technique, decimate captured image mostly by a factor of two using interpolation. The decimated low resolution image is used as the input and the original undedicated image act as true reference.

Most of the super resolution algorithm's performance is measured in comparison to the interpolation. It should be counted that there is a positive bias in the calculations of these parameters, which is in favor of interpolation. This is due to the fact that these parameters are calculated using the same high resolution reference from which the low resolution image is made.

For reconstruction based multiframe super resolution technique, more than two low resolution images of the scene are to be used as input. Often these images are decimated, shifted and noisy versions of it are created from single captured high resolution image. In short, the performance calculations in super resolution imaging algorithm, *f(r,c)* is original image and it is shifted and/or rotated and down sampled to generate set of low resolution input images. Using these low resolution images, the super resolution image f (r, c) is reconstructed. Based on *f(r,c)* and $\hat{f}(r, c)$, objective quality measures are calculated. The techniques are used to generate low resolution images from high resolution image and the techniques used to generate high resolution from low resolution images are irreversible.

2.4 Literature Survey

Digital image processing applications are rapidly growing in the field of desktop publishing, multimedia, video conferencing, High Definition Television (HDTV), process automation, robotics and medical image analysis has increased the need for very high resolution images.

Interpolation methodologies have been used over the years for reconstructing higher resolution image. These methods have one common goal to enhance the quality of image by increasing resolution of image so that it can help to improve quality of frames during communication in video conferencing and HDTV, providing the vision for object detection in automation and correct diagnoses in medical applications. Recently the active research is going on to develop the effective technique for the perfection to match the technology advances.

Tsai and Huang [4] were the first to consider the problem of obtaining a high-quality image from several down sampled and translationally displaced images in 1984 [4]. Their approach was formulating a set of equations in the frequency domain, by using the shift property of the Fourier transform. But they had not considered the optical blur or noise. Tsai-Huang's approach is computationally attractive, but has significant disadvantages. The assumption of ideal sampling is unrealistic. The possibility of an optical system point spread function, or even that of spatially integrating sensors is not addressed. Observation noise, blurring due to finite aperture time are not considered. To overcome these several extensions to the basic Tsai-Huang method have been proposed in literature. In short a finite object imaged by diffraction limited system can be resolved by extrapolation in the Fourier domain. This extrapolation of the spectrum of an object beyond the diffraction limit of the imaging system is called super-resolution [1]. However, in general, a super resolution is computationally complex and numerically ill-posed problem [44].

The differences among the several proposed works are subject to what type of reconstruction method is employed, which observation model is assumed, in which particular domain (spatial or frequency) the algorithm is applied, what kind of method is used to capture low resolution images, and so on.

The technical report by S. Borman and R.L. Stevenson [3] provides a comprehensive and complete overview on the super resolution image reconstruction algorithms until around 1998. They had defined Super-resolution as recovery of spatial frequency information beyond the diffraction limit of the optical system as well as removal of blur caused by the imaging system such as out of focus blur, motion blur, non-ideal sampling, etc.

Where x is the ideal undegraded image that is sampled at or above the Nyquist rate from a continuous scene which is assumed to be bandlimited. Now, let the parameters $L_1$and L_2 represent the down-sampling factors in the observation model for the horizontal and vertical directions, respectively. Thus, each observed LR image is of size N_1 X N_2. it is assumed that x remains constant during the acquisition of the multiple LR images therefore, the observed LR images result from warping, blurring, and subsampling operators performed on the HR image x. We are able express these models as follows:

$$y_k = W_k x + n_k \quad , k = 1, \ldots . , p, \qquad \text{------ 2.2}$$

Where matrix W_k represents, via blurring, motion, and subsampling, the contribution of HR pixels in x to the LR pixels in y_k.

At highest level, super-resolution techniques can be divided into frequency domain or spatial domain algorithms. Frequency domain approaches are, to a greater or lesser extent, unable to accommodate general scene observation models including spatially varying degradations, non-global relative camera/scene motion, general a-priori constraints or general noise models. Whereas spatial domain formulations can accommodate all these and provide enormous flexibility in the range of degradations and observation models which may be represented and are thus the methods of choice. Spatial domain observation models facilitate inclusion of additional data in the observation equation with the effect of reducing the feasible solution space.

Further authors have put forth three critical factors affecting super-resolution restoration. Firstly, reliable subpixel motion information is essential. Secondly, observation models must accurately describe the imaging system and its degradations. Thirdly, restoration methods must provide the maximum potential for inclusion of a-priori information.

In super resolution image reconstruction process, registration is the first and the most important step. The accuracy of registration is based on motion estimation and therefore accurate knowledge of relative scene locations sensed by each pixel in observed images is necessary for super resolution.

Irani and Peleg suggested an iterative back propagation (IBP) super resolution reconstruction approach of improving the resolution in their paper titled "Improving resolution by image registration" [39]. The high resolution image is estimated by back propagating the error (difference) between simulated low resolution images. Initially the high resolution image is guessed and low resolution images are constructed from it. Further, these are compared with low resolution images constructed from input image. The difference is calculated and used to improve initial guess by back projecting each value in difference image into its respective field in original guess image. This process is repeatedly used to minimize the error function. The authors have concluded that in given technique original high resolution frequencies are not fully restored because the blurring function is a low pass filter that filters out the high frequency information.

Researchers M. Irani and S. Peleg, in paper "Motion analysis for image enhancement: resolution, occlusion, and transparency" [40] have described methods for enhancing image sequences using the motion information computed by a multiple motions analysis method. The multiple moving objects are first detected and tracked using both a large spatial region and a large temporal region without assuming any temporal motion constancy. This paper has discussed in brief the approaches used for segmenting the image plane into different moving objects, computing their motion and tracking them throughout image sequence. The techniques for improving resolution of tracked objects, occluded segments of tracked objects and transparent moving objects are presented as well. It is concluded that quality of high resolution image is a function of good motion estimation and segmentation of tracked objects.

S. Park, M. Park and M. Kang in article titled "Super-Resolution Image Reconstruction: a Technical Overview" [44] have presented concepts of super resolution technology along with review of super resolution algorithms until around 2003 and issues to improve performance of super resolution algorithms. The authors have classified super resolution techniques as-Nonlinear interpolation approach, Frequency domain approach, Deterministic & Stochastic regularization approach and The Projection onto Convex Sets (POCS) approach. Further few issues in super resolution are presented by authors: registration error, blind super resolution image reconstruction, computational efficiency, color super resolution and compression issue.

Ur & Gross [41] presented spatial domain algorithm in paper titled "Improved resolution from sub-pixel shifted pictures". Assuming a known 2D translation, a fine sample grid image is created from the input images, using interpolation, and the camera blur is canceled using deblurring technique. The paper is based on geometric warps as pure translations; and the additive noise is white. In time domain, researchers have used Papoulis-Brown generalized sampling theorem [92-93] to obtain an improved resolution picture from an ensemble of spatially shifted pictures. However, these shifts are assumed to be known by the authors, which in practical may not be a feasible solution. The restoration process then uses a convolution method to remove blurs. The disadvantage is that the resulting high resolution image is not optimal and only one blurring model can be applied for all low resolution images.

The researchers Sina Farsiu, Robinson, Elad, and Milanfar, in article titled "Advances and Challenges in Super-Resolution" [2] have reviewed a variety of Super-Resolution methods and a detailed study of several very important aspects of Super-Resolution such as robustness, treatment of color, and dynamic operation modes is presented.

Authors have concluded that an inherent difficulty with inverse problems is the challenge of inverting the forward model without amplifying the effect of noise in the measured data. In the linear model, these results from the very high, possibly infinite and condition number for the model matrix M. Solving the inverse problem, as the name suggests, requires inverting the effects of the system matrix M. Also aliasing artifacts in images are visually very disturbing. Therefore, there is a need to apply a low-pass filter before sampling. This removes all aliasing but it also creates a blurred image.

In the paper Authors P. Vanwalle, Sbaiz, Vetterlia and Susstruk in "Super Resolution from Highly Under Sampled Images" [42], have presented a new method for the reconstruction of a high resolution image from a set of highly under sampled and thus aliased images. Authors have used the information in the entire frequency spectrum, including the aliased part, to create a sharp, high resolution image. The unknown relative shifts between the images are computed using a subspace projection approach. The projection has been decomposed into multiple projections onto smaller subspaces. Once the offset is known, the original signal is reconstructed as the solution of a set of linear equations in unknown basis components.

It is further emphasized by authors that if the signal is sampled at lower frequency the sampled signal is aliased, and the original signal cannot be reconstructed. However, all the frequency content is still present in the sampled signal. It would therefore be interesting to use all this frequency information to reconstruct the signal.

Based on their study, authors have drawn a few conclusions and have extended their work in [43] to exploit aliasing. In super-resolution signal reconstruction, aliased components contain valuable high-frequency information that can be used to recover a higher resolution reconstruction.

In paper "Super Resolution from Unregistered and Totally Aliased Signals Using Subspace Methods" [43], by Patrick Vandewalle, L Sbaiz, J Vandewalle and M Vetterli have studied methods to reconstruct a signal, including its high-frequency information, from multiple aliased sampled signals with relative offsets. When multiple copies are available, they have used the information that is inherently present in the aliasing to reconstruct a higher resolution signal. These different copies have unknown relative offsets; this is a nonlinear problem in the offsets and the signal coefficients. They are not easily separable in the set of equations describing the super-resolution problem. The offsets are unknown and are computed first. For the estimation of those offsets, they have explicitly used the information available in the aliased part of the spectrum and do not need extra measurements. They perform joint registration and reconstruction from multiple unregistered sets of samples.

Further authors have discussed practical issues related to technique proposed. For given technique, no sampling kernel was considered. Signal is sampled using Dirac function. Although this is not very much realistic, it is approximately obtained to make analysis simple. For one-dimensional signal, it is easy to calculate relative offset required. The image is two-dimensional, hence to use this technique for image, number of offsets increase, and hence in turn the computational complexity becomes a critical issue.

The accuracy of results is based on the estimation of offset. To calculate this offset iterative method is used. This method calculates approximate offset and takes more time. To calculate this offset the main limitation of these methods is their computational

complexity. The major advantages provided by this approach include General observation models, which may include Arbitrary motion models, Motion blurring, Optical system degradations, Effects of non-ideal sampling and ability to model complex degradations.

Tekalp, Ozkan and Sezan [6] propose a two-step procedure where the up sampling of the low resolution images and the restoration to correct for a sensor PSF are performed sequentially. The low resolution frames are registered and combined to form a non-uniformly sampled high resolution image which is then interpolated and resampled on a uniform grid to produce the reconstructed high resolution frame.

Sina Farsiu, M. Dirk Robinson, Michael Elad, and Peyman Milanfar [13] propose an alternate approach using L_1 norm minimization and robust regularization based on a bilateral prior to deal with different data and noise models. This computationally inexpensive method is robust to errors in motion and blurs estimation and results in images with sharp edges.

Sina Farsiu, Michael Elad, and Peyman Milanfar[14] propose a fast and robust hybrid method of super-resolution and demosaicing, based on a maximum a posteriori estimation technique by minimizing a multiterm cost function. The L_1 norm is used for measuring the difference between the projected estimate of the high-resolution image and each low resolution image, removing outliers in the data and errors due to possibly inaccurate motion estimation. Bilateral regularization is used for spatially regularizing the luminance component, resulting in sharp edges and forcing interpolation along the edges and not across them. Simultaneously, Tikhonov regularization is used to smooth the chrominance components. Finally, an additional regularization term is used to force similar edge location and orientation in different color channels. This approach cannot fully analyze subpixel motion estimation from colored filtered images.

Nathan A. Woods, Nikolas P. Galatsanos, and Aggelos K. Katsaggelos,[15] proposed two algorithms for the problem of obtaining a single high-resolution image from multiple noisy, blurred, and under sampled images. The first is based on a Bayesian formulation that is implemented via the expectation maximization algorithm as Bayesian approach offers the advantage of more reliable parameter estimates since all of the information that is known about the hidden variables is incorporated into the estimation process. The second is based on a maximum a posteriori formulation. In both of

formulations, the registration, noise, and image statistics are treated as unknown parameters. These unknown parameters and the high-resolution image are estimated jointly based on the available observations. Both of the proposed approaches produce superior registration estimates as compared to independent estimation of motion followed by restoration. The Bayesian method produces more accurate registration parameter estimates than the MAP approach. Issue of the sensitivity to errors in the blur is still a disadvantage for the super-resolution problem.

Giannis K. Chantas, Nikolaos P. Galatsanos, and Nathan A. Woods[16] proposed a maximum posteriori framework for the super-resolution problem, whose main two contributions are; first, the use of a new locally adaptive edge preserving prior for the super-resolution problem, second, an efficient two-step reconstruction methodology that includes first an initial registration using only the low-resolution degraded observations. This is followed by a fast iterative algorithm implemented in the discrete Fourier transform domain in which the restoration, interpolation and the registration subtasks of this problem are preformed simultaneously. Images reconstructed using the proposed nonstationary prior, are visually more pleasant and display less ringing at the edges. It results into faster processing (4-5 sec.) at cost of slight decrease in quality by estimating the registration parameter than real.

Russell Hardie,[17] proposed a computationally simple super-resolution algorithm using a type of adaptive Wiener filter (AWF). He used subpixel registration to position each LR pixel value on a common spatial grid that is referenced to the average position of the input frames. The positions of the LR pixels are not quantized to a finite grid as with some previous techniques. The output high-resolution (HR) pixels are obtained using a weighted sum of LR pixels in a local moving window. Using a statistical model, the weights for each HR pixel are designed to minimize the mean squared error and they depend on the relative positions of the surrounding LR pixels. Thus, these weights adapt spatially and temporally to changing distributions of LR pixels due to varying motion. Both a global and spatially varying statistical model are considered here. Since the weights adapt with distribution of LR pixels, it is quite robust. Advantages of the AWF SR algorithm are, it does not quantize the motion parameters and place the LR pixels on a discrete HR grid. Also, the filter weights for the AWF SR method are model-based and do not require empirical training images. Finally, no vector quantization is needed. Computational complexity of the method is quite low in

comparison to iterative SR algorithms, but for no translational motion, the complexity goes up drastically.

Authors Kim-Hui Yap, Li Chen, and Lap-PuiCha[18], presented a new framework that performs simultaneous image registration and HR image reconstruction. As opposed to other current methods that treat image registration and HR reconstruction as disjoint processes, the new framework enables image registration and HR reconstruction to be estimated simultaneously and improved progressively. Motion model used includes both translation as well as rotation.

Uma Mudenagudi, Subhashis Banerjee, and Prem Kumar Kalra[19] address the problem of super-resolution by multiple low-resolution inputs. The increased resolution can be in spatial or temporal dimensions, or even in both. They present a unified framework which uses a generative model of the imaging process and can address spatial super-resolution, space-time super-resolution, image deconvolution, single-image expansion, removal of noise, and image restoration. High-resolution image is modeled as Markov random field and use maximum posteriori estimate as the final solution using graph-cut optimization technique.

S. Derin Babacan, Rafael Molina, and Aggelos K. Katsaggelos, [20] propose super resolution methods where the HR image and the motion parameters are estimated simultaneously. Utilizing a Bayesian formulation, model the unknown HR image, the acquisition process, the motion parameters and the unknown model parameters in a stochastic sense. Employing a variational Bayesian analysis, they develop two algorithms which jointly estimate the distributions of all unknowns. The proposed framework has the following advantages: 1) Through the incorporation of uncertainty of the estimates, the algorithms prevent the propagation of errors between the estimates of the various unknowns; 2) the algorithms are robust to errors in the estimation of the motion parameters; and 3) using a fully Bayesian formulation, the developed algorithms simultaneously estimate all algorithmic parameters along with the HR image and motion parameters, and therefore they are fully-automated and do not require parameter tuning. HR image estimates with sharper edges and fewer ringing artifacts, are also very effective in preserving sharp image features while suppressing noise and motion artifacts. The unknown high resolution image, motion parameters and algorithm parameters, including the noise variances, are modeled within a hierarchical Bayesian framework.

Estimate all unknowns and algorithm parameters solely from the observed low resolution images without prior knowledge or user intervention.

Maria Teresa Merino and Jorge Nunez in "Super-Resolution of Remotely Sensed Images with Variable-Pixel Linear Reconstruction" [11] present a method known as Super-Resolution Variable-Pixel Linear Reconstruction (SRVPLR) proposed by Hook. The technique is useful for not only astronomical but also satellite remotely sensed images. But in satellite imaging, automatic registration is very difficult as subpixel accuracy is complex and image is highly distorted. Authors have put forth that it is preferable to use simple super resolution algorithm that performs only proper interpolation. The algorithm preserves photometry, and can weight input images according to the statistical significance of each pixel, and removes the effect of geometric distortion on both image shape and photometry.

Frequency domain algorithms mostly utilize the shifting property of the Fourier transform to model global translational scene motion, and take advantage of the sampling theory to enable effect restoration made possible by the availability of multiple observation images. Under the assumption of global translational motion, frequency domain methods are computationally highly attractive.

Tsai and Hunag were the first to consider frequency domain method, though computationally attractive but proposed approach has significant disadvantages. [05]. System matrix requires knowledge of the translation, which is not typically known a-priori; these parameters must be estimated before reconstruction.

Tekalp, Ozkan and Sezan [06] extended Tsai-Huang formulation by including the point spread function of the imaging system and observation noise. A simultaneous multi-frame image registration algorithm is proposed which shows to deliver reliable registration parameters even under the conditions of severe under sampling, provided a sufficiently large number of observation frames are available. An approach based on a least squares formulation implemented in a recursive fashion to improve computational efficiency and provides the advantage of a robustness in the case of an under or over determined system. To overcome the inability to accommodate non-global motion models, observation images are decomposed into overlapping blocks; translational motion is estimated for these blocks in the observation sequence frames. A extensions of the recursive least squares is that of recursive total least squares which is known to

provide some degree of robustness to errors in the observation model, which are likely, in the case of super-resolution reconstruction, to result from errors in motion estimation. A frequency domain technique relying on the shift property of the Fourier Transform to model the translation of the source imagery. DWT is applied in order to decompose an input image into different sub-bands. Then the high frequency sub-bands are manipulated to obtain HR image. Those components can be assembled back into the original signal without loss of information.

In the paper "Statistical Performance Analysis of Super Resolution" [75], Dirk Robinson & Milanfar have examined the performance bounds for super resolution algorithms using a set of low resolution images performing combined task of registration and fusion of low resolution data sets. The analysis revels that super resolution performance depends on a complex relationship between measurement SNR, the number of observed frames, and set of relative motion between frames, image contents, and imaging systems PSF. The analysis reveals that degradation in super resolution performance is considerable when motion are estimated from the data, rather than known a priori. But the analysis restricted for image sequences have simple translational motion only.

In the paper titled "Multi-Objective Super Resolution: Concept and Examples", [76] the authors Deepu Ranjan, S Chaudhari, M Joshi deal with issues related to motion estimation and modeling. Authors have considered that multiple observations of a scene with different types of cues, where each frame contains some additional information, even though there is no relative positional shift among frames. Further they have enlarged the capacity of super resolution technique to recover intensity values. In this fashion, they get super resolution image along with structural information of a scene at higher resolution. The extracted structural information is fed back to the super resolution algorithm which is used to generate the super resolution image in an iterative way. The structural information is embedded in observations and, using the formulations of DFD (depth from focus) and shape from shading (SFS) problems they have generated super resolution image and structure. The DFD method avoids correspondence and wrapping problem inherent in current super resolution techniques involving the motion cues a more natural depth related focus as a natural cue in real aperture imaging.

Patrick Vandewalle, Sabine Susstrunk and Martin Vetterli "A Frequency Domain Approach to Registration of Aliased Images with Application to Super-resolution" [46] have proposed a frequency domain technique to reconstruct high resolution image from set of aliased images. Author strongly claimed that an error in motion estimation translates most directly into degradation of resulting high resolution image. Further authors claim that the result obtained by interpolating one of the low resolution images is better solution than high resolution image obtained from set of low resolution images using incorrect motion estimation. The artifacts due to bad motion estimation are visually very noticeable. The second challenge is to apply information obtained from different registered images to reconstruction of sharp high resolution image.

One of the limitations of algorithm is that it works properly if captured images possess aliasing. If Optical low pass filter is applied to image before capturing to ensure that aliasing cannot occur. Then, the algorithm presented cannot perform better than regular interpolations.

Mahesh B. Chappalli and N. K. Bose [7] used wavelet coefficients thresholding for reducing spatial domain noise in wavelet-based super-resolution algorithms. The choice of optimal threshold is a tradeoff between noise filtering and blurring introduced by thresholding in second-generation wavelet super-resolution (SGWSR) algorithm.

TurgayCelik and TardiTjahjadi[8] proposed a complex wavelet-domain image resolution enhancement algorithm based on the estimation of wavelet coefficients. The HR image is reconstructed from the LR image, together with a set of wavelet coefficients, using the inverse Dual-Tree Complex Wavelet Transform (IDT-CWT). The set of wavelet coefficients is estimated from the DT-CWT decomposition of the rough estimation of the HR image. Generate the initial estimate (Y) of the HR image; decompose Y using one-level DT-CWT to create a low- and high-pass matrix structure $[LP_Y\ HP_Y]$; formulate a matrix structure $[X_L\ HP_Y]$ using $[LP_Y\ HP_Y]$ and the input LR image X_L; and generate the HR image by employing the IDT-CWT on $[X_L\ HP_Y]$.

Prakash P. Gajjar and Manjunath V. Joshi[9] propose a learning-based approach where first obtain an initial high-resolution (HR) estimate by learning the high frequency details from the available database. A discrete wavelet transform (DWT) based approach is proposed for learning that uses a set of low-resolution (LR) images and their corresponding HR versions. The prior model for the super-resolved image is chosen as an

Inhomogeneous Gaussian Markov random field (IGMRF) and the model parameters are estimated using the same initial HR estimate. A maximum a posteriori (MAP) estimation is used to arrive at the cost function which is minimized using a simple gradient descent approach. The missing high-frequency details are learned from a database consisting of LR images and their HR versions all captured by varying resolution settings of a MAP estimate. An inhomogeneous Gaussian MRF model is used as a prior. Both the model parameters as well as the decimation are estimated using the learned HR estimate. [09]

Hasan Demirel and Gholamreza Anbarjafari[10] propose an image resolution enhancement technique based on interpolation of the high frequency sub-band images obtained by discrete wavelet transform (DWT) and the input image. The edges are enhanced by introducing an intermediate stage by using stationary wavelet transform (SWT). DWT is applied in order to decompose an input image into different sub-bands. Then the high frequency sub-bands as well as the input image are interpolated. The estimated high frequency sub-bands are being modified by using high frequency subband obtained through SWT. Then all these sub-bands are combined to generate a new high resolution image by using inverse DWT (IDWT).

Table 2.1: PSNR (dB) Results for resolution enhancement from 128 x 128 to 512 x 512 of the technique compared with the conventional and state-of-art image resolution enhancement techniques [10]

	PSNR (dB)			
Techniques \ images	**Lena**	**Elaine**	**Baboon**	**Peppers**
Bilinear	26.34	25.38	20.51	25.16
Bicubic	26.86	28.93	20.61	25.66
WZP (db. 9/7)	28.84	30.44	21.47	29.57
Regularity-Preserving Image Interpolation[7]	28.81	30.42	21.47	29.57
NEDI [10]	28.81	29.97	21.18	28.52
HMM [11]	28.86	30.46	21.47	29.58
HMM SR [12]	28.88	30.51	21.49	29.60
WZP-CS [13]	29.27	30.78	21.54	29.87
WZP-CS-ER [14]	29.36	30.89	21.56	30.05
DWT SR [15]	34.79	32.73	23.29	32.19
CWT SR [5]	33.74	33.05	23.12	31.03
SWT SR	32.01	31.25	22.74	29.46
Proposed Technique	**34.82**	**35.01**	**23.87**	**33.06**

The state-of-art techniques used for comparison purposes are : —regularity-preserving image interpolation ;new edge-directed interpolation (NEDI) ;hidden Markov model (HMM) ;HMM-based image super resolution (HMM SR) ; WZP and cycle-spinning (WZP-CS) ; WZP, CS, and edge rectification (WZP-CS-ER) ; DWT based

super resolution (DWT SR) ; complex wavelet transform based super resolution (CWT SR) . Table –2.1 shows PSNR (dB) results compared with all above techniques.

M. Dirk Robinson, Cynthia A. Toth, Joseph Y. Lo, and Sina Farsiu[11] present a novel extension of the combined Fourier-wavelet deconvolution and denoising algorithm ForWarD to the multiframe SR application. First uses a fast Fourier-based multiframe image restoration to produce a sharp, yet noisy estimate of the high-resolution image, and then applies a space-variant nonlinear wavelet thresholding that addresses the non-stationary inherent in resolution-enhanced fused images. For better performance do the extensions to the ForWarD algorithm with more sophisticated redundant wavelet techniques such as curvelets or ridgelets.

HuiJi and Cornelia Fermuller [12] present an analysis and algorithm for the problem of super-resolution imaging as Super-resolution reconstruction entails solutions to two problems. One is the alignment of image frames and the other is the reconstruction of an HR image from multiple aligned LR images. Both are important for the performance of super-resolution imaging. Image alignment is addressed with a new batch algorithm, which simultaneously estimates the homographies between multiple image frames by enforcing the surface normal vectors to be the same.

Manjunath Joshi and Subhasis Choudhari in paper titled "Simultaneous estimation of super resolved depth map and intensity field using photometric cue"[13] have proposed regularization based technique to obtain the super resolution scene that simultaneously enhances the surface gradients and albeto representing the object shape and reflectance. To explore a structure preserving super-resolution technique, authors have investigated the usefulness of the photometric cue instead of the motion cue for super-resolving a scene. The sampled plenoptic function is sampled by taking the photographs of same scene with different light source positions. The plenoptic function is decomposed into a number of sub-functions and a generalized upsampling process with the prior-based regularization is used, the proposed method is only applicable to indoor scenes where the ambient illumination can be controlled.

In the technique proposed the 3-D shape preservation is used as a constraint while super-resolving a scene. Given the observations under different illuminant positions, method combines these observations to obtain the super-resolved image and the spatially enhanced scene structure simultaneously. The use of shape cue in the form of

photometric measurements, instead of the motion cue, eliminates the need for image registration with sub-pixel accuracy. Authors have modeled the high-resolution image, the structure, and the albeto of the surface as separate Markov random fields and super-resolve them using a suitable regularization scheme. The approach avoids the correspondence and wrapping problem inherent in current super resolution techniques that involve the motion cue in low resolution observations.

In paper "Simultaneous Estimation of Super-Resolved Scene and Depth Map from Low Resolution Defocused Observations" [14] authors Deepu Ranjan and Subhasis Choudhari have extended scope of super resolution to techniques from intensity domain to depth estimates to include high resolution depth information in a scene in addition to recovering intensity values. Authors have exploited this blur to recover the depth map through the depth from defocus formulation; and propose how the depth map can be estimated at a higher resolution than one that can be normally extracted from such observations. They have concluded that it is indeed possible to super resolve both intensity and depth maps using the depth related defocus as natural cue.

Researchers Elad and Feuer in "Restoration of a single super-resolution image from several blurred, noisy and undersampled measured images" [15] have proposed a method for super-resolution restoration from several geometrically warped, blurred, noisy, and down-sampled measured images, achieved by combining maximum likelihood (ML), MAP, and projection onto convex sets (POCS) approaches. The proposed approach is image restoration using single image, which is general that assumes explicit knowledge of linear space and time invariant blur, additive Gaussian noise, the different measured resolutions and smooth motion characteristics.

XinboGao, Qian Wang, Xuelong Li, Dacheng Tao, and Kaibing Zhang [21], in the process of reconstruction, fuzzy registration is used which mainly focuses on the correlation between pixels of the candidate and the reference images to reconstruct each pixel by averaging all its neighboring pixels. However, if some objects appear or disappear among LR images or different angle rotations exist among them, the correlation between corresponding pixels becomes weak, if the LR images are noised, the reconstruction quality will be affected seriously. To reduce these problems, they have used SR method based on the Zernike moment, consist of a set of independent and invariant moments with an arbitrarily high order.

EsmaeilFaramarzi, Dinesh Rajan, and Marc P. Christensen[22] presents, a unified blind method for multi-image super-resolution and multi-image blur deconvolution (MIBD) of low-resolution (LR) images degraded by linear space-invariant (LSI) blur, aliasing, and additive white Gaussian noise (AWGN). The proposed approach is based on alternating minimization (AM) of a new cost function with respect to the unknown high-resolution (HR) image and blurs. The regularization term for the HR image is based upon the Huber-Markov random field (HMRF) model, which is a type of variational integral that exploits the piecewise smooth nature of the HR image. The blur estimation process is supported by an edge-emphasizing smoothing operation, which improves the quality of blur estimates. The blur estimation is done in the filter domain using the gradients of the LR and HR images.

Feng Li, XiupingJia, Donald Fraser, and Andrew Lambert [23] propose a new super resolution (SR) method called the maximum a posteriori based on a universal Hidden Markov Tree (HMT) model for remote sensing images. The HMT theory is first used to set up a prior model for reconstructing super resolved images from a sequence of warped, blurred, subsampled and noise-contaminated low-resolution (LR) images. Because the wavelet coefficients of images can be well characterized as a mixed Gaussian distribution, an HMT model is better able to capture the dependences between multiscale wavelet coefficients. Computational loads depend on the number of the LR images and the size of each image which is large.

The authors Bahedir Gunturk &Gevrekci in research letter "High Resolution Image Reconstruction from Multiple Differently Exposed Images"[50] proposed a Bayesian super resolution algorithm based on an imaging model which includes camera response function, exposure time, sensor noise and quantization error besides spatial blurring and sampling. The basic theory of multiframe super resolution imaging is modeling a process relating an unknown high resolution image with multiple low resolution observations and then solves this inverse problem to obtain high resolution image based on certain assumptions. Major drawback of this technique is that if assumptions are wrong, false information may get added in the high resolution image.

In this paper, authors have made efforts to minimizing this error by modeling the imaging process using exposure time, sensor noise and quantization error all as an independent random variable with Gaussian distributions. The approach starts with an

initial guess obtained by interpolating one of the low resolution images. This reference image is updated iteratively. Each of iterations consist of image operations: warping, convolution, sampling and scaling. After spatial registration using feature based method, estimate the exposure time using least-squares estimation. The outliers are eliminated and homographies are estimated.

Authors Marcelo Victor Wust Zibetti and Joceli Mayer in paper "Outlier Robust and Edge Preserving Simultaneous Super resolution" [51] have proposed algorithm to reconstruct high resolution image using set of low resolution images. During reconstruction of high resolution images, there is need to estimate the motion and compensate it. But in the process of compensations the error may get included are, small differences in the motion compensated image, and another is, large errors, supposed to be outliers. Outliers degrade the super resolution results. So, to reduce their influence they have proposed a method to reduce the effect of outliers even without detection and removal.

Due to the dependency of the registration errors to super resolution imaging, several recent works have proposed super resolution algorithms, designed to be robust to such errors. Researchers, Guilherme Holsbach Costa, and José Carlos Moreira Bermudez in paper titled "Statistical Analysis of the LMS Algorithm Applied to Super-Resolution Image Reconstruction" [52] have proposed different registration algorithms for super resolution image reconstruction. A deterministic model for its stochastic behavior is proposed which permits the determination of the mean square high-resolution estimation error for a given level of registration error.

Wenze Sohao, Zhihui Wei in the paper "Efficient Image Magnification and Applications to Super Resolution Reconstruction" [53] have proposed an another magnification approach utilizing filtering based implementation scheme and novel regularization through coupling bilateral filtering with digital total variation model. The regularization theory is used to it with the help of some priori constraints for instance locations of sharp edges, fine textures etc. Ultimately a new simple, fast and robust approach is put forth for super resolution reconstruction.

In the paper "A computationally efficient super-resolution image reconstruction algorithm" [54] Nguyen et al. and Milanfar proposed a multichannel super resolution. Algorithm models each low resolution frame as a noisy, uniformly down-sampled

version of the high resolution image, which has been shifted and blurred. In this paper, authors consider only shifts of integral multiples of one high resolution pixel and non-integral shift is replaced with the nearest integral shift. The proposed approach is an efficient and robust for image super resolution and this work is bi-fold. First, robust approach for super resolution reconstruction employs Tikhonov regularization. To automatically calculate the regularization parameter, authors adopt the generalized cross-validation criterion which is a well-known technique for parameter estimation for over determined least squares problems, the derivation for underdetermined problems is new. Secondly, to accelerate conjugate gradient (CG) convergence, authors proposed circulant-type preconditioners, operations involving in these preconditioners can be done efficiently by FFTs, most important point is the reduction in number of CG iterations leading to significant improvement in runtime.

To address motion estimation under multiple object movement Huanfeng, Zhang, Huang and Pingxiang, in paper [55] titled, "A MAP Approach for Joint Motion Estimation, Segmentation & Super resolution" proposed a joint MAP formulation combining motion estimation, segmentation, and super resolution together. The formulation is solved by a cyclic coordinate process which considers the motion fields, segmentation fields, and high resolution image as unknowns and estimates them in combine using the available data.

The joint estimation approach is based on interdependence of desired high resolution image and motion estimates. As motion estimation and segmentation are interdependent. So, the success of motion segmentation is depends on the accuracy of the motion field, and vice versa. In the algorithm, all the processes are judiciously integrated within a MAP framework. it can suppress the artifacts around motion boundaries and occlusion regions without the need of interaction. The advantage of this algorithm is that the motion estimates, segmentation maps and high resolution image can benefit each other.

To minimize common space invariant blur effect, Tuan Pham, Vliet & Schutte [56], in their article "Robust Fusion of Irregularly sampled Data Using Adaptive Normalized Convolution" proposed the super resolution fusion as a separate step in between image registration and deblurring. They have presented a algorithm for image fusion from irregularly sampled data based on framework of Normalized Convolution

(NC). The first order NC with three bases can model the edges; the second order NC with six bases can further model ridges and blobs. A full first order NC needs nine convolutions and produces three output images: interfolded image and two directional derivative for x and y dimensions. The NC better interpolates uncertain data but it requires signal certainly known in advance. In proposed technique, robust certainty is assigned to each neighboring sample before local polynomial expansion around pixel.

Initially low resolution images are registered, then adjusting their weight factors followed by performing robust adaptive NC is performed and finally super resolution image is constructed using deblurring function. In NC, the local signal is approximated through a projection onto a subspace. The method is based on a robust polynomial fit over an adaptive neighborhood. The robust sample certainty minimizes the smoothing of sharp corners and tiny details because samples from other intensity distributions are effectively pay no attention in local analysis.

Researchers Bo-Won Jean, Park & Yang in their article [57] discussed existing resolution enhancement techniques, and they have proposed a resolution enhancement algorithm titled "Resolution Enhancement by Prediction of High Frequency Image Based on the Laplacian Pyramid" for predicting high frequency image based on Laplacian / Gaussian pyramid structure. High frequency image is estimated by using the features of Laplacian images. The normalized histogram of the Laplacian images is fitted to the Laplacian Probability Density Function (pdf) and the parameter of Laplacian pdf is estimated using Laplacian image pyramid. Along with a control function utilized to remove overshoot artifacts in reconstructed image. In the proposed algorithm only Y component is processed by algorithm, and the U and V components are interpolated using bilinear interpolation. Comparison of algorithm with interpolation with respect to computational cost and PSNR parameters shows better results than conventional approaches in terms of connectivity, sharpness at edges and smoothness in uniform region.

In the paper "Resolution Enhancement via Probabilistic Deconvolution of Multiple Degraded Images", authors F. Sroubek & J Flusser [58] present a maximum a posteriori (MAP) solution to the problem of obtaining a high resolution image from set of degraded low resolution images of the same scene. The main aspect of proposed fusion method is that no prior knowledge of blurring function is required. They have utilized

stochastic fusion method that performs multi-channel blind convolution and the super resolution simultaneously. Further authors claim that this approach provides the high quality fused image fully comparable to the ideal one

Y. He, K. Yap, L. Chen & L. Chau, in paper titled "Joint Image Registration and Super Resolution Using Nonlinear Least Squares Method" [59], proposed a new algorithm to integrate image registration into super resolution, achieved by fusing multiple blurred low resolution images to obtain a high resolution image. The registration and high resolution reconstruction is carried out jointly using an iterative scheme based on nonlinear least squares method to estimation of motion shift and high resolution image gradually. The image registration is estimated from the high resolution image iteratively rather than using low resolution images. The proposed framework for joint registration and reconstruction is favorable; results demonstrate that method is effective in performing image super resolution.

Cohen, Avrin and Dinstein in paper titled "Polyphase Back Projection Filtering for Resolution Enhancement of Image Sequences" [60], have proposed a method for resolution enhancement of image sequence by polyphase back projection filtering. The work is an extension of super resolution image sequence restoration algorithm proposed by Avrin and Dinstein [60]. The initial solution of super resolution image is prepared by interpolation of the first low resolution image. The imaging system is simulated for every super resolution image at a time, and the error between the simulated image and the corresponding low resolution image is calculated. This error is back projected to the corresponding super resolution image for resolution enhancement.

Authors Balaji N, Kenneth E in paper titled "A Computationally Efficient Super Resolution Algorithm for Video Processing using Partition Filters" [61], propose a algorithm to produce high-resolution video from low-resolution video using partition-based weighted sum (PWS) filters. First, subpixel motion parameters are estimated from the low resolution video frames. These are used to position the observed low resolution pixels into a high-resolution grid. Finally, PWS filters are employed to simultaneously perform nonuniform interpolation and perform deconvolution of the system point spread function. Authors claims that, in addition to super resolution image enhancement the proposed technique is a very useful to carry out non-uniform interpolation. The novelty

of this article is the innovative PWS filter training and implementation methodology for super resolution enhancement of video.

The authors Frank M. Candocia, and Jose C. Principe, in paper "Super-Resolution of Images Based on Local Correlations"[62] have developed an adaptive two-step paradigm for the super resolution. Initially, an unsupervised feature extraction is performed on local neighborhood information from a training image. These features are then used to cluster the neighborhoods into disjoint. A super-resolved image is obtained through the convolution of a low-resolution test image with the established family of kernels. The results of are accurate under assumption that there is much similar local structure among images and this similarity holds across the scales.

As super resolution is an ill posed problem with multiple LR images the obtained HR is not always a guaranteed solution and so number of authors tried to obtain the HR image by using single LR image with estimation of high frequency information from same image or from training sets.

Example-based super-resolution algorithms can roughly be characterized as nearest neighbor (NN)-based estimation: During the training phase, pairs of low-resolution and corresponding high-resolution image patches (sub windows of images) are collected. Then, in the super-resolution phase, each patch of the given low-resolution image is compared to the stored low-resolution patches, and the high-resolution patch corresponding to the nearest low-resolution patch and satisfying a certain spatial neighborhood compatibility is selected as the output. NN-based estimation suffers from overfitting when the target function is highly complex or the data is high-dimensional. Few Single image SR techniques already discussed are Turgay Celik and Tardi Tjahjadi[8] ,Prakash P. Gajjar and Manjunath V. Joshi[9] ,Hasan Demirel and Gholamreza Anbarjafari[10]

KwangIn Kim and Younghee Kwon [24], proposes a framework with an idea is to learn a map from input low-resolution images to target high-resolution images based on example pairs of input and output images. Kernel ridge regression (KRR) is adopted for this purpose. KRR leads to a better generalization than simply storing the examples as has been done in existing example-based algorithms and results in much less noisy images. However, this may introduce blurring and ringing artifacts around major edges as sharp changes are penalized severely. A prior model of a generic image class which

takes into account the discontinuity property of images is adopted to resolve this problem.

Young Cheul Wee and Hyun Joon Shin[25], proposed to construct a higher resolution image from a low resolution image using fractal coding. This super-resolution method utilizes a special type of orthogonal fractal coding method in which the fractal affine transform is determined by the range block mean and contrast scaling. The proposed non-adaptive fractal super-resolution procedure uses a fixed domain block and a fixed contrast scaling factor. Drawbacks of the proposed method are improvement of the visual quality does not match that of the numerical quality. Also this method exaggerates the contrast around edges to increase numerical precision; these exaggerations are not always visually pleasing.

Jianchao Yang, John Wright, Thomas S. Huang, and Yi Ma[26], given an approach, seek a sparse representation for each patch of the low-resolution input, and then use the coefficients of this representation to generate the high-resolution output. Jointly training two dictionaries for the low and high-resolution image patches, enforce the similarity of sparse representations between the low-resolution and high-resolution image patch pair with respect to their own dictionaries, but need future investigation is to determine the optimal dictionary size for natural image patches in terms of SR tasks.

Jian Sun, ZongbenXu, and Heung-Yeung Shum.[27] propose a gradient profile prior, which implies the prior knowledge of natural image gradients. In this prior, the image gradients are represented by gradient profiles, which are 1-D profiles of gradient magnitudes perpendicular to image structures. Using parametric gradient profile model, the prior knowledge of the gradient profiles is learned from a large collection of natural images. Based on this prior, propose a gradient field transformation to constrain the gradient fields of the high resolution image.

To reduce the problem for neighbor-embedding (NE)-based SR reconstruction, XinboGao, Kaibing Zhang, Dacheng Tao and Xuelong Li.[28] , apply a joint learning technique to train two projection matrices simultaneously and to map the original LR and HR feature spaces onto a unified feature subspace. Subsequently, the nearest neighbor selection of the input LR image patches is conducted in the unified feature subspace to estimate the reconstruction weights. Refine further the initial SR estimate, impose a global reconstruction constraint on the SR outcome based on the maximum a posteriori

framework. Still the construction of optimal GPPs rather than a fixed neighborhood size is a challenge.

Fei Zhou, Wenming Yang, and Qingmin Liao.[29] , they propose new dictionary learning (DL) method, two-step procedure for DL. First partition the training samples into different subsets, and then learn an incoherent sub-dictionary for every subset. Finally, the input patches are super-resolved using their corresponding sub-dictionaries. Adopt an incoherent dictionary for sparse representation, as well as a coherent learning for learning-based SR. To achieve the incoherent property, learn a sub-dictionary for every subset by the concept of equiangular tight frame (ETF).

Kaibing Zhang, XinboGao, Xuelong Li, and Dacheng Tao.[30], they believe that textures may be contained in multiple manifolds, corresponding to classes. Under this assumption, they present a novel example-based image super-resolution reconstruction algorithm with clustering and supervised neighbor embedding (CSNE). First, a class predictor for low-resolution (LR) patches is learnt by an unsupervised Gaussian mixture model. Then by utilizing class label information of each patch, a supervised neighbor embedding is used to estimate high-resolution (HR) patches corresponding to LR patches. Disadvantages of the proposed algorithm are, first, the computation of clustering for huge training patches is a time-consuming so need to find a representative training set. Second, more efficient methods for patch matching, to be used to speed up the SR process.

Kaibing Zhang, XinboGao, Dacheng Tao, and Xuelong Li.[31], propose an approach by learning multiscale self-similarities from an LR image itself. The proposed SR approach is based upon an observation that small patches in natural images tend to redundantly repeat themselves many times both within the same scale and across different scales. To synthesize the missing details, establish the HR-LR patch pairs using the initial LR input and it's down sampled version to capture the similarities across different scales and utilize the neighbor embedding algorithm to estimate the relationship between the LR and HR image pairs. Also accumulate the previous resultant images as training examples for the subsequent reconstruction processes. A drawback of the proposed SR method is that a fixed number of K-NN used in the example learning-based detail synthesis tends to result in blurring effects.

Min-Chun Yang and Yu-Chiang Frank Wang. [32] proposed framework. advance support vector regression (SVR) with image sparse representation. which offers excellent generalization in modeling the relationship between images and their associated SR versions. SR framework learns and selects the optimal SVR model when producing an SR image. They do not require training low and high-resolution image.

Shuyuan Yang. Min Wang. Yiguang Chen. and Yaxin Sun.[33] . proposed a multiple-geometric-dictionaries-based clustered sparse coding scheme for SISR. Firstly. a large number of high-resolution (HR) image patches are randomly extracted from a set of example training images and clustered into several groups of "geometric patches." from which the corresponding "geometric dictionaries" are learned to further sparsely code each local patch in a low-resolution image. A clustering aggregation is performed on the HR patches recovered by different dictionaries. followed by a subsequent patch aggregation to estimate the HR image. They have added a self-similarity constraint on the recovered image in patch aggregation to reveal new features and details.

Most of single-image super-resolution methods fail to consider the local geometrical structure in the space of the training data. To take this issue into account, Xiaoqiang Lu, Yuan Yuan, and Pingkun Yan.[34], proposes a method named double sparsity regularized manifold learning (DSRML). DSRML can preserve the properties of the aforementioned local geometrical structure by employing manifold learning.

Haichao Zhang, Yanning Zhang, HaisenLi, and Thomas S. Huang.[35] propose an algorithm via Bayesian modeling with a natural image prior modeled by a high-order Markov random field (MRF). The minimum mean square error (MMSE) criteria are used for estimating the HR image. A Markov chain Monte Carlo (MCMC) based sampling algorithm is presented for obtaining the MMSE solution, as it is less sensitive to the local minima problem. As the proposed method is an MCMC sampling-based generative approach, it is not as fast as the MAP solution.

Lingfeng Wang, Shiming Xiang. GaofengMeng, Huaiyu Wu, and Chunhong Pan. [36], propose an effective edge-directed super-resolution method to handle preserving local edge structures. An adaptive self-interpolation algorithm is first proposed to estimate a sharp high-resolution gradient field directly from the input low-resolution image. The obtained high- resolution gradient is then regarded as a gradient constraint or an edge-preserving constraint to reconstruct the high-resolution image.

Hongteng Xu, Guangtao Zhai, and Xiaokang Yang .[37] propose algorithm using local fractal analysis. They treat the pixels of a natural image as a fractal set, the image gradient as a measure of the fractal set. The fundamental of approach is the invariance of the bi-Lipschitz transform of fractal dimension. According to the scale invariance feature of fractal dimension, estimate the gradient of a high-resolution image from that of a low-resolution. High resolution image is further enhanced by preserving the local fractal length of gradient during the up-sampling process. In this the image gradient was used as a sole measure of fractal, which can be insufficient for some complicated image contents.

To determine and learn these statistical features of natural images, the authors Olcay Kursun and Oleg Favorov In paper "Single frame super resolution by a Cortex based mechanism using high level visual features in natural images" [63] have used SINBAD (Set of Interacting Back propagating Dendrites) to reconstruct high resolution image. SINBAD method concludes missing pixel values better way and authors have explained how it can be used to reconstruct super resolution image using single low resolution image. The results show that SINBAD interpolation is visually significantly better by filling the reconstructed image with realistic fine spatial details, such as sharp lines and edges. But, not for certain images where few lines and edges are broken down into separate segments in reconstructed image.

Researchers W. T. Freeman, T. R. Jones, and E. C. Pasztor, in the paper titled "Example based Super resolution" [64] discussed the methods that achieve high resolution enlargement of pixel based images as the super resolution algorithms. They have proposed example based, training based, single image, and one pass super resolution algorithm. Their algorithm needs only nearest neighbor search training set to derive a vector from every patch of local image data. Authors have stressed on Sharpening by amplifying existing image detail, aggregating from multiple frames and Single-frame super-resolution, estimate missing high resolution detail, not present in the original image. During the training, the algorithm gain knowledge of the fine details that correspond to different image regions available at a low-resolution and later uses these learning to forecast fine details in other images. If only local image information is sufficient to predict the missing high-resolution details, the training set patches can be used for super-resolution. Authors noticed that their approach does not work properly. But when they have used it globally instead of locally and better results are achieved.

Authors employed two different approaches to make use of neighborhood relationships in super-resolution algorithms. The first uses a Markov network to probabilistically model the relationships between high- and low-resolution patches and between neighboring high-resolution patches. It is an iterative algorithm, which converges quickly. The second approach is a one-pass algorithm based on local relationship information; it is a fast and approximate solution to the Markov network. Major steps of method are- construct high-resolution image using conventional interpolation from low resolution image and predict the missing image details based on patches. When the data resolution or noise degradations match those of the images to which it is applied the algorithm results are best.

Defining Super-resolution by making use of only one low resolution observations, authors C V Jijji & S. Chaudhari [65] in paper titled "Single Frame Image Super Resolution through Contourlet Learning" have proposed a learning based, single frame super resolution reconstruction method. The method makes use of contourlet transform which is able of capture the smoothness along the contours using the directional decomposition. The main idea of approach is to reconstruct the super resolution image using single low resolution image with the help of database of several high resolution images. The contourlet transform is used to learn the best features from high resolution image database during the up sampling of the image. The paper revels that when an image is interpolated, a region without any edges does not suffer any degradation. But, region containing edges is blurred while up sampling. The algorithm learns the mapping of a low resolution edge to its high resolution representation locally using the training data.

A novel approach propose by Hong Chang, Dit Yan Yeng in the paper titled as "Super Resolution through Neighbor Embedding" [67]. Where given a low-resolution image as input and method recovers its high resolution counterpart using a set of training examples from scenes of the same or different types. In proposed method, a feature vector of the patch is reconstructed using its neighbors in the feature space. For each patch in the low-resolution image, algorithm first calculates the reconstruction weights of its neighbors in feature vector set by minimizing the local reconstruction error. The high-resolution implant is then estimated using the training image pairs while preserving local geometry. At the end impose local compatibility and smoothness constraints between adjoining patches in the target high-resolution image through overlapping. Authors have

given certain research directions. One is to select a good feature to represent image patch that can preserve neighborhood better. The other is to choose a good reconstruction function when given some high resolution neighbor patches.

A new approach "A New Method of Images Super Resolution Restoration by Neural Network" is proposed by Liming Zhang and Fengzhi Pan [68] for generating a higher resolution image the original one by combining intra-frame interpolation and linear restoration of residual errors by neural networks. The proposed technique has short training time as trained with only one image, good generalization and small computation consumption and easily implemented on real time to magnify other images accurately. This method yields correct results if assumptions are correct and original high resolution image is available to estimate the residual error else proposed strategy will not work.

In the paper "Improving a Single Down-sampled Image Using Probability Filtering Based Interpolation and Improved Poisson Maximum a Posteriori Super Resolution" [70] Min Cheng Pan, has presented method consists of interpolation and smoothing simultaneously by exploiting probability filter coupled with a pyramidal decomposition. Afterward, the improved Poisson Maximum a Posteriori (MAP) super resolution is performed to reconstruct high spatial frequency spectrum of interpolated image. Further exploit and use the inter-correlation among the colors to improve performance as it would extend adaptive capability by incorporating image characteristics.

Authors M Joshi, S Choudhari and R Panuganti in paper [72] titled "A Learning Based Method for Image Super Resolution From zoomed Observations" propose use of the homogeneous MRF to model the high resolution field for learning purposes. Utilize a learning based approach where the parameters of the super resolved image are learned from the most zoomed observations and used to estimate zoomed entire scene. The MRF parameters are estimated using a maximum Pseudo likelihood (MPL) estimator to reduce the computations. Use observations at arbitrary levels of resolution (scale) and estimated while super resolving the entire scene.

First order MRF is used to model the intensity process. Metropolis-Hasting algorithm is used to set initial values of parameters as unity. Using initial parameter set super resolved scene is obtained iteratively. The results are compared with bilinear interpolation results. The zoom factor two is found quite well. For zoom factor four is

difficult task in terms of results. Again, the prior term with second order neighborhood shows that there is no perceptual improvement with an additional order introduced in prior term. But, the computation goes up drastically while learning the scene prior.

Authors Shuangteng Zhang, Yihong Lu in paper in "Image Resolution Enhancement Using a Hopfield Neural Network" have proposed a neural network based technique. First establish the observation model, closely relates physical image acquisition process. Then based on the model a cost function is created and minimized by using a Hopfield neural network to enhance the resolution of the images. This method takes into account the PSF (Point Spread Function) and additive noise. The Hopfield neural network is a single-layer feedback neural network, consisting of N interconnected neurons with connecting weights.

Authors Heng Lain, in paper "Variational Local Structure Estimation for Image Super Resolution" [74] has proposed an algorithm which does not use training images or database of images. This technique consider that each low resolution pixel value is a linear combination of neighboring pixel values and uses local structure to construct filter based on estimated local structure of an image for interpolation. The resulting filter reflects both local pixel variance and global image information.

Authors S. Baker and T. Kanade in the paper "Limits on super-resolution and how to break them," [77] have presented limits and techniques to break them. They have proposed a super resolution algorithm based on different kind of constraints, in additional to the reconstruction constraints attempts to identify local features in low resolution images and then enhances their resolution appropriately. The algorithm developed modifies the prior term in the cost to include the results of a set of recognition decisions, so referred as recognition-based super resolution. Recognition-based prior is a function of a collection of recognition decisions. The algorithm learns a recognition based prior for specific classes of objects, scenes or images. Algorithm applied for super resolution of both for faces and text claims the significantly better results in terms of qualitative and in terms of RMS pixel error than traditional reconstruction based super resolution algorithms. Conclusions drawn are, firstly, information content is fundamentally limited by the dynamic range of images. The second is, strong class based priors can provide more information than the simple smoothness priors, used in existing super resolution algorithm.

2.5 Overview of Literature Survey

Image registration is critical for the success of multi-frame SR reconstruction, where spatial samplings of the HR image are fused. The image registration problem is well known as ill-posed and is more difficult in the SR setting, where the observations are low-resolution images with heavy aliasing artifacts. The performance of the standard image registration algorithms decreases as the resolution of the observations goes down, resulting in more registration errors. Degradations caused by these registration errors are visually more annoying than the blurring effect resulting from interpolation of a single image. Motion estimation is used in a range of image and video processing tasks. A computationally effective method for subpixel image registration employed specifically for HR restoration, is presented. It is the gradient constraint method, based on Taylor series expansion, and it is used extensively in this thesis.

In Super-resolution reconstruction via the spatial domain approach, it is simple to include a local motion model as a global model using the spatial domain formulation. Simple inclusion of linear degradations such as motion blurring resulting from a non-zero aperture time, spatially varying or invariant blurs, missing pixels and so on. Inclusion of spatial domain a-priori knowledge for regularization, Markov random fields as well as the spatial domain POCS formulation provided is almost trivially simple, yet very powerful methods to incorporate a-priori constraints into the reconstruction process. Optimizations involved in spatial domain methods are more complex than their frequency domain counterparts. The increased flexibility of spatial domain methods tend to come at the cost of much increased computational requirements. Super-resolution reconstruction via the frequency domain approach has significant advantages: Simplicity, Computational complexity, Intuitive super-resolution mechanism. Significant disadvantages are Global translation motion model, Degradation models; difficult to include spatially varying degradation models in the frequency domain, Inflexibility regarding motion models; due to the inability to formulate Fourier domain transformations which are equivalent to spatially varying motion. Comparisons of Frequency Domain and Spatial Domain techniques is given in table 2.2 which deals with the formulation of the observation, motion and degradation models.

Table 2.2: Comparison of Frequency Domain and Spatial Domain Techniques

	Frequency Domain Techniques	Spatial Domain Techniques
Observation model	Frequency domain	Spatial domain
Motion models	Global translation	Almost unlimited
Degradation model	Limited	LSI or LSV
Noise model	Limited	Very flexible, even spatially varying
SR Mechanism	Dealiasing	Dealiasing & BW extrapolation using a-priori constraints
Simplicity	Very simple	Generally complex
Computational Cost	Low	High
A-priori constraints	Limited	Almost unlimited
Regularization	Limited	Excellent
Extensibility	Poor	Excellent
Performance	Good for specific applications	Good

The spatial domain formulation essentially reduces to projection on a HR grid and interpolation of non-uniformly spaced samples. Several techniques are given: nearest-neighbor, weighted average, least-squares plane fitting, normalized convolution using a Gaussian kernel, Popoulis-Gerchberg algorithm, and iterative reconstruction. It should be noted, that most optical systems cannot be modelled as ideal impulse samplers.

Since super resolution involves estimating data or parameters that are unknown, it is natural to model images as probability distribution. In particular, recursive least squares (RLS), least mean squares (LMS), and steepest descent (SD) are considered. Projection onto Convex Sets (POCS), constraint sets are defined which limit the solution space for the HR reconstruction. However drawbacks are, notably non uniqueness of solution, dependence on the initial guess, and slow convergence.

Although many SR algorithms have been proposed, most of them suffer from several impractical assumptions, e.g., the shift or rotation between LR images is global, the motion occurring between LR images is known exactly, or the LR images are noise

free. However, the imaging procedure is generally much more complicated and may include local warping, blurring, decimation, and noise contamination. As super resolution is an ill posed problem and number of authors tried to obtain the HR image by using single LR image with estimation of high frequency information by learning HR-LR relation from training sets. The correlation between low resolution images and corresponding high resolution images is learnt from a database of known low and high resolution image pairs. This learning is then applied to a new low resolution image to obtain its most likely high resolution image.

The researches on SR reconstruction mainly considered the situation that degraded model is linear, results provided are mostly based on subjective measurements, and it is difficult to find an unbiased comparison on which SR methods are more appropriate for a given task. There must be considerations like if more than one input images are present then use multi frame SR approach and if one or more HR training images are available then use single image SR approach. If registration step is not required then single frame SR can be used. Also, if HR training is not available but different LR images are available for same scene then, one must have to use multi frame SR. This does not provide a clear method of comparing different implementations suitability for a desired application, so one have to implement SR method based on problem model which can be generalized to all SR reconstruction problems.

The super resolution process can be generalized into three important phases: the preprocessing, the reconstruction, and the post processing. Though a wide variety of super resolution approaches are proposed, most of them suffer from drawbacks. It is observed that there is scope to develop the efficient technique for super resolution to satisfy today's demand of high resolution images.

Chapter 3

Design and Implementation of Super Resolution Algorithms

In the process of Image Registration two or more images of the scene are aligned with reference to a particular image of the same scene. These images are captured at different circumstances or time instances, for a range of perspectives, and additionally might be by a variety of sensors. The images are captured using a variety of sensors at different instance of time and at different point of view. Therefore image registration is necessary to identify a superior representation of any change in the scene/object over a considerable period of time. Image registration is utilized expansively in medical sciences, remote sensing and computer vision. This chapter discusses the several significant approaches in conjunction with contributions and drawbacks of the registration techniques in the view of SR.

Registration results are used in reconstruction phase of SR, where inter pixel information available is used in high resolution grid to obtain HR image. This chapter covers the different reconstruction techniques where multiple low resolution images are used. A hybrid approach of super resolution image reconstruction technique and structure for SR image quality measure is derived at the end. Here six different approaches for SR reconstruction are considered and analyzed for their performance to obtain high resolution image with more high frequency information and improved quality. For all the reconstruction algorithms, for registration step, an iterative planar motion estimation algorithm based on Taylor series expansions is used for accurate motion estimation which is found to be best.

In this chapter finally the Particle Swarm Optimization (PSO) based image Reconstruction algorithm has been design and implemented using multiple LR images. This technique is based on statistics and machine learning approach where missing high frequency details of low resolution image are learned from an appropriate LR images.

3.1 Introduction

Image Registration is inferred as the process of superimposing two or more images of the same scene with respect to a base image. Registration process transforms geometrically the different sets of data into a specific required reference co-ordinate system. The divergence between these images are introduced due to the dissimilar imaging conditions. Image Registration is an essential and must require step to obtain the final information from a combination of a large number LR images captured by the source with different orientation. Based on the manner of image acquisition, the application of Image Registration can be separated out into Multi-view Analysis, Multi-temporal Analysis, Multi-modal Analysis groups.

The performance of hybrid approach using log-polar (L-P) Fast Fourier Transform (FFT), an iterative planar motion estimation algorithm based on Taylor series expansions is found better. It is an iterative algorithm to find the rotation angle by using a affine transformation created using Gaussian pyramid. It estimates the linear motion and rotation parameters to sub-pixel accuracy using hybrid approach. It is a robust global registration which consists of combination of the L-P FFT and spatial domain method.

After registration, next step is to interpolate the subpixel information obtained from LR images on regular HR grid and compensate for blur and noise. Accuracy and quality of reconstruction is largely dependent on selection of appropriate registration process, and depends on accurate motion parameter estimation and set of training images. This chapter covers in detail the different reconstruction approaches and the novel combination of registration and reconstruction for super resolution has been suggested.

The work proposes Super Resolution Reconstruction algorithm using PSO with multiple LR images to obtain the SR image. In this method, PSO is used by tuning of parameters of patch size, overlap and K nearest neighbor. By applying certain mathematical procedures for maximizing the PSNR to improve fitness value and gives several enhancements as compared to other method.

3.2. Image Registration Techniques

Image registration techniques can be classified based on criteria [76-77] :Dimensionality, Domain of transformation, Type of transformation, Registration Quality, Parameters of Registration, Subject of Registration, Object of Registration, Nature of Registration basis, Interaction and Modalities involved.

Registration identifies the variation between images, which can be divided into three types:

- Differences which we wish the registration algorithm to account for, and thereby *remove*
- Those which are of interest to us, and so should not be accounted for, and therefore will be *exposed* after registration,
- Those which are not of interest to us, but which we are unable to remove, and which are called uncorrected distortions.

To obtain registration parameters, a range of possibilities for the search space is set of transformations, can be either *global* or *local*. The most common types of transformations are rigid, affine, projective, perspective, and global polynomial. The affine transformation is used in the proposed registration technique in this research for the registration, consisting of a combination of a rotation, a translation, and a scale change.

Image Registration for Super-Resolution

Image registration is decisive for the success of multiframe SR reconstruction, where subpixel spatial samplings of the HR image are reoriented. Robust registration is a key component of successful multi-frame processing aimed at super-resolution. Spatial domain registration methods gives accurate estimation of sub-pixel motion. However, success rely on the availability of a priori information, and are therefore limited in terms of dynamic range of the global relative motions between camera and scene. On the other hand, Fourier domain-based correlation techniques provide fast and reasonably accurate estimates of global shifts, rotation and uniform scale change, and tend to perform well over a large range of frame-to-frame motion magnitudes.

In the process of recording a digital image, there is a natural loss of spatial resolution caused by the optical distortions, motion blur due to limited shutter speed, noise that occurs within the sensor, during transmission, and insufficient sensor density. Thus, the recorded image suffers from blur, noise, and aliasing effects. The aim of SR techniques is to restore HR image from many degraded and aliased LR images. The information combined from various observations of the same scene allows us SR reconstruction of the scene. Model of the LR image acquisition process provide us input for processing the image through various steps to obtain SR image with more quality.

Observation model provides idea to relate LR images to SR image which can be implemented with various ways of processing with different success ratio for different types of images.

Frequency domain algorithms mostly utilize the shifting property of the Fourier Transform to model global translational scene motion, and take advantage of the sampling theory to enable effect of restoration made possible by the availability of multiple observation images.

Spatial domain methods has General observation models, which may include:– Arbitrary motion models, Motion blurring due to non-zero aperture time, Optical system degradations, Effects of non-ideal sampling, Ability to model complex degradations.

In the following sub-section, various registration techniques are discussed which are implemented, analyzed and utilized for the reconstruction process. These techniques are not only analyzed for registration parameter estimation accuracy but also compared for their potential benefit for the result of super-resolution.

3.2.1 Vandewalle's Frequency Domain Registration Algorithm

Vandewalle et al had proposed a planar motion estimation method. Registration of aliased low resolution images is carried out through Fourier transformation. It estimates the movement parameter with sub-pixel precision based on algorithm which is in frequency domain and it estimates the motion parameters between the reference low resolution (LR) image and each of the other LR images. It is restricted to only planar motion parallel to the image plane consist of horizontal and vertical shifts, Δx and Δy, and a planar rotation angle φ.

The reference image is $f_1(x,y)$ and its shifted and rotated version is $f_2(x,y)$. $|F_1(u,v)|$ and $|F_2(u,v)|$ are the magnitudes of their Fourier transform hence $|F_2(u,v)|$ is a rotated version of $|F_1(u,v)|$ since the magnitude of the Fourier Transform is affected by rotation only.

Firstly it estimates the rotation angle φ from the amplitudes ($|F_1(u,v)|$ and $|F_2(u,v)|$) then compensate the shifted LR for the rotation, and compute the shifts Δx and Δy from the phase difference of $F_1(u,v)$ and $F_2(u,v)$. The shift parameters Δx and Δy can thus be computed as the slope of the phase difference. Following is the sequence to implement registration algorithm.

Consider A set of M low-resolution images $f_{LR,m}$ ($m = 1, 2, \ldots, M$) with Fourier transform $F_{LR,m}$. and $f_{LR,1}$ is the reference image.

1. Compute the Fourier transforms $F_{LR,m}$ of all low-resolution images.
2. The rotation angle between every image $f_{LR,m}$ ($m = 2, \ldots, M$) and the reference image $f_{LR,1}$ is estimated from the amplitudes of the Fourier transforms.
3. Then compute the polar coordinates (r, θ) of the all image samples.
4. For every angle α, compute the average value $h_m(\alpha)$ of the Fourier coefficients for which $\alpha-1 < \theta < \alpha+1$ and $0.1\rho < r < \rho_{max}$. The angles are expressed in degrees and $h_m(\alpha)$ is evaluated for every 0.1 degrees. A typical value used for ρ_{max} is 0.6 which is based on experimental analysis.
5. Then find the maximum of the correlation between $h_1(\alpha)$ and $h_m(\alpha)$ between -30 and 30 degrees. This is the estimated rotation angle φ_m.
6. Rotate image $f_{LR,m}$ by $-\varphi_m$ to cancel the rotation for accurate Shift estimation.
7. The horizontal and vertical shifts between every image $f_{LR,m}$ ($m = 2, \ldots, M$) and the reference image $f_{LR,1}$ are estimated.
8. Compute the phase difference between image m and the reference image as $\angle(F_{LR,m}/F_{LR,1})$. For all frequencies $-u_s + u_{max} < u < u_s - u_{max}$ write the linear equation describing a plane through the computed phase difference with unknown slopes Δx.
9. Find the shift parameters Δx_m as the least squares solution of the equations.

The results of the registration for LR images with known rotation and shift have been observed, which are presented in chapter 4, section 4.1. Table 4.1 and graphs in Figure No. 4.1 and 4.2 for known value of rotational and translational motion. Results are shown in terms of three registration parameters, angle of rotation, horizontal and vertical shift. Vandewalle's frequency domain rotation estimation accuracy is less. Due to which rotation compensation is not accurate which in turn results in large error in shift estimation.

3.2.2 Marcel Frequency Domain Registration Algorithm

This algorithm is also based on frequency domain. It estimates the motion parameters between the reference low resolution (LR) image and each of the other LR images. The movement parameters are estimated with sub-pixel precision based on frequency domain transformed LR images.

Algorithms estimate the motion parameters as per following strategy. To obtain the phase correlation function. Let the image I_2 be a shifted version of the image I_1 by (Δx, Δy), then

$$I_2(x,y) = I_1(x - \Delta x,\ y - \Delta y) \qquad \text{----------3.1}$$

Relationship due to the shift property of the FT is.

$$I_2(u,v) = I_1(u,v)\, e^{-j(u\Delta x + u\Delta y)} \qquad \text{----------3.2}$$

Therefore, a shift in the spatial domain will produce a phase difference in the frequency domain. Here normalized cross power spectrum is utilized and it is given as

$$\frac{I_2(u,v) I_1(u,v)}{|I_2(u,v) I_1(u,v)|} = e^{-j(u\Delta x + u\Delta y)} \qquad \text{------3.3}$$

The (PC) function is finally obtained by taking the Inverse Fourier Transform (IFT) of the cross-power spectrum, which gives a $\delta(\Delta x, \Delta y)$) as result nothing but the shift of test image in x and y direction denoted by Δx, Δy respectively. Following is the sequence to implement registration algorithm.

Consider A set of M low-resolution images f_{LRm} (m = 1, 2, ... ,M) with Fourier transform F_{LRm}. and f_{LR1} is the reference image

1. Compute the Fourier transforms F_{LRm} of all low-resolution images.
2. Obtain the phase correlation between each LR image and the reference LR image.
3. The phase correlation between LR images is used to calculate the normalized cross power spectrum.
4. The phase correlation (PC) function is obtained by taking the Inverse Fourier Transform (IFT) of the cross-power spectrum.
5. Then obtain the $\delta(\Delta x, \Delta y)$ nothing but the shift of test image in x and y direction denoted by Δx, Δy respectively.

The results of the registration for LR images with known rotation and shift have been observed, which are presented in chapter 4. Table 4.2 and Figure No. 4.3 shows the registration estimation results for linear motion estimation in terms of horizontal and vertical shift. Drawback of this algorithm is that it won't estimate the rotation parameters and depend on x and y movement only which affect the estimation accuracy. It results in poor shift estimation.

3.2.3 Hybrid Approach using L-P FFT Registration Algorithm

In this algorithm to minimize the processing time and improve the accuracy the concept of pyramid has been implemented. The pyramid generation. In the Pyramid generation process obtain the group of images with decreasing spatial resolution by subsampling sequential by an arbitrary factor in both x and y direction.

A Gaussian pyramid technique is used for creating a series of images which are weighted down using a Gaussian average and scaled down. When this technique is used multiple times, it creates a stack of successively smaller images, with each pixel containing a local average that corresponds to a pixel neighborhood on a lower level of the pyramid.

Spatial domain methods are providing accurate estimation of sub-pixel motion, but these techniques depend on the availability of a priori information with limited dynamic range of global relative motions. A Gaussian pyramid approach is one standard method to extend the region of convergence of spatial domain techniques. Alternatively, Fourier domain-based correlation techniques, the log-polar FFT (L-P FFT) method provide fast and reasonably accurate estimates of global shifts, rotation, and uniform

scale change, and learn to perform well over a wide range of frame-to-frame motion magnitudes.

In hybrid approach robust global registration uses combination of the L-P FFT and spatial domain technique. Initial results are obtained using the output of the L-P FFT method, act as initial guess for a spatial domain technique. Explore the normalized gradient correlation (NGC) while carrying out the coarse L-P FFT registration, for improving performance of the L-P FFT method with respect to robustness and dynamic range of scale factor estimates. The log-polar FFT (L-P FFT) algorithm is able to estimate global x- and y-axis translations, rotation and uniform scale change as described by the following affine coordinate transformation between two images f_1 and f_2:

$$f_2(x,y) = f_1(xs\ cos\theta_0 + ys\ sin\theta_0 + t_x, -xs\ sin\theta_0 + ys\ cos\theta_0 + t_y) \text{ --3.4}$$

Where t_x and t_y represent translations along the x- and y-axis respectively, θ_0 is rotation, and s is the uniform scale factor applied to both axes. Following is the sequence to implement L-P FFT registration algorithm.

1. Compute FFT of each LR image: $F_1 = \mathcal{F}\{f_1\}$ and $F_2 = \mathcal{F}\{f_2\}$, and magnitudes $M_1 = |F_1|$ and $M_2 = |F_2|$.
2. Map the Fourier magnitudes from Cartesian to log-polar coordinates (log ρ, θ).
3. Compute the global correlation between $M_1(\log \rho, \theta)$ and $M_2(\log \rho - \log s, \theta - \theta_0)$.
4. Find peak in the correlation surface, the location of which provides estimates of rotation $\hat{\theta}_0$ and $\hat{s}$ scale.
5. Create two rotated image, using $(\hat{\theta}_0, \hat{s})$ and $(\hat{\theta}_0, \hat{s} + 180^o)$ and 180° ambiguity is due to the conjugate symmetry of the Fourier transform.
6. Compute global correlations between the baseline image and the two scaled and rotated images given the two possible solutions for rotation angle.
7. Repeat the steps 1 to 6 for all images in the Gaussian pyramid consist of a series of scaled down images of LR image.

8. Find the peak in each of the two correlation surfaces, the larger peak resolves the angle ambiguity and its location provides estimates of translation $\hat{t}_x$ and $\hat{t}_y$.

The results of the registration for LR images with known rotation and shift have been observed, which are presented in chapter 4. Table 4.3 and graphs in Figure No. 4.4 and 4.5 for known motion results are shown in terms of three registration parameters, angle of rotation, horizontal shift and vertical shift. The Hybrid approach derived using L-P FFT performance is better that all other techniques in terms of both rotation estimation and shift estimation. Due to accurate subpixel motion estimation this approached is used in proposed super resolution techniques.

3.3 SR image Reconstruction algorithms

SR Image reconstruction is a mathematical process that generates high resolution image from data acquired from different LR images in registration due to subpixel shift. Using the registration information of input images, construct a composite image on non-uniformly spaced sampling points. In the next step, obtain uniformly spaced sampling points by direct or iterative reconstruction procedure. After getting a high resolution image with non-uniform interpolation, restoration is carried out to remove blurring. Six different approaches for SR reconstruction are implemented and their performance has been compared.

3.3.1 Modified Interpolation SR Reconstruction Algorithm

In registration the pixels of low resolution images are mapped on HR grid. There may be few possibilities that some of the locations on HR grid are missing or wrong pixel values are mapped. In such cases interpolation technique help to calculate the missing information or correct the information up to certain extend. Hence in this research the modified interpolation technique has been suggested. This modified interpolation technique maintains the resolution of original HR grid and estimate the value of missing pixel with the help of neighboring pixel information.

Compute the coordinates of the pixels from the N images, using shift and rotation estimation of each LR image, out of the result consider row and column indices within range of HR grid. Next convert an irregularly distributed point data set into a

regular, equally spaced, rectangular grid of points and place this information at proper place on HR grid. To convert from irregular data to a regular grid, the data must be resampled by interpolation. Following is the sequence to implement interpolation algorithm.

1. All LR images placed in cell array (s{1}, s{2},....) in YC_bC_r format.
2. Use Y component of LR images in cell array, and estimate the shift and rotation information Δx and Δy and phase estimation φ.
3. Find the center of each LR image and covert estimated φ into radians and compensate each LR by respective estimated φ.
4. Compute the coordinates of the pixels from the N images, map the pixels of LR images to appropriate position on HR grid.
5. This HR grid is modified by using bicubical interpolation technique.

The reconstruction results of the interpolation approach have been observed, which are presented in chapter 4. Table 4.10 represents the results in terms of SSI, MSE, SNR, PSNR, entropy and execution time respectively. The graphical comparison is given in the Figure No. 4.22 to Figure No.4.27 for SSI, MSE, SNR, PSNR, entropy and execution time parameters respectively. In this technique due to interpolation there is a chances to modify the value of all pixels unnecessary. Hence performance of this algorithm is poor as it introduces noise.

3.3.2 Popoulis-Gerchberg (PG) SR Reconstruction Algorithm

In PG method extrapolation theory has been applied to perform image super-resolution by extrapolating the spectrum beyond the diffraction limit of a finite object.

This approach for SR employs only shift estimation obtained in registration stage and rotation estimation φ is discarded for SR reconstruction. In reconstruction process obtain initial estimation using subpixel information using multiple LR images. The initial estimated image is a higher dimensional grid with some pixels are known and some are unknown. The values of unknown pixels are initially set to zero. Then the image is low pass filtered with a normalized cut off frequency of σ; maximal allowable frequency which results in blurring due to the Unknown pixels will have some values and known pixel values changes after filtering. Hence in this technique the original values of the known pixels are again restored and minimizes the problem of blurring.

This process of filtering and restoring is repeated iteratively to yield HR image. Following is the sequence to implement PG SR algorithm.

1. Obtain the initial high resolution grid by putting the known pixels values from the LR images by converting pixel position to the reference frame.
2. The position on the HR grid is calculated by rounding the magnified pixel positions to nearest integer locations.
3. Unknown pixel values are initialized to zero.
4. Set the high-frequency components to zero beyond the threshold value in frequency domain. This is effectively a low-pass filtering of the image.
5. The known pixel values in spatial domain are set to the original values and retain modified unknown pixel values.
6. Repeat the process of low pass filtering and setting the known pixel value i. e. step 4 and 6 till the acceptable results are not achieved.

The reconstruction results of the Popoulis-Gerchberg (PG) method for SR have been observed, which are presented in chapter 4. Table 4.7 represents the results in terms of SSI, MSE, SNR, PSNR, entropy and execution time respectively. The graphical comparison is given in the Figure No. 4.22 to 4.27 for SSI, MSE, SNR, PSNR, entropy and execution time parameters respectively.

The method is fast but has some shortcomings. The algorithm assumes that, the LR images are down-sampled versions of the expected HR image without any low-pass filtering totally free from noise. Due to the steep cut off in the frequency domain, ringing artifacts near the edges in resultant HR image.

3.3.3 Robust Super Resolution Reconstruction Algorithm (Robust SR):

Robust SR is preferred in case when LR images are corrupted heavily or certain pixel values lies on an abnormal distance (outliers) from other values may be due to relative motion of scene and capturing device. In this algorithm a robust estimator is used in an iterative process to accomplish super resolution. However success of such approach is highly dependent on accuracy of the model used for the imaging process.

To handle it a Maximum a Posteriori solution of stochastic optimization and prior smoothness assumptions are used to minimize the effect of inconsistent measurement. As to handle outliers, algorithm imposes the smoothness on LR images. However it results in a suppression of high frequency information. To handle the abnormalities robust median based estimator is used. The estimator will discard inconsistent measurements in connection with the imaging model, moving objects and parallax. In the next step, all up-sampled LR images are combined into single image via median and then high pass filtered for high frequency retention. Algorithm is robust to exceptions and irregularities due to model inaccuracies and motion object. In this case resolution of inliers regions is improved if occupies large portion of image. Equation specifies the imaging model used.

Let us consider n LR images as $g_1, g_2, \ldots, g_n$. The image formation g_k from super resolved image as

$$\overrightarrow{Y_k} = D_k C_k \vec{X} + \overrightarrow{E_k} \quad \text{------ 3.5}$$

$\vec{X}$ is HR image recorded in a vector.

$\overrightarrow{Y_k}$ is k^{th} input image g_k recorded in a vector.

$\overrightarrow{E_k}$ is k^{th} normality distributed additive noise recorded in vector.

$\overrightarrow{F_k}$ is k^{th} the geometric warp function.

$\overrightarrow{C_k}$ is k^{th} blurring matrix

$\overrightarrow{D_k}$ is k^{th} decimation function.

The gradient of the k^{th} LR image($\overrightarrow{B_k}$) is calculated using the equation 3.6 and sum of the gradient ∇L has been calculated using equation 3.7

$$(\overrightarrow{B_k}) = F_k^T C_k^T D_k^T \left(D_k C_k F_k \vec{X} - \overrightarrow{Y_k}\right) \quad \text{----------3.6}$$

$$\nabla L(\vec{X}) = \sum_{k=1}^{n} \overrightarrow{B_k} \quad \text{---------- 3.7}$$

The gradient based iterative minimization is used to updates the solution. Iteratively the solution is estimated by

$$\overrightarrow{X}^{n+1} = \vec{X}^n + \lambda \nabla L(\vec{X}) \quad \text{---------- 3.8}$$

Where λ is scale factor which is define as the step size in the direction of the gradient. In a proposed research work value of λ has been considered as 0.05 and max 50 iteration.

To have the robustness use scaled pixel wise median, given as

$$\nabla L\left(\vec{X}\right)(x,y) \approx n.median\left\{\overrightarrow{B_k}(x,y)\right\}_{k=1}^{n} \qquad \text{--------3.9}$$

The median estimator approximates the mean accurately. Median is robust when outlier measurements are organized non-symmetrically w.r.t. mean. But need to minimize error i.e. large projection error should have small influence on the computed solution. Following is the sequence of steps for Robust SR algorithm

1. Use luminance component of all LR images to estimate shifts in y and x direction and estimated angle of rotation using reference LR.
2. Resize the reference LR by factor using nearest neighbor method act as initial estimation. Here factor is the enlargement factor for reconstruction.
3. Initialization defines the step size for the iterative gradient method.
4. Start with an estimate of HR image, use an up-sampled version of the first LR image as an initial estimate.
5. Define blur filter mask and normalize it, also define sharpen filter mask.
6. Compute the gradient of the total squared error of reassembling the HR image as:
   - I. First an initial estimate is shifted by Δx and Δy in –ve direction by using circular shift then rotated it by estimated φ for respective LR, to fit it at the estimated place.
   - II. Then apply blur filter by using symmetric method.
   - III. Consider the pixels of this HR grid corresponding to LR grid only and from them subtract the respective LR images, this difference again resize by factor.
   - IV. In next step filter it by using sharpen filter and again rotate it by estimated φ in opposite direction and shift by Δx and Δy in +ve direction by circular shift as need to be consistent with initial estimate.
   - V. Repeat this procedure for all LR images and result stored in array G one by one.

VI. Take the median of G, element by element. Once the median is available, go in its direction with a step size of lambda.

7. New solution of HR is estimated by using previous HR estimate and the median obtained in step 6.
8. The new HR estimate is modified using step 6 to 7 iteratively for the defined number of iterations.

The Robust super resolution reconstruction is implemented and results for SR have been observed, which are presented in chapter 4. Table 4.6 represents the results in terms of SSI, MSE, SNR, PSNR, entropy and execution time respectively. The graphical comparison is given in the plots given in Figure No. 4.22 to 4.27 for SSI, MSE, SNR, PSNR, entropy and execution time parameters respectively. This algorithm is not suitable to use for images where the effect of outlier is not observed.

3.3.4 Iterative Back Projection (IBP) SR Reconstruction Algorithm

SR using IBP (SR–IBP) methods efficiently satisfies the basic reconstruction constraints, in spatial domain applications, it allows easy inclusion of data and also it is a computationally efficient approach.

In this SR algorithm based on iterative back projection. The error between the observed LR and the corresponding LR formed using an estimate of the SR image is used iteratively to refine the SR estimations. The equation for result refinement is

$$g^{n+1}(p) = g^{n}(p) + \sum_{m} \left((y_k(\mathrm{m}) + \hat{y_k}(\mathrm{m})) \frac{(h_{Mp}^{BP})^2}{c \sum_m h_{Mp}^{BP}} \right) \qquad \text{---3.10}$$

Where g^n is the estimate of the SR image at the nth iteration, y_k is the Kth LR image, $\hat{y_k}$ Is the k^{th} LR image as approximated from g^n, and h^{BP} is a back projection kernel. The algorithm's initial estimate is an up-sampled version of the base or reference LR image, by the factor needed by SR. Following is the sequence of steps for IBP algorithm.

1. Define the matrix G of size of initial estimation and let us consider initial estimation matrix as G.

2. For each LR image compensate for shift and rotation and then use low pass filter as normalize blur filter.
3. Retain only the initial LR pixels locations on HR grid and then subtract from them the respective LR pixels, then apply sharpening filter to estimated HR grid.
4. Thereafter rotate the HR grid by the estimated angle φ in opposite direction and crop it to required size of HR estimate and then shift it by the amount of estimated shift value in the process of registration.
5. Copy the result in matrix G for each LR image. After working on all LR images matrix G carries result contributed by all LR images as a single matrix, and it behaves as gradient matrix because the process of subtraction used before sharpening.
6. Then subtract the scaled gradient from previous estimated HR to obtain the new estimated HR.
7. Calculate the error matrix which is difference of current estimated HR and previous estimated HR. the elements of error matrix are normalized in the range of 0 to 1 and then calculated the cost of normalized error matrix.
8. Again start the computation of gradient for all images with current estimate. Repeat it up to predefined number of iteration or cost of normalized error matrix is less that acceptable values.
9. Finally estimated HR grid is the SR solution.

Algorithm need to initialize with scaling factor λ=0.1 and maximum number of iteration for the iterative gradient method which is considered as 100 and acceptable value of error is less than 10^{-4} using trial and error method. The normalized blur filter and sharpen filter have been considered with the size of 3 x 3 matrix.

The Iterative Back Projection approach for reconstruction is implemented and results for SR have been observed, which are presented in chapter 4. Table 4.9 represents the results in terms of SSI, MSE, SNR, PSNR, entropy and execution time respectively. The graphical comparison is given in the Figure No. 4.22 to 4.27 for SSI, MSE, SNR, PSNR, entropy and execution time parameters respectively. However, inferior convergence rate, sensitivity to the initial choice of image affects the performance of SR IBP.

3.3.5 Projection on Convex Sets (POCS) based SR Reconstruction Algorithm

POCS, is a method to find a point in the intersection of two closed convex sets. It is set theoretic Method where constraint sets limit the feasible solution space of the SR reconstruction. Constraints are defined as convex sets in the vector space containing all possible SR reconstructions. Define the sets that consist of desirable characteristics of the solution, like positivity, smoothness, bounded energy, fidelity to data and so on. The solution space of the problem is estimated by the intersection of the convex constraint sets. POCS is an iterative approach in which for every point in the vector space, identify a point that satisfies all the convex constraint sets. This technique of POCS use in this algorithm to find the value of missing pixels from set of different orientation images. The coefficients of 5x5 blur filter are estimated to help for the implementation of POCS.

Initial estimation of HR grid is contributed by all compensated LR images which is further normalize by filtering. Thereafter iteratively improve the solution by obtaining high frequency information from initial estimation and retaining original HR grid information. Find normalize error between previous and current solution, if it is less than minimum specified (e.g. 10^{-4}) then stop else current solution act as initial estimation up to maximum 50 iterations for better result. Following is the sequence of steps for IBP algorithm.

POCS - reconstruct high resolution image using Projection on Convex Sets to reconstruct SR image algorithm need inputs, those are LR images in cell array, estimated shifts in x and y direction obtained in registration and factor for SR.

1. Up-sample the reference LR by factor of SR in rows and columns, with all added pixels having value zero. Copy this up-sampled version of LR which is Initial estimate of HR.

2. Up-sample one of the remaining LR images by the factor of SR in rows and columns, with all added pixels having value zero.

3. Shift the up-sampled LR images in x and y direction by corresponding estimated shift value.

4. Replace all zero value elements of up sampled reference image with corresponding elements in shifted up sampled LR image.

5. Repeat step 2 to 4 for all LR images to act initial estimation of HR contribution by all LR images.

6. Define blur filter of size 5x5 matrix and filter the initial estimate contribution by all LR images.

7. Modify the pixel value of the matrix which is obtained after the blur filtering by replacing the original HR grid information contributed by all LR images except the pixel those are modified from zero to nonzero value due to process of filtering.

8. Calculate the error matrix which is difference of current estimated HR and previous estimated HR. the elements of error matrix are normalized in the range of 0 to 1 and then calculated the cost of normalized error matrix.

9. Then iteratively refine this solution by blur filtering and retaining original HR grid pixel information contribution by all LR images up to predefined number of iteration or cost of normalized error matrix is less that acceptable values.

10. Finally estimated HR grid is the SR solution.

The POCS based algorithm for reconstruction is implemented and results for SR have been observed, which are presented in chapter 4. Table 4.8 represents the results in terms of SSI, MSE, SNR, PSNR, entropy and execution time respectively. The graphical comparison is given in the plots in Figure No. 4.22 to 4.27 for SSI, MSE, SNR, PSNR, entropy and execution time parameters respectively.

3.3.6 Structure-Adaptive Normalized Convolution (SANC) SR Reconstruction Algorithm

Normalized convolution (NC) is a technique for local signal modeling from projections onto a set of basis functions. NC uses an applicability function to localize the polynomial fit, which is an isotropic, radially decaying function with size

proportional to the scale of analysis, usually employed is a Gaussian function. First-order NC with three bases can model edges, and second-order NC with six bases can further model ridges and blobs but at the expense of increased computation. A complete first-order NC requires nine convolutions and produces three output images: an interpolated image f_I and two directional derivatives f_x, f_y in the x-and y-dimensions.

Robust NC requires the signal certainty to be known in advance. However, in case of Robust NC a robust certainty is assigned to each neighboring and the robust certainty, being a Gaussian function of residual error $f - \hat{f}$, assigns low weights to potential outliers, which effectively exclude them from the analysis.

$$c(s, s_0) = \exp\left(\frac{|f(s) - \hat{f}(s, s_0)|^2}{2\sigma_r^2}\right), \qquad \text{-------- 3.11}$$

Where, $f(s)$ is an intensity measured at position s and $\hat{f}(s, s_0)$ is an estimated intensity at s using an initial polynomial expansion at the center of analysis s_0. The photometric spread σ_r define an acceptable range of the residual error $(f - \hat{f})$. Residual error less than σ_r get a certainty close to one. With this adaptive certainty, NC becomes a weighted least-squares estimator that behaves as a normal least-squares estimator under Gaussian noise and it is robust against outliers, solved by an iterative weighted least-squares minimization. The process is repeated until convergence is observed.

Structure-adaptive normalized convolution has the adaptive applicability function make certain that only samples sharing similar intensity and gradient information are gathered for the local polynomial expansion.

To construct an adaptive kernel at an output pixel, the local image structure around that pixel of interest must be known in advance. We compute an initial estimate of the output intensity I and gradient information $I_x = \partial I/\partial x$ and $I_y = \partial I/\partial y$ using first-order robust NC. Local structure information including orientation of angle φ and anisotropy A is computed from the eigenvectors {u, v} and the corresponding eigenvalues (λ_u , λ_v) of a principal component analysis of the local gradient vectors $\nabla I = [I_x\ I_y]^T$ a.k.a. the gradient structure tensor (GST) method.

$$GST = \overline{\nabla I \nabla I^T} = \begin{bmatrix} \overline{I_x^2} & \overline{I_x I_y} \\ \overline{I_x I_y} & \overline{I_y^2} \end{bmatrix} = \lambda_u u u^T + \lambda_v u u^T \ , \qquad \text{--------- 3.12}$$

Sample density is computed as a sum of sample certainty over an unnormalized Gaussian-weighted neighborhood of scale $\sigma_c(s_0)$, a Gaussian kernel whose middle weight equals one.

$$d(s_0\sigma_c) = \sum exp\left(-\frac{(s-s_0)^2}{2\sigma_c^2(s_0)}\right) c(s-s_0) \quad \text{----- 3.13}$$

We define a local scale $\sigma_c(s_0)$ as the scale at which $d(s_0, \sigma_c)$ is equal to a constant C (C = 3 for first-order NC). Then set to this scale to minimize smoothing in regions with high sample density.

To estimate this local scale, the certainty of each irregular sample is split to its four nearest HR grid points. The accumulation of all grid-stamped sample certainties forms a density image on the HR grid.

Robust Fusion of Irregularly Sampled Data Using Adaptive Normalized Convolution, in this case the local signal is approximated through a projection onto a subspace. The window function of adaptive NC is adapted to local linear structures which leads to more samples of the same modality being gathered for the analysis, to increase signal-to-noise ratio and reduces diffusion across discontinuities. For fusion of irregularly sampled data surface interpolation is used. Apply robust certainty and a structure-adaptive applicability function to the polynomial Facet model and use it for fusion of irregular sampled data. Correct the localization by introducing a Gaussian applicability to the operator, which will put more prominence on fitting the central pixels. Robust signal certainty estimated directly from the intensity difference between the current sample and its neighbors. The guiding parameters for the adaptive applicability function are worked out from gradient information of the input data.

Structure-adaptive applicability function is adaptive applicability function is an anisotropic Gaussian function whose main axis is rotated to align with the local dominant orientation:

$$a(s-s_0) = p(s-s_0)\, exp\left[-\left(\frac{x\cos\emptyset + y\sin\emptyset}{\sigma_u(s_0)}\right)^2 - \left(\frac{-x\sin\emptyset + y\cos\emptyset}{\sigma_v(s_0)}\right)^2\right] \quad \text{--3.14}$$

Where σ_u and σ_v are the directional scales of the anisotropic Gaussian kernel. σ_v is the scale along the elongated orientation and is greater than or equal to σ_u The two

directional scales are adjusted by the local scale σ_c estimated earlier. The local scale σ_c allows the applicability function to shrink or grow based on how population density of the neighborhood.

The tuning parameter $\alpha > 0$ sets an upper-bound on the eccentricity of the applicability function. We use $\alpha = 0.5$ for a maximum eccentricity of 3 when the anisotropy A = 1.

Computational complexities is linear with reference to the number of input samples. Robust NC with an isotropic applicability function runs much faster than adaptive NC. Therefore Adaptive NC is performed as a second pass after a robust NC. it is selectively applied to highly anisotropic pixels (pixels with anisotropy A> 0.5). whose results improve significantly from the first pass.

For super-resolution fusion of low-resolution image sequences the Robust as well as Adaptive NC is applied to the motion-corrected LR samples. Deconvolution finally reduces the blur and noise caused by optics and sensor integration.

Super-resolution fusion approach

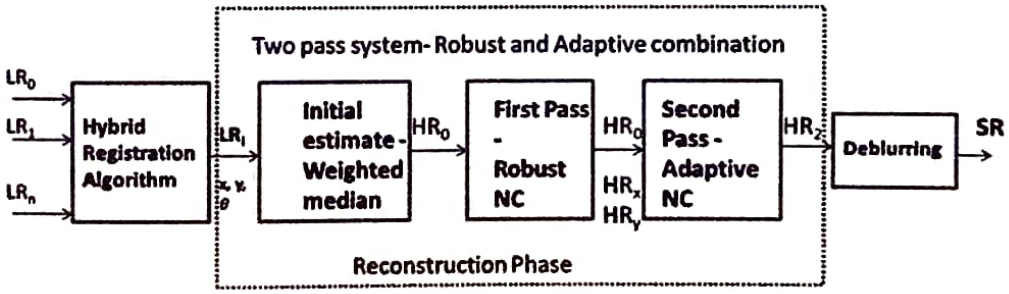

Figure No. 3.1: Robust Adaptive Normalized Convolution Super-Resolution Process

As shown in Figure No. 3.1 the fusion block is divided into three sub steps, first estimate HR_0 is constructed by a locally weighted median operation. HR_0 is then used as an initial estimate for a first-order robust NC, which produces a better estimate of the HR image HR_1 and two derivatives HR_x and HR_y in x-and y-directions. The derivatives are then used to construct anisotropic applicability functions for the second phase of

convolution by adaptive NC. Implementation details of each fusion sub step are already conversed.

The algorithm perform two iterations of robust NC, followed by one iteration of adaptive NC for highly oriented pixels. As the fill factor is low, many details previously aliased in the LR images are now visible in the factor times HR image without the need of deconvolution. Following is the sequence of steps for SANC algorithm.

For each LR image perform following set of operation

I. Each LR image is up sampled to HR grid size and compensated for estimated motion parameters. Initially compensate for the rotation of LR image by estimated angle φ.
II. In next phase compensate for estimated shift Δx and Δy by shifting the image by same distance in reverse direction.
III. Now put pixels from up sampled and compensated LR image of respective co-ordinates to HR estimation grid.
IV. Collect result of all LR images and put in an array of HR grid.
V. Then apply the normalized convolution algorithm.

Normalized convolution algorithm steps:

1. Initialization by setting all certainties, parameters for the applicability function-- alpha, beta and max radius and Radius of the filters used in the convolution. Certainty optimization is for noise robustness and optional noise cancelation.
2. For all rows indices of estimated HR grid elements of LR consider coordinates within the radius of R_{max} and their values and certainty.
3. Find their dx and dy distances from center.
4. Find Euclidian distance from (i,j) to every other point of interest (x,y)
5. Apply applicability function using alpha, beta and R_{max} with infinite values truncated to 1.
6. Define basis functions matrix of order 6 x 6 second orders Normalize Convolution consist of

   First column—all elements 1

Second column—x distance of coordinates from centre

Third column-- y distance of coordinates from centre

Forth column—dx^2

*Fifth column—x * y*

Sixth column—dy^2

7. Perform the matrix multiplication diag(c)* diag(a) which is an N × N diagonal matrix constructed from an element-by-element product of the signal certainty c and the sampled applicability a.
8. Then optimize the Moore-Penrose pseudo inverse of matrix. Which is used to solve a system of linear equations when does not have a unique solution or many solutions.
9. Invert singular values in the result only if they are greater than 10^{-5} for entire matrix.
10. This is the end of first pass of HR Reconstruction. Call the second pass of adaptive normalized convolution with result of first pass as initial estimates and certainties.

Structure-Adaptive Normalized Convolution steps:

It finds basis functions matrix of order 6 x 6 second order Normalize Convolution. This final processing is done as a second pass, only on pixels that have a high anisotropy. Second pass, which will sharpen all edges.

1. Define mask for derivative in x and y directions.
2. Using Gaussian filter 7x 7 to normalize the image.
3. Find I_x, I_y, I_x^2, I_y^2, $I_x * I_y$, terms of GST equation.
4. Create the density image in which the certainty of each irregular sample is split to its four nearest HR grid points.
5. Find Scale-space responses using Gaussian of sigma 2^1.
6. Reconstruction process redefines a new R_{max} so that the applicability function will be oriented for all lines of the HR image.
7. Consider rows, columns, values of pixels and certainty in local region of radius R_{max}. For all columns of the HR image, find GST then adaptive applicability function.

8. The second pass is applied where the anisotropy is high (>0.5). Use tuning parameter to set an upper-bound on the eccentricity of the applicability function.

The Structure-adaptive Normalized Convolution (SANC) method for reconstruction is implemented and results for SR have been observed, which are presented in chapter 4. Table 4.11 represents the results in terms of SSI, MSE, SNR, PSNR, entropy and execution time respectively. The graphical comparison is given in the plots in Figure No. 4.22 to 4.27 for SSI, MSE, SNR, PSNR, entropy and execution time parameters respectively. Along with the objective, subjective results are also presented graphically in the Figure No. 4.38 and 4.39 of user study report for comparison with other techniques and similarity with original respectively. Improved results are observed at the cost of execution time which is system dependent.

3.4 Reconstruction of SR Algorithm using PSO with Multiple LR Images

The proposed system has Particle Swarm Optimization (PSO) as an integral part. It applies for each split image. In PSO the solutions are represented as chromosomes. The chromosomes, it is a string of genes that represents a solution, are evaluated for fitness values and they are ranked from best to worst based on fitness value. The process is accomplished by repeating applications of three genetic operators: selection, crossover, and mutation. First, the better offspring are selected to become parents to produce new chromosomes. Each particle maintains the P best and Swarm maintains its global best value i.e. G best value.

In this algorithm it has completely connected swarm, meaning that all the particles share information, any particle knows what is the best position ever visited by any particle in the swarm. Each particle has a position (1) and a velocity (2) which are calculated as follows:

$$x_{i,d}(it+1) = x_{i,d}(it) + v_{i,d}(it+1) \quad -- \quad 3.15$$

$$v_{i,d}(it+1) = xv_{i,d}(it)\ (previous\ update\ velocity)$$

$$(cognitive) \quad + C_1 * Rnd(0,1) * [pb_{i,d}(it)x_{i,d}(it)]$$

$$+C_2 * Rnd(0,1) * [gb_d(it)x_{i,d}(it)] \ (social) \quad ---3.16$$

i :- Is particle's index- used as a particle identifier.

d :- Is dimension being considered, each particle has a position and a velocity for each dimension

it : - iteration number as algorithm is iterative.

$X_{i,d}$:- position of the particle i in dimensions d

$v_{i,d}$:- velocity of the particle i in dimensions d

C_1 – acceleration constant for cognitive component

C_2 – acceleration constant for social component

Rnd: – stochastic component of algorithm, a random value

(between 0 to 1)

$Pb_{i,d}$:- location in the dimension d with the best fitness of all the visited locations in that dimension of particle i

Overview of Sequence of operations performed

1. Collect LR Images

2. Apply Segmentation techniques for all LR images.

3. Apply KNN

4. Find Fitness Value for each pixel and sort that fitness value for finding best fitness value. The best fitness value is known as solution.

5. If it is the best value the particle has achieved so far, the particle stores that value as 'personal best'(PB).

6. The best fitness value achieved by any particle during current iteration is stored as 'global best'(GB), by using Global Best Particles.

7. The pixel from different LR has different global best value, pixel with highest GB will be placed on the HR grid.

8. Apply Bicubic Interpolation for locations not having pixel value assigned.

9. Apply Bilateral Filter to remove noise.

Experimental results show that this approach can effectively obtain high resolution image and is summarized in five steps.

I. For each patch x_t^q in image X_t do.

II. Find the set N_q of K nearest neighbors in X_s.

III. Calculate the reconstruction weights of the neighbors for minimizing the error of reconstructing x_t^q

$$\varepsilon^q = \left\| x_t^q \sum_{x_s^p N^q} w_{qp} x_s^p \right\|^2 \qquad 3.17$$

w_{qp} is the weight of x_s^p with following constrains

$$\sum_{x_s^p N^q} w_{qp} = 1 \; and \; w_{qp} = 0 \; for \; any \; x_s^p \notin N_q \qquad 3.18$$

IV. Compute the high-resolution embedding y_t^q using the appropriate high-resolution features of the K nearest neighbors available from different LR images with higher reconstruction weights.

$$y_t^q \sum_{x_s^p \in N_q} w_{qp} y_s^p \quad t = I, \ldots, n \qquad 3.19$$

Architecture of Proposed System

Architecture of proposed system is as shown in Figure No. 3.2. PSO is applied for Reconstruction Phase of Image. PSO used to optimize three parameter are explored are Number of K nearest neighbors for neighbor embedding, Patch size and Degree of overlap between adjacent patches.

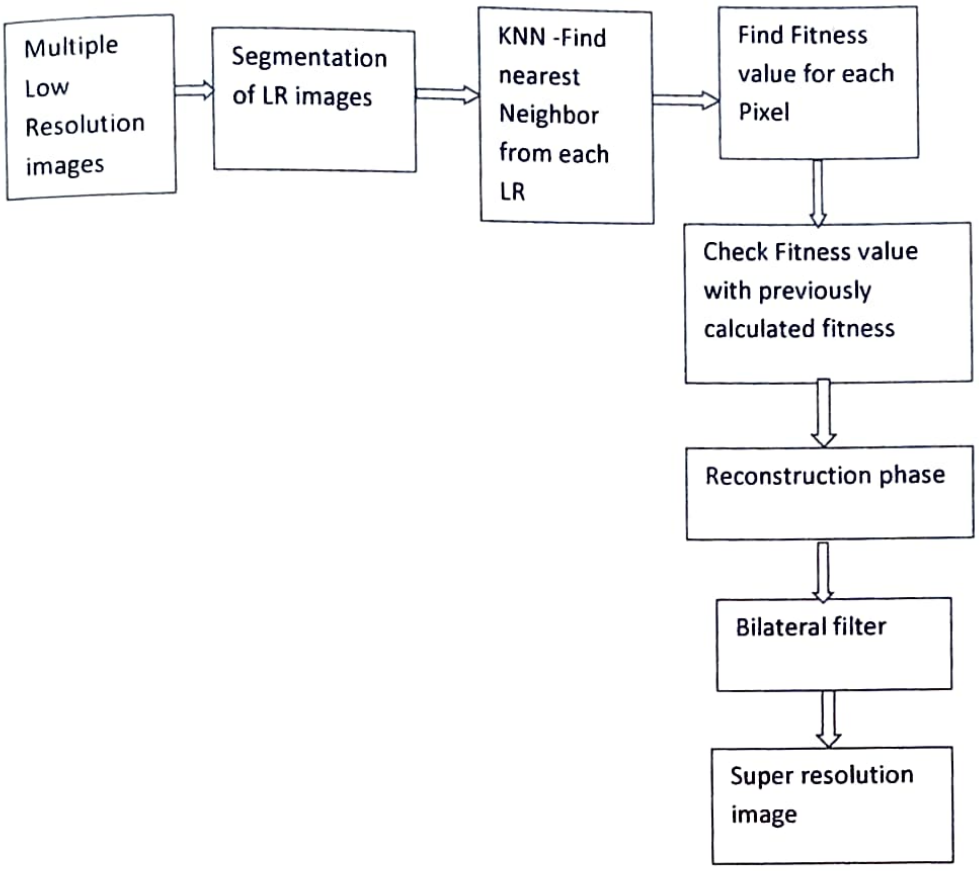

Figure No. 3.2 Architecture of Proposed System

Following is sequence of steps used for reconstruction of SR using PSO with multiple LR images algorithm.

Carry out following step 1 to 9 for each LR image

1. Create initial up sampled image by using bicubic interpolation
2. Generate initial population with three parameters for each particle includes patch size, overlap and K nearest neighbor.
3. while (all pixel not cover)
4. For each Particle i=1 to P do
5. Evaluate PSNR as a fitness value through neighbor
6. End for

7. If the fitness value is better than the best fitness value (P Best) in history
8. Set current value as new P Best
9. End if
10. Using result of all LR images Update global best by choosing the particle with the best fitness value of all the particles as the G Best
11. End while
12. Reconstruct and Display HR using GB.

The block Diagram of system is shown in Figure No. 3.3 gives the details of the system components.

The results of the implementation of technique have been observed, which are presented in chapter 4. Table 4.21, and Figure No. 4.47, 4.48 and 4.49 represents the results in terms of MSE, SNR and PSNR in decibel. The PSNR as well as subjective quality is also improved by using reconstruction algorithm using PSO with multiple LR images.

Chapter 4

Results

The multiple image super resolution image reconstruction algorithms are developed and implemented in MATLAB R2014a and R2015a. Sample results are given in this chapter. The proposed algorithm is tested over the range of natural standard images, natural camera captured images and synthetic images.

This chapter presents the results of SR reconstruction techniques using multiple LR images. This chapter is divided into three parts to present the results of various SR reconstruction approaches.

First part will discuss the results of registration techniques used for SR reconstruction using multiple LR images and their performance analysis. The techniques presented in the thesis has been tested with both real and synthetic data. We have used standard images of same scene but with different resolutions. These images are down sampled, shifted in x and y direction and/or rotated through small angle so as to obtain the number of LR images with different orientation. Decimation factor used to obtain LR images is four. Each LR image will have different angle of rotation and x and y shifts, which are used for testing of registration algorithms. With known shift and rotation of LR images registration algorithms are verified and results are compared with actual registration parameters available.

In second part, multiple LR images are used for testing of reconstruction techniques. The quality measures used for reconstruction techniques are structural similarity index (SSI), mean square error (MSE), Signal to noise ratio (SNR), Peak signal to noise ratio (PSNR), Entropy and execution time (T) of algorithm which is important factor for real time processing.

In third part, the reconstruction using PSO for multiple LR images has been carried out and results are presented where PSNR is used as quality measure.

Also the techniques can be better tested if set of varying frequency and varying resolution images are used for testing. For super resolution imaging the real reference high resolution image does not exist. We have captured images of varying resolutions of different scenes. It is difficult to capture the real image with different orientation and hence to test the algorithms the real scenes has been captured by varying the resolution only. The algorithm is tested over set of these images. The low resolution captured Images is given as input LR images and the real captured high resolution image is used as real reference image for computation of PSNR. For standard images the decimated images are used as input LR images and the original undecimated image is used as HR reference image.

Set of images used include standard, natural and synthetic. Input low resolution images and reconstruct high resolution images using super resolution techniques based on multiple LR images.

4.1 Registration Algorithms Results

The three approaches are selected for registration process, these are – Vandewalle's frequency domain registration, Marcel frequency domain registration and Hybrid approach using L-P FFT respectively. The registration parameters are restricted for x and y linear translational motion in horizontal and vertical direction and rotation of entire image plane only.

To verify the accuracy of the above registration algorithms it is needed to develop the set of LR images with known angle of rotation and shift along horizontal and vertical direction with subpixel movement. The set of images has been generated with known shift and angular rotation are called as Test1, Test2, Test3, Test4 and Test5. The registration algorithms are applied and rotation and shift in x and y direction has been calculated. Then difference of calculated angle of rotation and shift parameters with respect to known value of angle and shift has been noted and called as error in registration. The result of algorithms - Vandewalle's registration, Marcel registration, and Hybrid approach are presented.

4.1.1 Results of Vandewalle's Frequency Domain Registration Algorithm

The comparison of estimated value of angle of rotation in radians and translation motion in terms of x and y shift with the known value for LR images (LR1, LR2, LR3 and LR4) for test 1 to test 5 and error of estimation is shown in Table 4.1 and in Figure No. 4.1 and 4.2 for rotation, x shift and y shift respectively.

Table 4.1- Comparison for Vandewalle Frequency Domain Registration Algorithm for LR images with known Rotation and Shift Variation

Test case	images	Known angle Θ , x and y shift			Estimated angle Θ , x and y shift			Error in Estimation		
		Θ	x	y	Θ	x	y	Δ Θ	Δx	Δy
Test 1	LR1	0	0	0	0	0	0			
	LR2	0	-0.0015	-0.0015	-0.1	-0.01094	-0.01696	0.1	0.00944	0.01546
	LR3	0	0.001	0.002	-0.1	-0.009256	-0.01149	0.1	0.010256	0.01349
	LR4	0	-0.005	0.003	-0.1	-0.013885	-0.01158	0.1	0.008885	0.014581
Test 2	LR1	0	0	0	0	0	0			
	LR2	0	0.0001	0.0002	0	8.249E-05	-8.7E-05	0	1.75E-05	0.000287
	LR3	0	0.0003	0.0004	0	-0.000569	0.000265	0	0.000869	0.000135
	LR4	0	0.0005	0.0006	-0.1	0.0165477	-0.0064	0.1	-0.01605	0.007
Test 3	LR1	0	0	0	0	0	0			
	LR2	-0.0015	-0.0015	-0.0025	0	-0.000537	-0.00185	-0.0015	-0.00096	-0.00065
	LR3	-0.0025	-0.0025	0.003	0	-0.003513	0.005016	-0.0025	0.001013	-0.00202
	LR4	0.0025	0.0015	0.0015	-0.1	-0.020447	-0.00078	0.1025	0.021947	0.002284
Test 4	LR1	0	0	0	0	0	0			
	LR2	-0.002	-0.001	-0.002	0	-0.000471	-0.00383	-0.002	-0.00053	0.001834
	LR3	-0.006	0.002	0.001	-0.1	-0.036304	0.014249	0.094	0.038304	-0.01325
	LR4	-0.006	-0.002	0.002	-0.1	-0.037779	0.015401	0.094	0.035779	-0.0134
Test 5	LR1	0	0	0	0	0	0			
	LR2	0.0015	0.0012	0.0016	0	0.0012568	0.002075	0.0015	-5.7E-05	-0.00047
	LR3	-0.0015	-0.0018	0.0022	0	-0.001799	0.001557	-0.0015	-8.6E-07	0.000643
	LR4	-0.002	-0.0024	-0.0008	0	-0.003034	-0.00109	-0.002	0.000634	0.000292

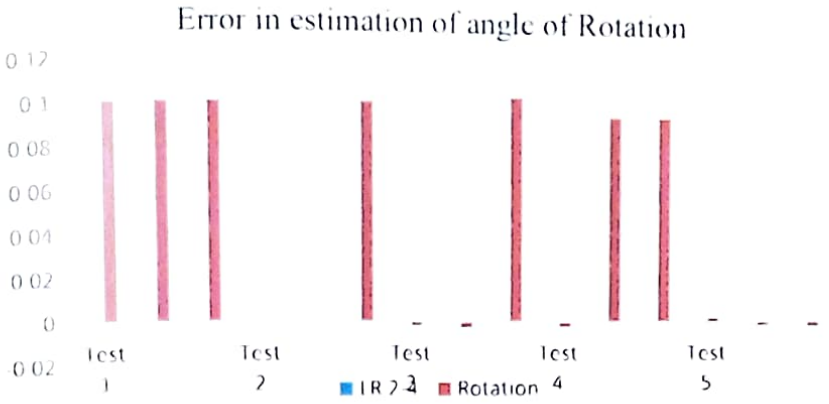

Figure No. 4.1 Plot of error in estimation of angle of rotation

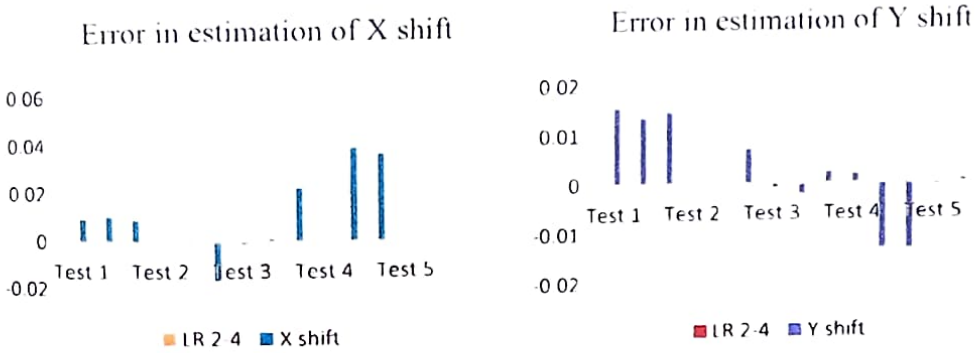

Figure No. 4.2 Plot of error in estimation of x and y shift

From observations of Table 4.1 and error Plot from Figure No. 4.1 and 4.2 it is found that the registration algorithm estimate the x and y shift with subpixel accuracy and results are more improved when only translational motion is present between the LR images. When rotational as well as translational motion is given the rotation estimation error is large in most of the cases. Due to error in rotation estimation the x and y shift is estimation error also increases.

4.1.2 Results of Marcel Frequency Domain Registration Algorithm

The result of estimated value of translation motion in terms of x and y shift are compared with the known value for LR images (LR1, LR2, LR3 and LR4) for test 1 to test 5 and error of estimation is shown in Table 4.2 and in Figure No. 4.3 for x shift and y shift respectively.

Table 4.2- Comparison for Marcel Frequency Domain Registration Algorithm of LR Images with Known Rotation and Shift Variation

Test case	images	Known angle Θ , x and y shift			Estimated angle Θ , x and y shift		Error in Estimation	
		Θ	x	y	x	y	Δx	Δy
Test 1	LR1	0	0	0	0	0		
	LR2	0	-0.0015	-0.0015	-0.2	-0.2	0.19850	0.19850
	LR3	0	0.001	0.002	0.3	0.5	-0.29900	-0.49800
	LR4	0	-0.005	0.003	-0.8	0.6	0.79500	-0.59700
Test 2	LR1	0	0	0	0	0		
	LR2	0	0.0001	0.0002	0.2	0.2	-0.19990	-0.19980
	LR3	0	0.0003	0.0004	0.4	5.68	-0.39970	-5.67960
	LR4	0	0.0005	0.0006	2.365	0.6	-2.36450	-0.59940
Test 3	LR1	0	0	0	0	0		
	LR2	-0.0015	-0.0015	-0.0025	-0.3	-0.4	0.29850	0.39750
	LR3	-0.0025	-0.0025	0.003	-0.3	0.5	0.29750	-0.49700
	LR4	0.0025	0.0015	0.0015	0.7	0.3	-0.69850	-0.29850
Test 4	LR1	0	0	0	0	0		
	LR2	-0.002	-0.001	-0.002	-0.2	0.3	0.19900	-0.30200
	LR3	-0.006	0.002	0.001	0.8	0.6	-0.79800	-0.59900
	LR4	-0.006	-0.002	0.002	-0.4	0.5	0.39800	-0.49800
Test 5	LR1	0	0	0	0	0		
	LR2	0.0015	0.0012	0.0016	0.5	0.3	-0.49880	-0.29840
	LR3	-0.0015	-0.0018	0.0022	-0.4	0.6	0.39820	-0.59780
	LR4	-0.002	-0.0024	-0.0008	-0.2	-0.3	0.19760	0.29920

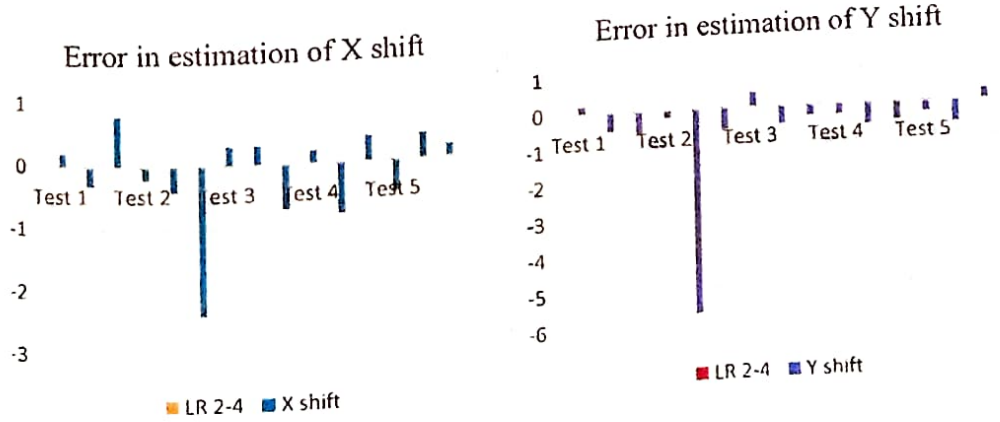

Figure No. 4.3 Plot of error in estimation of x and y shift

From the Table 4.2 it is observed that the rotation is not estimated by algorithm. Figure No. 4.3 revels that the accuracy of estimation of the shift in x and y direction is poor. Due to large error for estimation of shift in x and shift in y direction this approach is not suitable for registration step of super resolution, as it place the pixel at a location multiple pixel away from actual position.

4.1.3 Results of Hybrid Approach using LP-FFT Registration Algorithm

The comparative results of estimated value of angle of rotation in radians and translation motion in terms of x and y shift with the known value for LR images (LR1, LR2, LR3 and LR4) for test 1 to test 5 and error of estimation is shown in Table 4.3 and in Figure No. 4.4 and 4.5 for rotation, x shift and y shift respectively.

Table 4.3 Comparison for Hybrid Approach using L-P FFT Registration Algorithm for LR Images with Known Rotation and Shift Variation

Test case	images	Known angle Θ , x and y shift			Estimated angle Θ , x and y shift			Error in Estimation		
		Θ	x	y	Θ	x	y	Δ Θ	Δx	Δy
Test 1	LR1	0	0	0	0	0	0			
	LR2	0	-0.0015	-0.0015	-8.48E-04	-0.001549335	-0.002316366	0.00085	0.00005	0.00082
	LR3	0	0.001	0.002	-0.00011199	0.000889974	0.001231082	0.00011	0.00011	0.00077
	LR4	0	-0.005	0.003	-0.000696299	-0.005043927	0.001729568	0.00070	0.00004	0.00127
Test 2	LR1	0	0	0	0	0	0			
	LR2	0	0.0001	0.0002	-1.81E-04	0.000156916	0.000260225	0.00018	-0.00006	-0.00006
	LR3	0	0.0003	0.0004	-5.46E-05	0.000234299	0.000357176	0.00005	0.00007	0.00004
	LR4	0	0.0005	0.0006	4.21E-05	0.00048472	0.000565969	-0.00004	0.00002	0.00003
Test 3	LR1	0	0	0	0	0	0			
	LR2	-0.0015	-0.0015	-0.0025	-0.000750086	-0.001012934	-0.002073018	-0.00075	-0.00049	-0.00043
	LR3	-0.0025	-0.0025	0.003	-0.002237845	-0.002218209	0.003116771	-0.00026	-0.00028	-0.00012
	LR4	0.0025	0.0015	0.0015	0.001398531	0.001873117	0.001708446	0.00110	-0.00037	-0.00021
Test 4	LR1	0	0	0	0	0	0			
	LR2	-0.002	-0.001	-0.002	-0.001187579	-0.000485146	-0.002963312	-0.00081	-0.00051	0.00096
	LR3	-0.006	0.002	0.001	-0.003700714	0.00303332	0.000694135	-0.00230	-0.00103	0.00031
	LR4	-0.006	-0.002	0.002	-0.004240272	-0.001322711	0.001518439	-0.00176	-0.00068	0.00048
Test 5	LR1	0	0	0	0	0	0			
	LR2	0.0015	0.0012	0.0016	0.001241442	0.001115511	0.001541289	0.00026	0.00008	0.00006
	LR3	-0.0015	-0.0018	0.0022	-0.001509832	-0.002143113	0.002047351	0.00001	0.00034	0.00015
	LR4	-0.002	-0.0024	-0.0008	-0.001848232	-0.002819736	-0.000801259	-0.00015	0.00042	0.00000

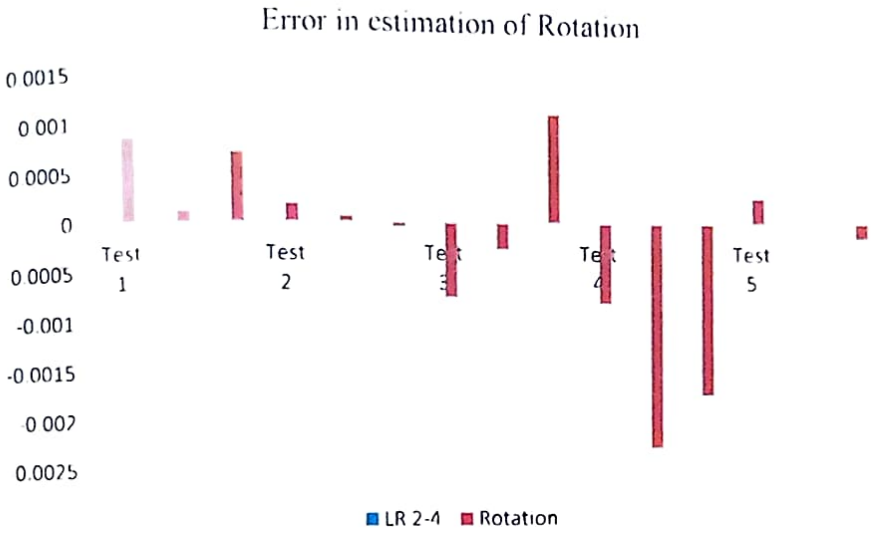

Figure No. 4.4 Plot of error in estimation of angle of rotation

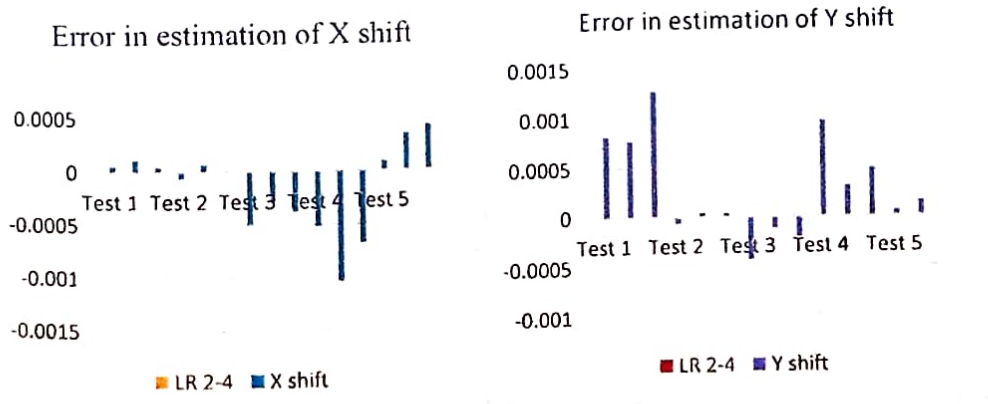

Figure No. 4.5 Plot of error in estimation of x and y shift

From observations of Table 4.3 and error Plot from Figure No. 4.4 and 4.5 it is found that the registration algorithm estimate the x and y shift with subpixel accuracy and results are improved than Vandewalle's frequency domain and Marcel frequency domain registration algorithms.

This hybrid approach exploits the features frequency and spatial domain processing. Accuracy of rotation estimation is good, which allow us to detect the

shift more accurately. So pixel motion parameters are estimated with error less that the inter pixel distance which will place the pixel with subpixel movement more accurately on HR grid during reconstruction. Therefore this method is recommended for registration phase of SR in this research work.

4.1.4 Comparative Results of Registration Methods

The registration algorithms (Vandewalle's frequency domain registration, Marcel frequency domain registration and Hybrid approach using L-P FFT) are tested for the same set of images with similar orientations and their comparative results are presented. Since the results of Marcel frequency domain strategy are very poor and not comparable to other algorithms and hence these are not shown in a comparison. Only the results of Vandewalle's frequency domain registration, and Hybrid approach using L-P FFT are presented here. The results of these two are compared in Table 4.4 and 4.5 for known angle of rotation and shift in x and y direction for selection of best suitable approach. These results are also presented graphically in the Figure No. 4.6, 4.7, 4.8 and 4.9 for angle of rotation and shift in x and y direction respectively.

Table 4.4 Comparison for Vandewalle's Frequency Domain Registration and Hybrid Approach using L-P FFT Registration Algorithm for LR Images with known rotation and shift variation

Test case		Known angle Θ , x and y shift			Estimated angle Θ , x and y shift by Vandewalle's frequency domain registration			Estimated angle Θ , x and y shift by Hybrid approach using L-P FFT		
	Images	Θ	Θ	x	Θ	x	Θ	x	Δx	Δy
Test 1 – IM4	LR1	0	0	0	0	0	0	0	0	0
	LR2	-0.0015	-0.0015	-0.0025	0	-0.000537	-0.001849	-0.00075	-0.001013	-0.002073
	LR3	-0.0025	-0.0025	0.003	0	-0.003513	0.0050158	-0.00224	-0.002218	0.0031168
	LR4	0.0025	0.0015	0.0015	-0.1	-0.020447	-0.0007841	0.001399	0.0018731	0.0017084
Test 2- IM5	LR1	0	0	0	0	0	0	0	0	0
	LR2	-0.002	-0.001	-0.002	0	-0.00047	-0.00383	-0.00119	-0.00049	-0.00296
	LR3	-0.006	0.002	0.001	-0.1	-0.0363	0.014249	-0.0037	0.003033	0.000694
	LR4	-0.006	-0.002	0.002	-0.1	-0.03778	0.015401	-0.00424	-0.00132	0.001518
Test 3- IM7	LR1	0	0	0	0	0	0	0	0	0
	LR2	0.0015	0.0012	0.0016	0	0.001257	0.002075	0.001241	0.001116	0.001541
	LR3	-0.0015	-0.0018	0.0022	0	-0.0018	0.001557	-0.00151	-0.00214	0.002047
	LR4	-0.002	-0.0024	-0.0008	0	-0.00303	-0.00109	-0.00185	-0.00282	-0.0008

Table 4.5 Comparison for Vandewalle's Frequency Domain Registration and Hybrid Approach using L-P FFT Registration Algorithm for LR Images with known rotation only.

Test case		Known angle Θ , x and y shift			Estimated angle Θ , x and y shift by Vandewalle's frequency domain registration			Estimated angle Θ , x and y shift by Hybrid approach using L-P FFT		
	Images	Θ	x	y	Θ	x	y	Θ	x	y
Test 1 -IM4	LR1	0	0	0	0	0	0			
	LR2	0.004	0	0	-0.1	-0.021022	-0.004331	0.002556	-3.67E-04	-1.31E-04
	LR3	0.005	0	0	-0.1	-0.021038	-0.005602	0.003405	-4.60E-04	-1.64E-04
	LR4	0.003	0	0	-0.1	-0.020891	-0.00393	0.002191	-1.63E-04	-2.37E-04
Test 2- IM5	LR1	0	0	0	0	0	0			
	LR2	-0.002	0	0	0	0.00059	-0.00025	-0.00098	0.000356	-0.00019
	LR3	-0.003	0	0	-0.1	-0.0379	0.011701	-0.00177	0.000635	-0.00031
	LR4	-0.004	0	0	-0.1	-0.03742	0.01185	-0.00213	0.000821	-0.00031
Test 3- IM7	LR1	0	0	0	0	0	0			
	LR2	0.0001	0	0	0	0.000267	-6.35E-05	8.06E-05	2.33E-05	9 74E-06
	LR3	0.0002	0	0	0	0.00036	-0.0002	0.000148	2.61E-05	-1.03E-05
	LR4	0.0003	0	0	0	0.000312	-0.00025	0.000256	2.08E-05	1.98E-05

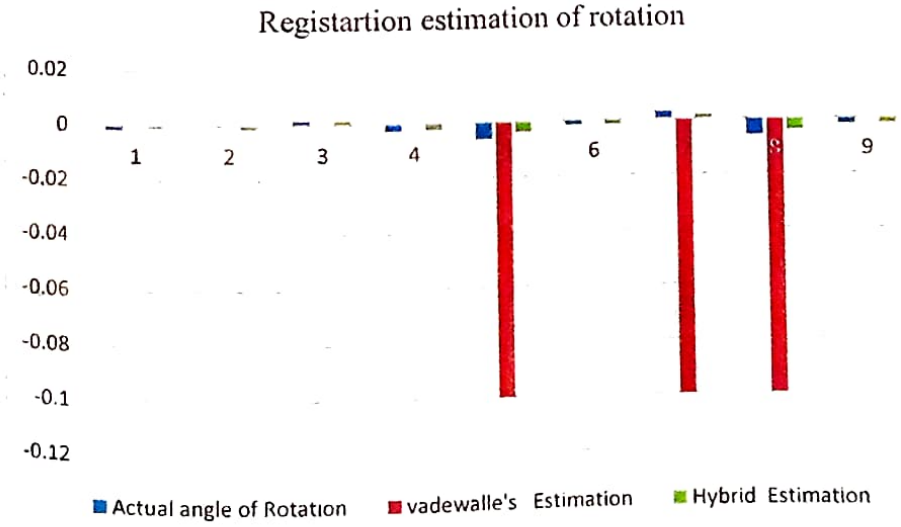

Figure No. 4.6 Comparison of estimation of angle of rotation for LR images with known rotation and shift variation

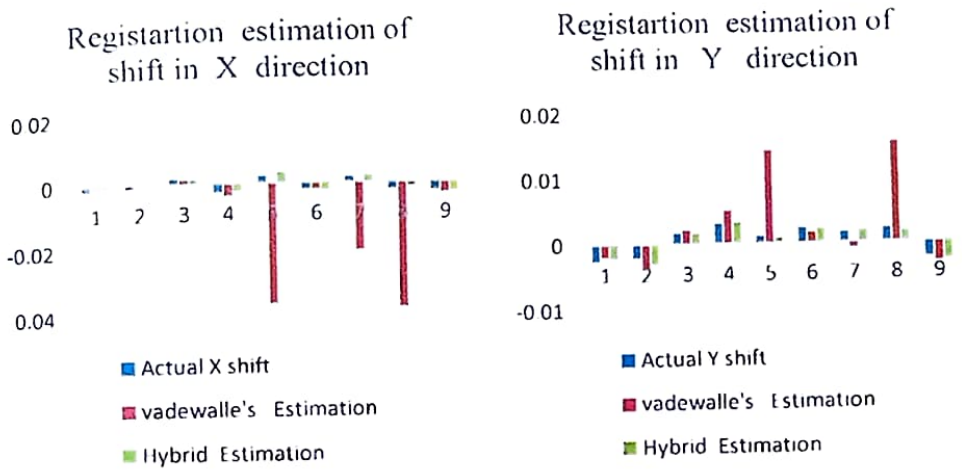

Figure No. 4.7 Comparison of estimation of shift in X and Y direction for LR images with known rotation and shift variation

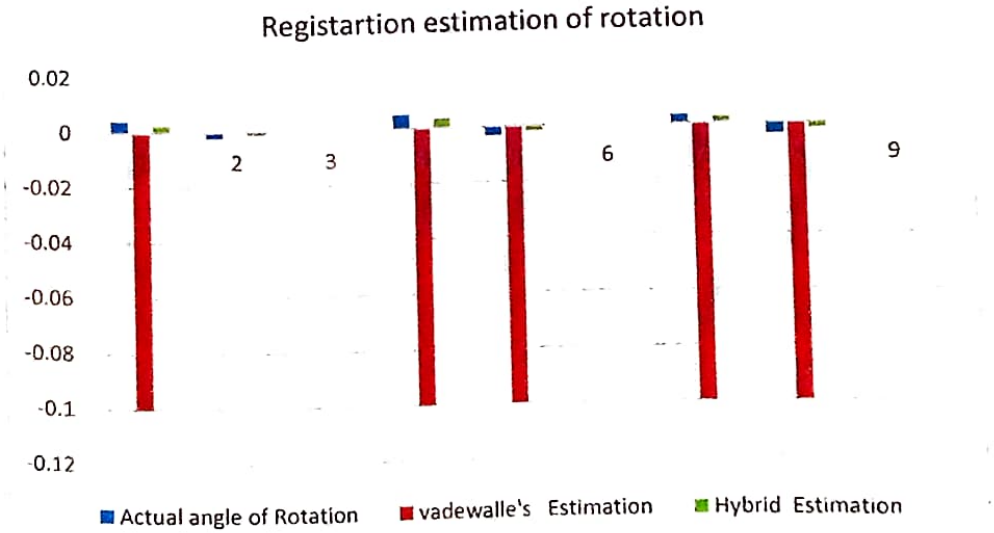

Figure No. 4.8 Comparison of estimation of angle of rotation for LR images with known rotation only (without shift)

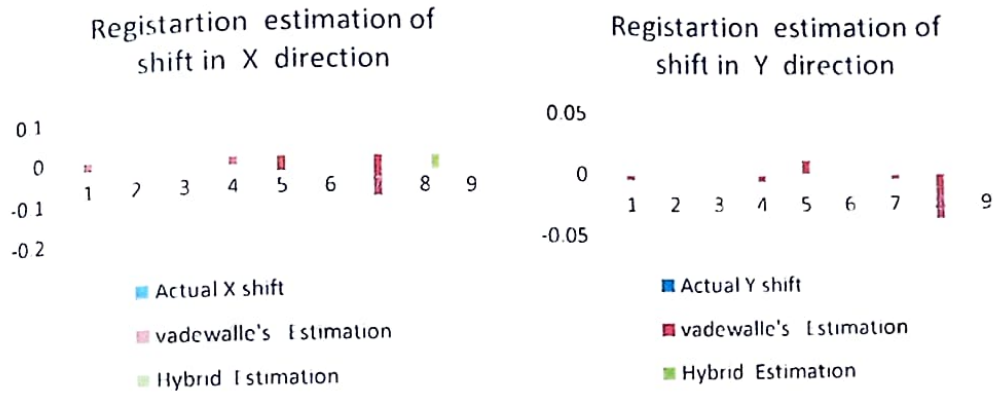

Figure No. 4.9 Comparison of estimation of shift in X and Y direction for LR images with known rotation only (without shift)

Vandewalle approach and hybrid method these two algorithms provide accurate shift and rotation of LR images in terms of subpixel shift. Performance of hybrid approach using L-P FFT is found better than frequency domain Vandewalle's planer motion estimation.

Finally from the results it is concluded that Vandewalle's frequency domain and Hybrid approach using L-P FFT is better. The average percentage error in determination of registration parameter in hybrid approach using L-P FFT method is very small average value 25% to 35% for rotation detection which result into registration of pixels at the right position between two pixels of LR images. The error is further reduces to average value 1% to 5% in determination of x and y subpixel movement which is better than other methods. These small errors may place the pixel at the correct position on a regular high resolution grid for super resolution. From the graphs it is observed that the estimation of Vandewalle's approach is suddenly having large errors for LR images with small details which makes it unsuitable. But Hybrid approach using L-P FFT technique always provide the more accurate value, without sudden large variations.

4.2 Reconstruction Algorithms Based on Multiple LR Images

The performances of six reconstruction algorithms are verified and presented using various sets of LR images. Sample results are presented here. The algorithm performance is analyzed and compared using objective and subjective approach.

The quality of reconstruction is measured using the parameters such as - Structural Similarity Index (SSI), Mean Square Error (MSE), Signal To Noise Ratio (SNR), Peak Signal To Noise Ratio (PSNR), Entropy and Execution Time (T).The Structure-adaptive Normalized Convolution (SANC) approach results are observed to be better than others. Hence only the results of SANC are compared with other algorithms and subjective criteria are used for this algorithm only to measure the performance.

4.2.1 Robust Super Resolution Reconstruction Algorithm: This algorithm is tested for large number of cases with variety of images. The results are shown in the Table 4.6, where measuring parameters used are SSI, MSE, SNR, PSNR, Entropy, Execution time.

Table 4.6- Result of Reconstruction using Robust SR Algorithm

Image	SSI	MSE	SNR	PSNR	Entropy	Execution Time (sec)
Castle	0.999185	554.567424	7.155625	20.691260	6.485585	2.031039
Huts	0.989761	4854.275829	2.935269	11.269559	6.469064	3.620634
building	0.997025	969.343164	6.431848	18.266028	7.142442	1.559287
Pot	0.998923	121.438086	10.23252	26.353161	6.502382	1.207651
Pheasant	0.998624	215.558566	6.847835	24.795151	6.014875	1.510896
Pepper	0.996397	838.952665	6.181924	18.893429	7.132976	1.542026
Aeroplane	0.998023	393.714497	6.499815	22.17899	5.91146	1.548439
starfish	0.996839	782.834052	6.101643	19.194107	7.088275	1.590389
Zebra	0.996404	1413.659931	4.736051	16.627354	6.573833	1.829953

From the result it is found that the algorithm's execution time is small, the SNR and PSNR are in the range of 2.93 to 10.23 and 11.26 dB to 24.79 dB respectively, and ringing artifacts are observed at the edges.

Figure No. 4.10 and Figure No. 4.11 show the result of robust SR reconstruction algorithm in the form of images. It includes high resolution original image, LR images with different orientation with angle θ, shift x and shift y and the SR image obtained after reconstruction. Here the high resolution image as shown in Figure No. 4.10 has resolution of 512x512 and LR images have resolution of 128x128. Here the high resolution image as shown in Figure No. 4.11 has resolution of 320x480 and LR images have resolution of 80x120.

High resolution Original Image

LR1 image (angle θ=0, shift x=0, shift y=0)

LR2 image(θ=0.0025,shift x=0.025,shift y=-0.004)

LR3 image(θ=-0.012, shift x=-0.0015,shift y0.003)

LR3 image(θ=-0.0045,shiftx=-0.002,shifty=-0.025)

SR image obtained after reconstruction

Figure No. 4.10 :Result of image 'Castle' using Robust SR Algorithm

High resolution Original Image

LR1 image (angle θ=0, shift x=0, shift y=0)

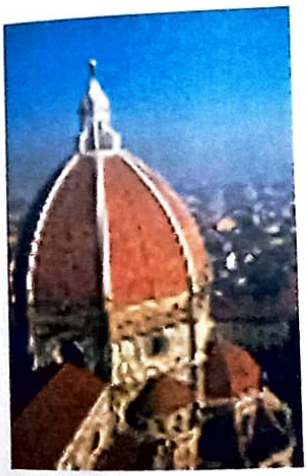

LR2 image(θ=0.003, shift x=0.001,shift y=-0.002)

LR3 image(θ=-0.002, shift x=0.005,shift y=0.03)

LR4 image(θ=0.001, shift x=-0.02,shift y=-0.015)

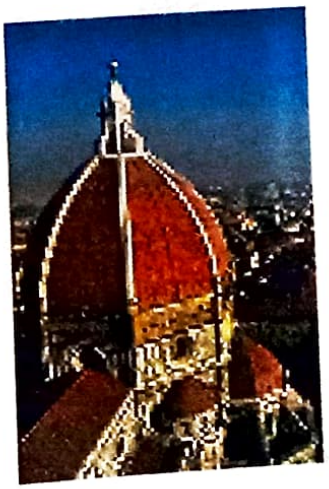

SR image obtained after reconstruction

Figure No. 4.11 :Result of image 'building' using Robust SR Algorithm

4.2.2 Popoulis-Gerchberg (PG) SR Reconstruction Algorithm: This algorithm is tested for large number of cases with variety of images. The results are shown in the Table 4.7, where measuring parameters used are SSI, MSE, SNR, PSNR, Entropy, Execution time.

Table 4.7- Result of Reconstruction using Popoulis-Gerchberg (PG) Algorithm

Image	SSI	MSE	SNR	PSNR	Entropy	Execution Time (sec)
Castle	0.999484	121.990364	10.443769	27.267548	6.442303	3.170428
Huts	0.994863	639.609294	7.336318	20.071656	6.681323	1.860928
building	0.996875	760.704286	6.958157	19.318645	7.102447	2.480875
Pot	0.998806	314.058236	8.169243	20.559134	6.329257	2.539845
Pheasant	0.998574	200.19082	7.008441	24.661866	5.766085	2.509426
Pepper	0.997284	720.920412	6.511175	19.55193	6.974351	2.475615
Aeroplane	0.998204	360.658496	6.690241	22.457049	5.26011	2.518521
starfish	0.997337	612.646389	6.633942	20.258705	6.96968	2.575418
Zebra	0.996036	821.956456	5.913532	18.982315	6.241778	2.55083

From the result it is found that the algorithm's execution time is small, the SNR and PSNR are in the range of 5.9 to 10.4 and 18.9 dB to 27.2 dB respectively, and blurring artifacts are observed at the edges and in the region of larger intensity variations.

Figure No. 4.12 and 4.13 show the result of Popoulis-Gerchberg (PG) SR reconstruction algorithm in the form of images. It includes high resolution original image, LR images with different orientation with angle θ, shift x and shift y and the SR image obtained after reconstruction. Here the high resolution image as shown in Figure No. 4.12 has resolution of 512x512 and LR images have resolution of 128x128. Here the high resolution image as shown in Figure No. 4.13 has resolution of 320x480 and LR images have resolution of 80x120.

High resolution Original Image

LR1 image (angle θ=0, shift x=0, shift y=0)

LR2 image(θ=0.0025, shift x=0.025,shift y=-0.004)

LR3 image(θ=-0.012, shift x=-0.0015,shift y0.003)

LR3 image(θ=-0.0045,shiftx=-0.002,shifty=-0.025)

SR image obtained after reconstruction

Figure No. 4.12 :Result of image 'Castle' using Popoulis-Gerchberg (PG) Algorithm

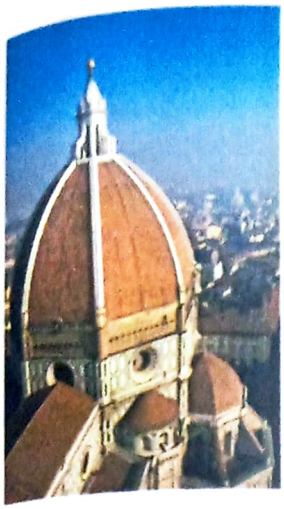

High resolution Original Image

LR1 image (angle θ=0, shift x=0, shift y=0)

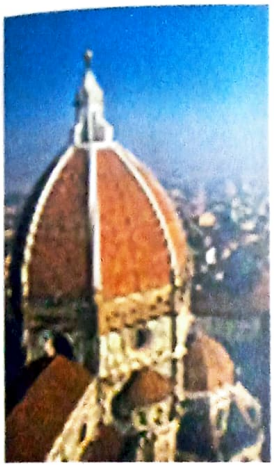

LR2 image(θ=0.003, shift x=0.001,shift y=-0.002)

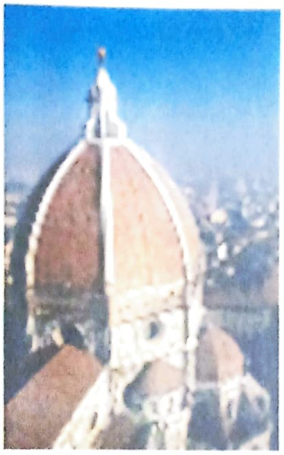

LR3 image(θ=-0.002, shift x=0.005,shift y=0.03)

LR4 image(θ=0.001, shift x=-0.02,shift y=-0.015)

SR image obtained after reconstruction

Figure No. 4.13 :Result of image 'building' using Popoulis-Gerchberg (PG) Algorithm

4.2.3 POCS based SR Reconstruction Algorithm: This algorithm is tested for large number of cases with variety of images. The results are shown in the Table 4.8. where measuring parameters used are SSI, MSE, SNR, PSNR, Entropy, Execution time.

Table 4.8- Result of Reconstruction using POCS Based Reconstruction Algorithm

Image	SSI	MSE	SNR	PSNR	Entropy	Execution Time - T
Castle	0.999548	165.2582	9.784582	25.949173	6.522563	3.182275
Huts	0.99509	775.791459	6.917167	19.233354	6.760229	1.855642
building	0.997118	711.565684	7.103161	19.608654	7.110289	2.535371
Pot	0.998811	250.846254	8.657256	22.198527	6.392639	2.52059
Pheasant	0.998729	152.831074	7.594603	26.08187	6.015255	2.518529
Pepper	0.997557	614.442385	6.858205	20.245992	7.119771	2.565376
Aeroplane	0.998336	280.693516	7.23456	23.614351	5.85158	2.538828
starfish	0.997679	552.365059	6.85886	20.708542	7.024257	2.59035
Zebra	0.996437	746.496582	6.122637	19.400525	6.407398	2.593112

From the result it is found that the algorithm's execution time is small, the SNR and PSNR are in the range of 6.12 to 9.78 and 19.23 dB to 25.94 dB respectively, and small ringing artifacts and blurring is are observed at the edges and smoothing over entire resultant image.

Figure No. 4.14 and 4.15 show the result of POCS based SR reconstruction algorithm in the form of images. It includes high resolution original image, LR images with different orientation with angle θ, shift x and shift y and the SR image obtained after reconstruction. Here the high resolution image as shown in Figure No. 4.14 has resolution of 512x512 and LR images have resolution of 128x128. Here the high resolution image as shown in Figure No. 4.15 has resolution of 320x480 and LR images have resolution of 80x120.

High resolution Original Image

LR1 image (angle θ=0, shift x=0, shift y=0)

LR2 image(θ=0.0025, shift x=0.025,shift y=-0.004)

LR3 image(θ=-0.012, shift x=-0.0015,shift y=0.003)

LR3 image(θ=-0.0045,shiftx=-0.002,shifty=-0.025)

SR image obtained after reconstruction

Figure No. 4.14 :Result of image 'Castle' using POCS based SR Reconstruction Algorithm

High resolution Original Image

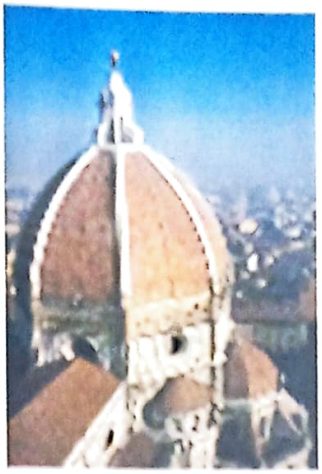

LR1 image (angle θ=0, shift x=0, shift y=0)

LR2 image(θ=0.003, shift x=0.001,shift y=0.002)

LR3 image(θ=0.002, shift x=0.005,shift x=0.03)

LR4 image(θ=0.001, shift x=-0.02,shift y=0.015)

SR image obtained after reconstruction

Figure No. 4.15 :Result of image 'building' using POCS based SR Reconstruction Algorithm

4.2.4 Iterative Back Projection (IBP) SR Reconstruction Algorithm: This algorithm is tested for large number of cases with variety of images. The results are shown in the Table 4.9, where measuring parameters used are SSI, MSE, SNR, PSNR, Entropy, Execution time.

Table 4.9- Result of Reconstruction using IBP SR Algorithm

Image	SSI	MSE	SNR	PSNR	Entropy	Execution Time (sec)
Castle	0.999083	622.606883	6.904327	20.188664	6.494244	0.970368
Huts	0.987561	6866.042269	2.182359	9.763739	6.056308	2.219939
building	0.997024	972.337031	6.425152	18.252635	7.143394	1.103732
Pot	0.998912	124.694659	10.175055	26.351281	6.504439	0.930469
Pheasant	0.998624	216.897179	6.834392	24.768265	6.01571	1.069079
Pepper	0.99639	844.082535	6.168687	18.866954	7.133838	1.124527
Aeroplane	0.998007	398.927099	6.471254	22.121868	5.917961	1.11371
starfish	0.996828	789.589004	6.082986	19.156793	7.08866	1.117915
Zebra	0.996398	1419.671771	4.726836	16.608924	6.574483	1.211691

From the result it is found that the algorithm's execution time is smaller than Robust SR, POCS based SR and PG SR algorithms. The SNR and PSNR are in the range of 2.18 to 10.17 and 9.76 dB to 24.76 dB respectively, and small ringing artifacts and step edges are observed at the curved sharper and slanted edges resultant image is sharper than POCS based and IBP SR algorithm.

Figure No. 4.16 and 4.17 show the result of IBP SR reconstruction algorithm in the form of images. It includes high resolution original image, LR images with different orientation with angle θ, shift x and shift y and the SR image obtained after reconstruction. Here the high resolution image as shown in Figure No. 4.16 has resolution of 512x512 and LR images have resolution of 128x128. Here the high resolution image as shown in Figure No. 4.17 has resolution of 320x480 and LR images have resolution of 80x120.

High resolution Original Image

LR1 image (angle θ=0, shift x=0, shift y=0)

LR2 image(θ=0.0025, shift x=0.025,shift y=-0.004)

LR3 image(θ=-0.012, shift x=-0.0015,shift y0.003)

LR3 image(θ=-0.0045,shiftx=-0.002,shifty=-0.025)

SR image obtained after reconstruction

Figure No. 4.16 :Result of image 'Castle' using IBP SR Algorithm

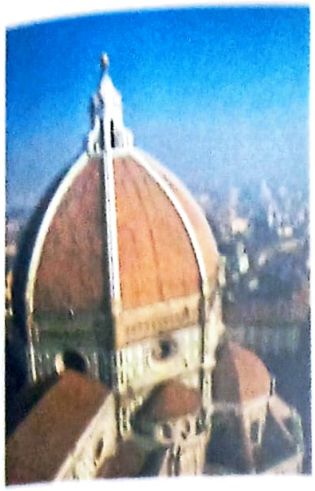

High resolution Original Image

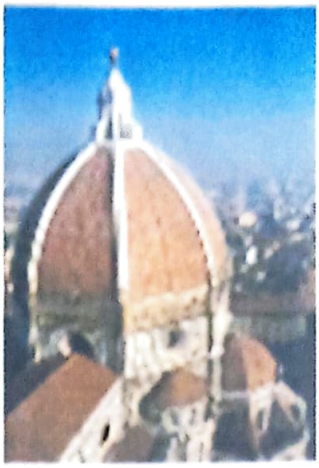

LR1 image (angle θ=0, shift x=0, shift y=0)

LR2 image(θ=0.003, shift x=0.001,shift y=-0.002)

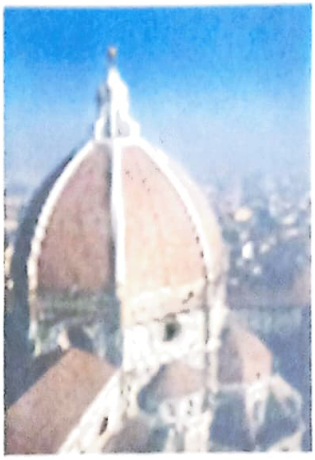

LR3 image(θ=-0.002, shift x=-0.005,shift y=0.03)

LR4 image(θ=0.001, shift x=-0.02,shift y=-0.015)

SR image obtained after reconstruction

Figure No. 4.17 :Result of image 'building' using IBP SR Algorithm

4.2.5 Modified Interpolation SR Reconstruction Algorithm: This algorithm is tested for large number of cases with variety of images. The results are shown in the Table 4.10, where measuring parameters used are SSI, MSE, SNR, PSNR, Entropy, Execution time.

Table 4.10- Result of Reconstruction using Modified Interpolation SR Algorithm

Image	SSI	MSE	SNR	PSNR	Entropy	Execution Time (sec)
Castle	0.999756	107.402819	10.720318	27.820647	6.433289	0.86289
Huts	0.994962	576.783862	7.560826	20.520673	6.716738	0.579808
building	0.997766	527.068468	7.754901	20.912133	7.104952	0.524357
Pot	0.998958	177.593481	9.407159	25.636533	6.46465	0.533942
Pheasant	0.998777	149.017734	7.649472	26.398424	6.016255	0.529334
Pepper	0.997858	524.963952	7.199964	20.929509	7.119672	0.523963
Aeroplane	0.997858	524.963952	7.199964	20.929509	7.119672	0.528726
starfish	0.998136	359.977146	7.788617	22.568054	7.067908	0.52855
Zebra	0.998136	359.977146	7.788617	22.568054	7.067908	0.533590

From the result it is found that the algorithm's execution time is smaller than all other implemented reconstruction algorithms, Robust SR, POCS based SR and PG SR, IBP SR and SANC SR algorithms. The SNR and PSNR are in the range of 7.19 to 10.72 and 20.52 dB to 27.82 dB respectively, and smaller ringing artifacts are observed at the curved sharper edges.

Figure No. 4.18 and 4.19 show the result of IBP SR reconstruction algorithm in the form of images. It includes high resolution original image, LR images with different orientation with angle θ, shift x and shift y and the SR image obtained after reconstruction. Here the high resolution image as shown in Figure No. 4.18 has resolution of 512x512 and LR images have resolution of 128x128. Here the high resolution image as shown in Figure No. 4.19 has resolution of 320x480 and LR images have resolution of 80x120.

High resolution Original Image

LR1 image (angle θ=0, shift x=0, shift y=0)

LR2 image(θ=0.0025, shift x=0.025,shift y=-0.004)

LR3 image(θ=-0.012, shift x=-0.0015,shift y0.003)

LR3 image(θ=-0.0045,shiftx=-0.002,shifty=-0.025)

SR image obtained after reconstruction

Figure No. 4.18 :Result of image 'Castle' using Modified Interpolation SR Algorithm

High resolution Original Image

LR1 image (angle θ=0, shift x=0, shift y=0)

LR2 image(θ=0.003, shift x=0.001,shift y=-0.002)

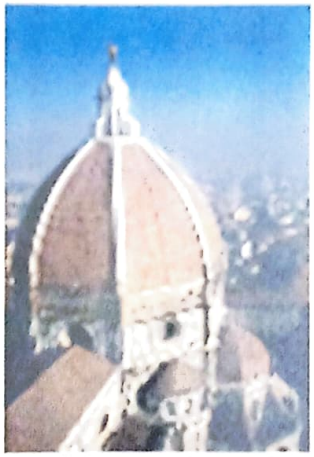

LR3 image(θ=-0.002, shift x=0.005,shift y=0.03)

LR4 image(θ=0.001, shift x=-0.02,shift y=-0.015)

SR image obtained after reconstruction

Figure No. 4.19 :Result of image 'building' using Modified Interpolation SR Algorithm

4.2.6 Structure-Adaptive Normalized Convolution (SANC) SR Reconstruction Algorithm: This algorithm is tested for large number of cases with variety of images. The results are shown in the Table 4.11, where measuring parameters used are SSI, MSE, SNR, PSNR, Entropy, Execution time.

Table 4.11- Result of Reconstruction using SANC SR Algorithm

Image	SSI	MSE	SNR	PSNR	Entropy	Execution Time (sec)
Castle	0.999617	41.58337	12.780798	31.941607	6.46031	59.97066
Huts	0.994901	664.649294	7.852929	20.904878	6.73949	33.03786
building	0.998795	269.075211	9.214868	23.832067	7.170895	30.76503
Pot	0.9854	791.061309	6.840504	19.503222	5.978297	28.59218
Pheasant	0.999349	84.346072	8.885337	28.870155	6.497063	32.39679
Pepper	0.998688	302.005152	8.400539	23.33066	7.144615	30.82093
Aeroplane	0.997953	331.802993	7.87132	22.922001	7.249873	30.72106
starfish	0.998199	239.357311	7.855902	22.702625	7.081407	31.61127
Zebra	0.993373	6127.98033	1.551189	14.25763	5.261749	32.73032

From the result it is found that the algorithm's execution time very large than all other implemented reconstruction algorithms, Robust SR, POCS based SR and PG SR, IBP SR and modified interpolation SR algorithms. The SNR and PSNR are in the range of 1.55 to 12.78 and 14.25 dB to 31.94 dB respectively, and result of reconstruction shows smaller details in image are better that all other algorithms for different type of images, synthetic, standard and natural with larger variation of contrast. Almost for all cases SSI is larger in SA-NC algorithm.

Figure No. 4.20 and 4.21 show the result of SANC SR reconstruction algorithm in the form of images. It includes high resolution original image, LR images with different orientation with angle θ, shift x and shift y and the SR image obtained after reconstruction. Here the high resolution image as shown in Figure No. 4.20 has resolution of 512x512 and LR images have resolution of 128x128. Here the high resolution image as shown in Figure No. 4.21 has resolution of 320x480 and LR images have resolution of 80x120.

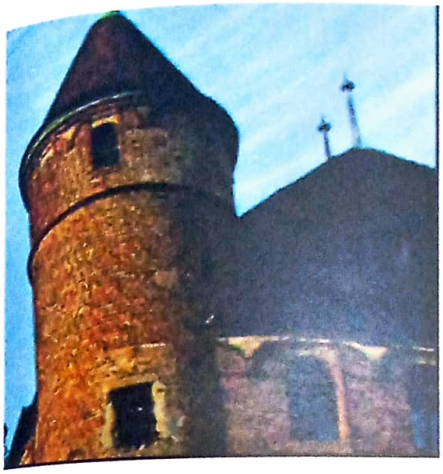

High resolution Original Image

LR1 image (angle θ=0, shift x=0, shift y=0)

LR2 image(θ=0.0025, shift x=0.025,shift y=-0.004)

LR3 image(θ=-0.012, shift x=-0.0015,shift y0.003)

LR3 image(θ=-0.0045,shiftx=-0.002,shifty=-0.025)

SR image obtained after reconstruction

Figure No. 4.20 :Result of image 'Castle' using SANC SR Algorithm

High resolution Original Image

LR1 image (angle θ=0, shift x=0, shift y=0)

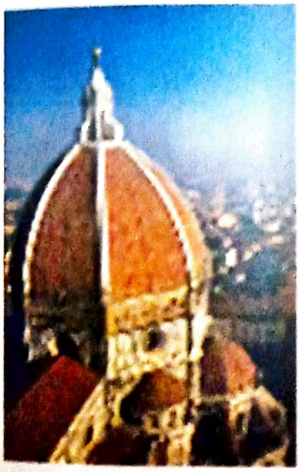

LR2 image(θ=0.003, shift x=0.001,shift y=-0.002)

LR3 image(θ=-0.002, shift x=0.005,shift y=0.03)

LR4 image(θ=0.001, shift x=-0.02,shift y=-0.015)

SR image obtained after reconstruction

Figure No. 4.21 :Result of image 'building' using SANC SR Algorithm

4.2.7 Comparative Results of Reconstruction Algorithms:

The six algorithms used for reconstruction are compared with respect to performance measuring parameters SSI, MSE, SNR, PSNR, Entropy and execution time in the Figure No. 4.22 to Figure No. 4.27 respectively. Average value of entropy is found better in SANC algorithm except in case 9 where image has repeated structures. The comparison reveals that robust SR and SANC SR algorithms performance is better that other implemented SR techniques. Moreover, SANC SR results resolve smaller details better than Robust SR algorithm. The results of SANC SR are consistent for different sets of images. The result of SA_NC are having better subjective quality than Robust SR. The subjective measures also in agreement to the quality of reconstruction of SANC than other reconstruction techniques.

Figure No. 4.28 to Figure No. 4.37 show the result of SANC SR reconstruction algorithm in comparison to all other reconstruction algorithms in the form of images. It includes the SR image obtained after reconstruction using IBP SR, Modified interpolation SR, SANC SR, POCS based SR, PG SR and Robust SR. Here the Super resolution results have been considered with SR factor of four. Super resolved images shown in Figure No. 4.28 to Figure No. 4.31 have resolution of 480x320, Figure No. 4.32 has resolution of 320x480 and Figure No. 4.33 to Figure No. 4.37 have resolution of 512x384.

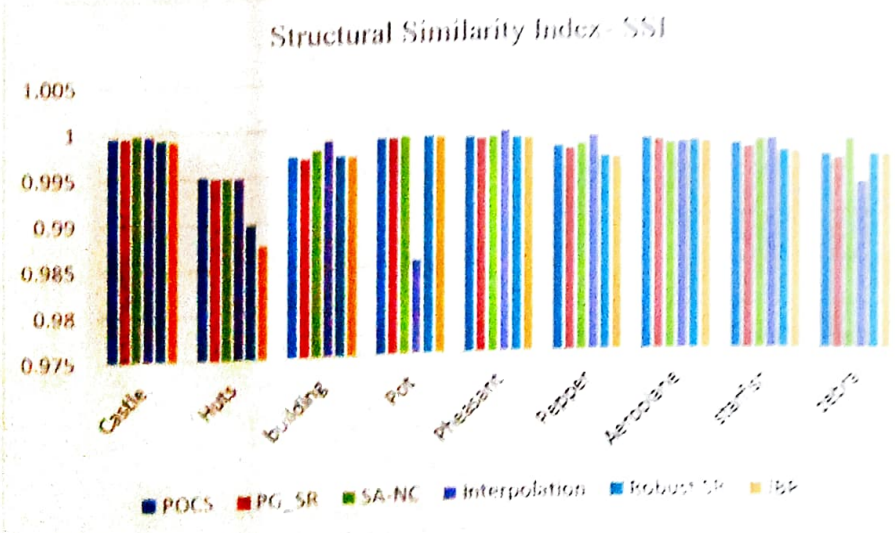

Figure No. 4.22 Plot of SSI for reconstruction algorithms using multiple LR images

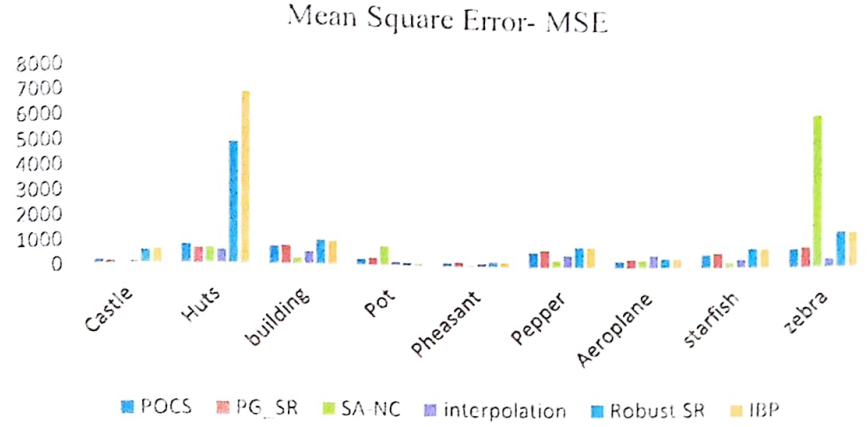

Figure No. 4.23 Plot of MSE for reconstruction algorithms using multiple LR images

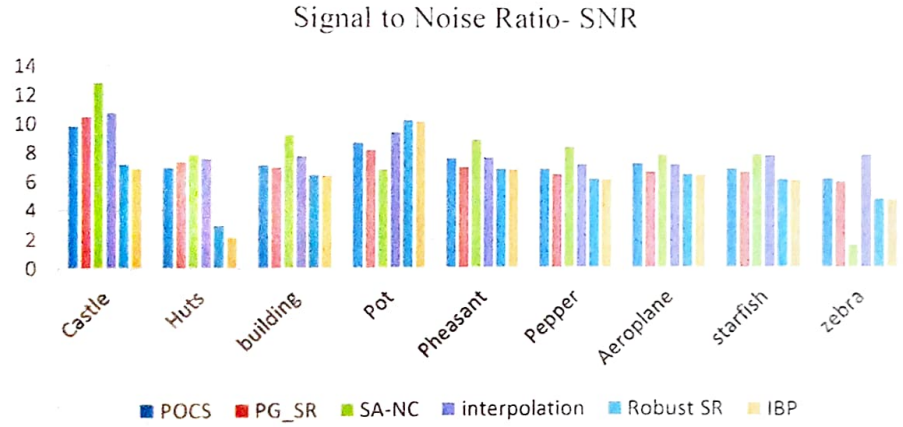

Figure No. 4.24 Plot of SNR reconstruction algorithms using multiple LR images

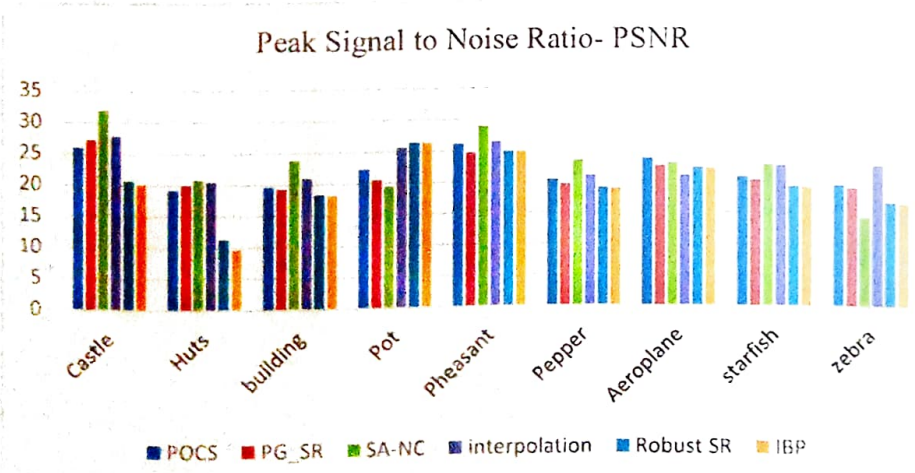

Figure No. 4.25 Plot of PSNR for reconstruction algorithms using multiple LR images

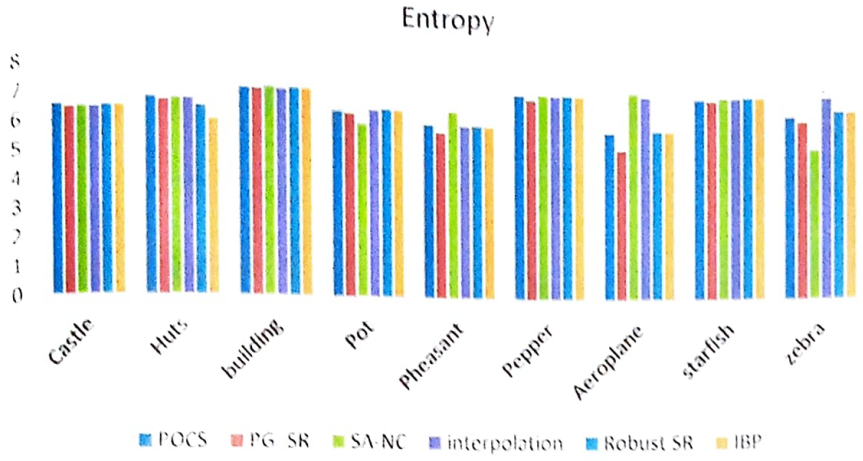

Figure No. 4.26 Plot of Entropy for reconstruction algorithms using multiple LR images

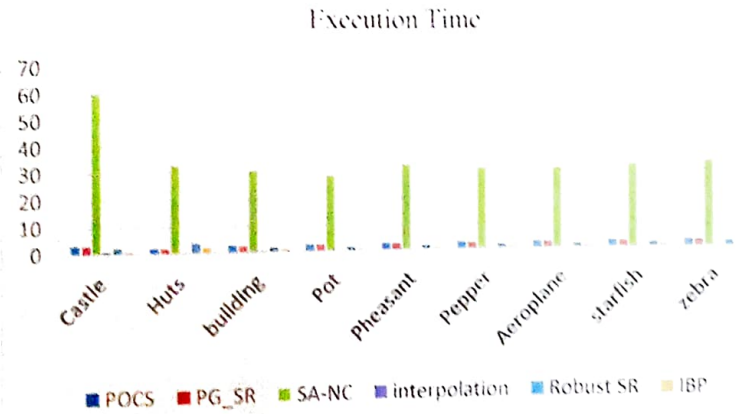

Figure No. 4.27 Plot of Execution Time in seconds for reconstruction algorithms using multiple LR images

IBP SR processing result

Modified Interpolation SR processing result

SANC SR processing result

POCS based SR processing result

PG_SR processing result

Robust SR processing result

Figure No. 4.28 :Result of image 'starfish' using reconstruction algorithms (480X320)

IBP SR processing result

Modified Interpolation SR processing result

SANC SR processing result

POCS based SR processing result

PG_SR processing result

Robust SR processing result

Figure No. 4.29 :Result of image 'Huts' using reconstruction algorithms (480X320)

IBP SR processing result

Modified Interpolation SR processing result

SANC SR processing result

POCS based SR processing result

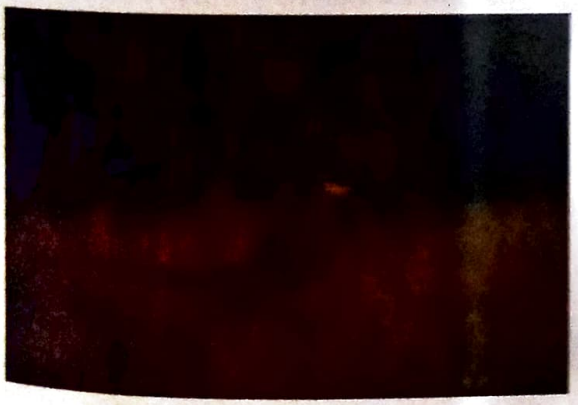

PG_SR processing result

Robust SR processing result

Figure No. 4.30 :Result of image 'Pheasant' using reconstruction algorithms (460X320)

IBP SR processing result

Modified Interpolation SR processing result

SANC SR processing result

POCS based SR processing result

PG_SR processing result

Robust SR processing result

Figure No. 4.31 :Result of image 'Aeroplane' using reconstruction algorithms (480X320)

IBP SR processing result

Modified interpolation SR processing result

SANC SR processing result

PCA based SR processing result

PG_SR processing result

Robust SR processing result

Figure No. 4.32 :Result of image 'Pepper' using reconstruction algorithms (320X480)

IBP SR processing result

Modified Interpolation SR processing result

SANC SR processing result

POCS based SR processing result

PG_SR processing result

Robust SR processing result

Figure No. 4.33 :Result of image 'captured image-1' using reconstruction algorithms (512x348)

IBP SR processing result

Modified Interpolation SR processing result

SANC SR processing result

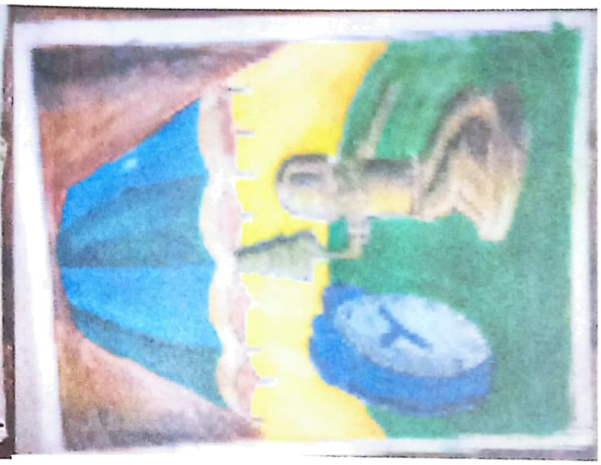

POCS based SR processing result

PG_SR processing result

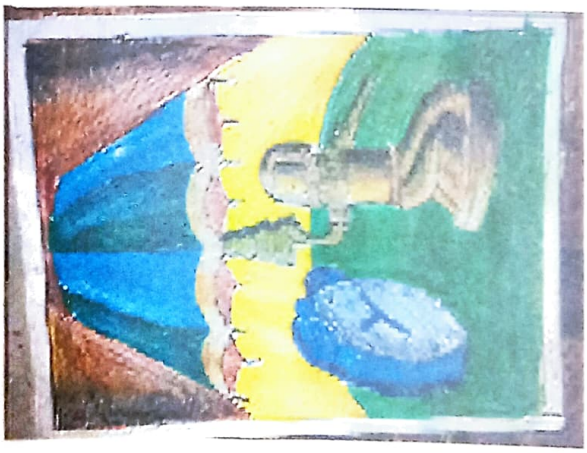

Robust SR processing result

Figure No. 4.34 :Result of image 'captured image-2' using reconstruction algorithms (512x348)

IBP SR processing result

Modified Interpolation SR processing result

SANC SR processing result

POCS based SR processing result

PG_SR processing result

Robust SR processing result

Figure No. 4.35 :Result of image 'captured image-3' using reconstruction algorithms (512x348)

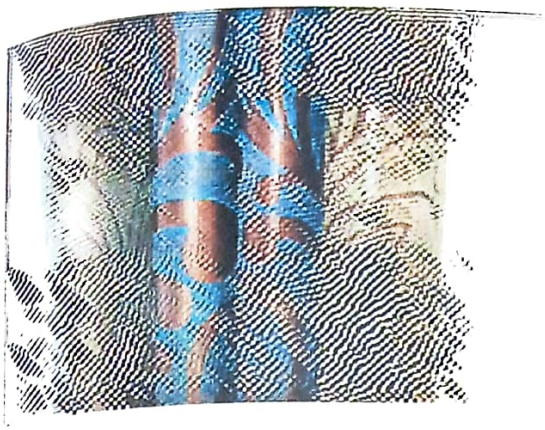

IBP SR processing result

Modified Interpolation SR processing result

SANC SR processing result

POCS based SR processing result

PG_SR processing result

Robust SR processing result

Figure No. 4.36 :Result of image 'captured image-4' using reconstruction algorithms (512x348)

IBP SR processing result

Modified Interpolation SR processing result

SANC SR processing result

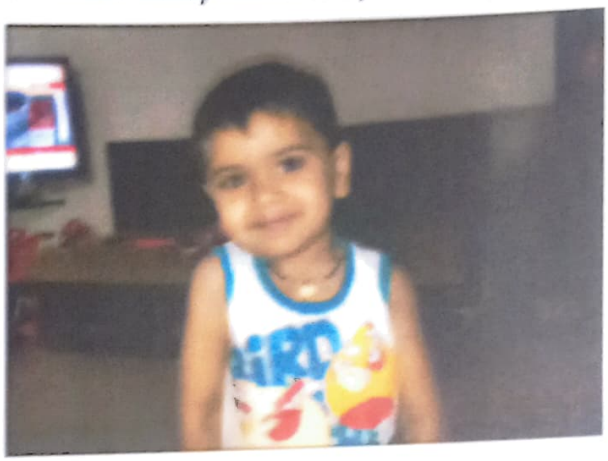

POCS based SR processing result

PG_SR processing result

Robust SR processing result

Figure No. 4.37 :Result of image 'captured image-5' using reconstruction algorithms (512x348)

The subjective approach is also used to verify the visual quality of the processed images. In the subjective approach the original high resolution images are compared with resultant images of all implemented algorithms. Here the five rating factors 1to 5 viz 1- worst, 2- bad, 3-average, 4- good, 5- best are suggested. The opinion of 50 persons of diverse background has been taken and presented here. Table 4.12 to Table 4.17 depicts the results.

Table 4.12 Voting Count for the Robust SR Algorithm

Image	Worst(1)	bad (2)	Average(3)	Good (4)	Best(5)
Castle	3	10	30	7	0
Huts	40	6	4	0	0
building	5	15	21	6	3
Pot	2	10	30	6	2
Pheasant	6	17	21	3	3
Pepper	7	12	25	3	3
Aeroplane	6	10	28	4	2
starfish	2	6	25	10	7
zebra	14	21	15	0	0

Table 4.13 Voting Count for the PG SR Algorithm

Image	Worst(1)	bad (2)	Average(3)	Good (4)	Best(5)
Castle	15	25	10	0	0
Huts	17	24	9	0	0
building	8	21	19	2	0
Pot	14	27	9	0	0
Pheasant	16	28	5	1	0
Pepper	12	21	15	2	0
Aeroplane	13	23	12	2	0
starfish	10	19	18	3	0
zebra	11	21	15	3	0

Table 4.14 Voting Count for the POCS Based SR Algorithm

Image	Worst(1)	bad (2)	Average(3)	Good (4)	Best(5)
Castle	8	15	25	2	0
Huts	7	14	26	3	0
building	12	19	18	1	0
Pot	17	22	11	0	0
Pheasant	14	18	16	2	0
Pepper	11	23	14	2	0
Aeroplane	16	20	14	0	0
starfish	10	17	20	3	0
zebra	12	17	19	2	0

Table 4.15 Voting Count for the IBP SR Algorithm

Image	Worst(1)	bad (2)	Average(3)	Good (4)	Best(5)
Castle	9	13	23	3	2
Huts	14	13	20	2	1
building	9	15	19	5	2
Pot	5	11	22	7	5
Pheasant	6	7	25	8	4
Pepper	13	8	23	6	0
Aeroplane	8	12	22	6	2
starfish	6	8	25	7	4
zebra	4	4	10	27	5

Table 4.16 Voting Count for the Modified Interpolation SR Algorithm

Image	Worst(1)	bad (2)	Average(3)	Good (4)	Best(5)
Castle	7	10	28	3	2
Huts	3	5	26	11	5
building	6	12	25	5	2
Pot	5	11	22	7	5
Pheasant	6	7	25	8	4
Pepper	13	8	23	6	0
Aeroplane	8	12	22	5	3
starfish	6	8	25	7	4
zebra	4	4	10	27	5

Table 4.17 voting count for the SANC SR Algorithm

Image	Worst(1)	bad (2)	Average(3)	Good (4)	Best(5)
Castle	2	2	12	28	6
Huts	2	2	16	25	5
building	0	2	18	24	6
Pot	8	12	25	3	2
Pheasant	3	3	15	28	1
Pepper	3	2	20	26	4
Aeroplane	1	2	24	20	3
starfish	0	2	19	26	3
zebra	20	25	5	0	0

The subjective observations of robust SR algorithm are graphically shown in Figure No. 4.38, for PG SR algorithm are graphically shown in Figure No. 4.39, for

POCS based SR algorithm are graphically shown in Figure No. 4.40, for IBP SR algorithm are graphically shown in Figure No. 4.41, for Modified Interpolation SR algorithm are graphically shown in Figure No. 4.42 and for SANC SR algorithm are graphically shown in Figure No. 4.43.

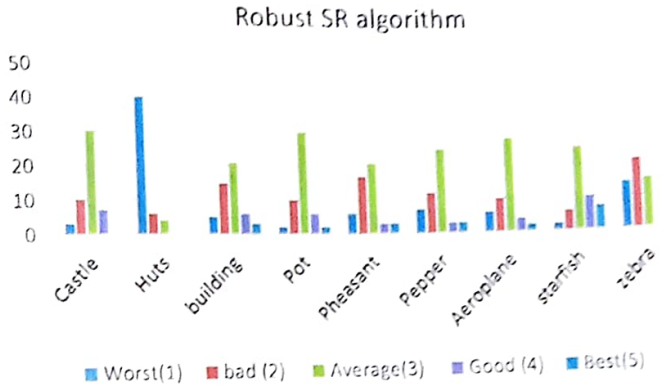

Figure No. 4.38 Plot of voting count for the Robust SR algorithm

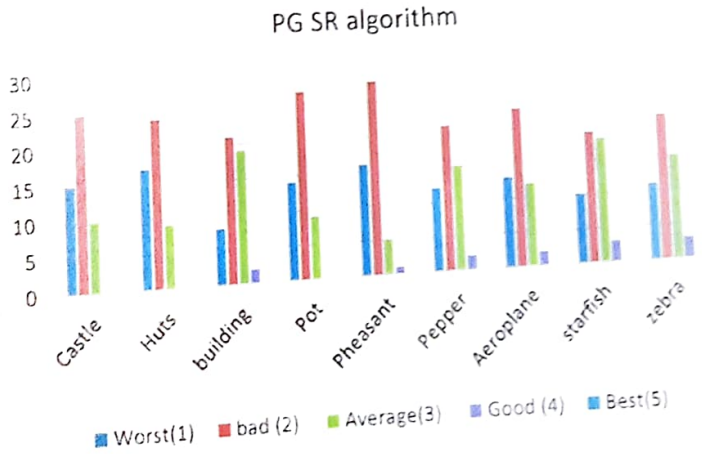

Figure No. 4.39 Plot of voting count for the PG SR algorithm

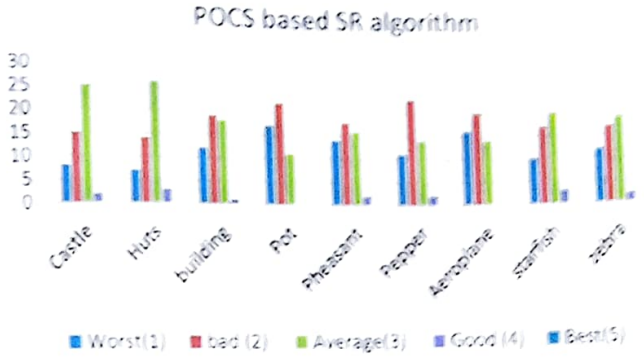

Figure No. 4.40 Plot of voting count for the POCS based SR algorithm

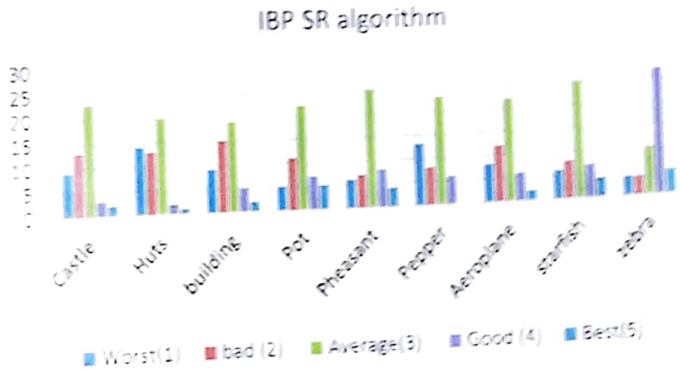

Figure No. 4.41 Plot of voting count for the IBP SR algorithm

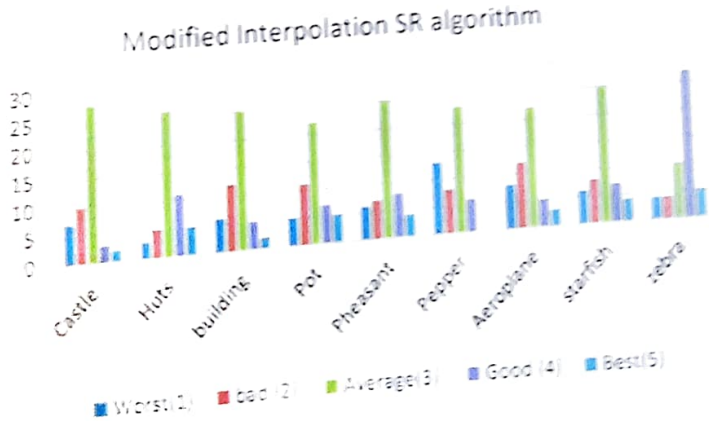

Figure No. 4.42 Plot of voting count for the Modified Interpolation SR algorithm

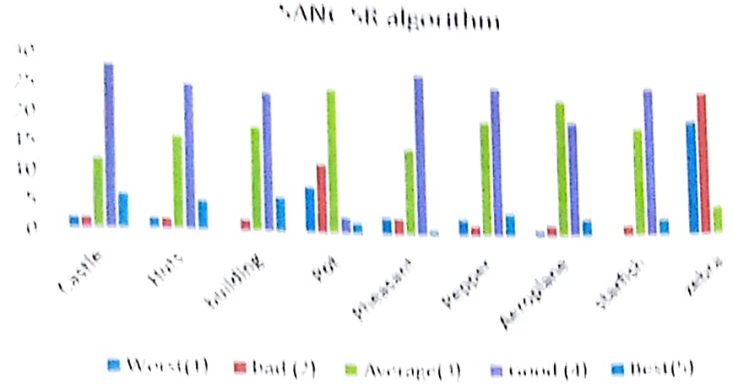

Figure No. 4.43 Plot of voting count for the SANC SR algorithm

The subjective comparison of implemented reconstruction algorithms for all the test images are given in following Tables. Table 4.18 shows the count of voted 'average' for the algorithms of different test image. Table 4.19 shows the count of voted 'average' for the algorithms of different test image. Table 4.20 shows the count of voted 'average' for the algorithms of different test image.

Table 4.18 Voting Count for the grade Average of Algorithms

Image	Robust SR	PG SR	POCS based SR	IBP SR	Mod. Interpolation SR	SANC SR
Castle	30	10	25	23	28	12
Huts	4	9	26	20	26	16
building	21	19	18	19	25	18
Pot	30	9	11	22	22	25
Pheasant	21	5	16	25	25	15
Pepper	25	15	14	23	23	20
Aeroplane	28	12	14	22	22	24
starfish	25	18	20	25	25	19
zebra	15	15	19	10	10	5

Table 4.19 Voting Count for the grade Good of Algorithms

Image	Robust SR	PG SR	POCS based SR	IBP SR	Mod. Interpolation SR	SANC SR
Castle	7	0	2	3	3	28
Huts	0	0	3	2	11	25
building	6	2	1	5	5	24
Pot	6	0	0	7	7	3
Pheasant	3	1	2	8	8	24
Pepper	3	2	2	6	6	26
Aeroplane	4	2	0	6	5	20
starfish	10	3	3	7	7	26
zebra	0	3	2	27	27	0

Table 4.20 Voting Count for the grade Best of Algorithms

Image	Robust SR	PG SR	POCS based SR	IBP SR	Mod. Interpolation SR	SANC SR
Castle	0	0	0	2	2	6
Huts	0	0	0	1	5	5
building	3	0	0	2	2	6
Pot	2	0	0	5	5	2
Pheasant	3	0	0	4	4	4
Pepper	3	0	0	0	0	4
Aeroplane	2	0	0	2	3	3
starfish	7	0	0	4	4	3
zebra	0	0	0	5	5	0

For the comparison of implemented algorithms for the different test images in above Table only the average, good and best grade have been considered. These comparative results are also presented graphically. The subjective observations of all test images for all implemented algorithms graphically shown in Figure No. 4.44, Figure No. 4.45 and Figure No. 4.46 for the grade 'average' 'good' and 'best' respectively.

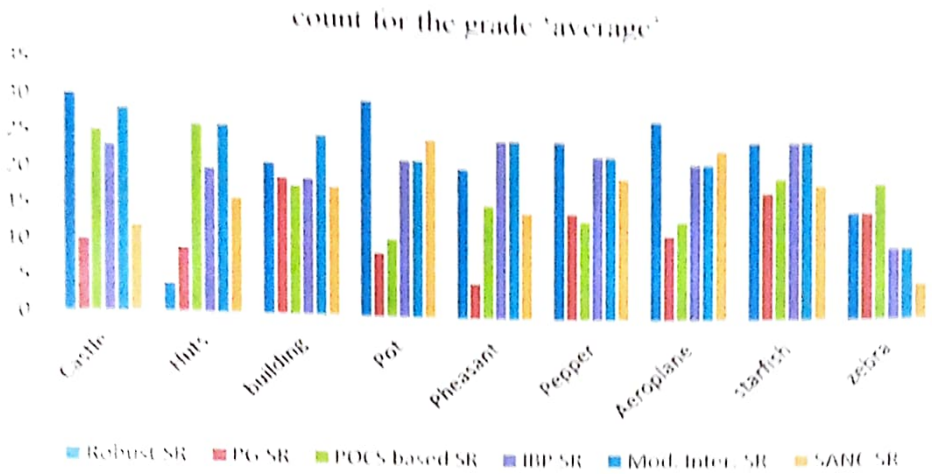

Figure No. 4.44 Plot of voting count for the grade 'average'

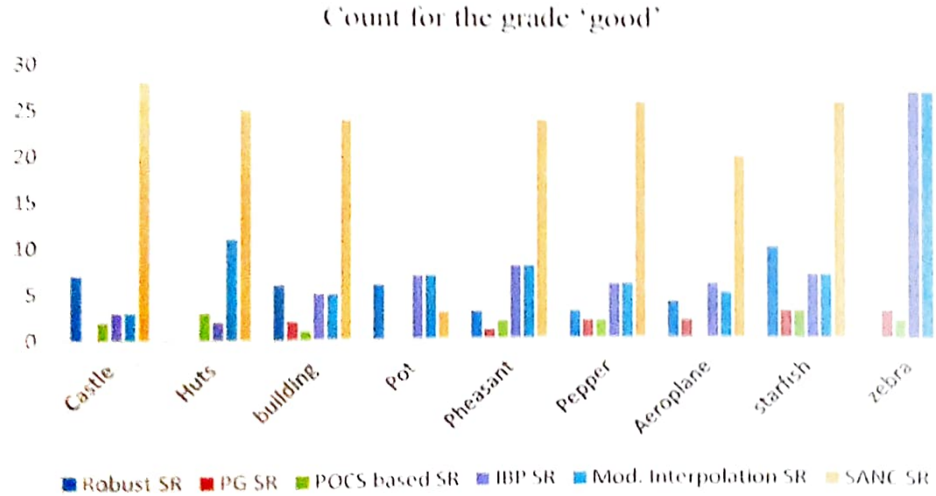

Figure No. 4.45 Plot of voting count for the grade 'good'

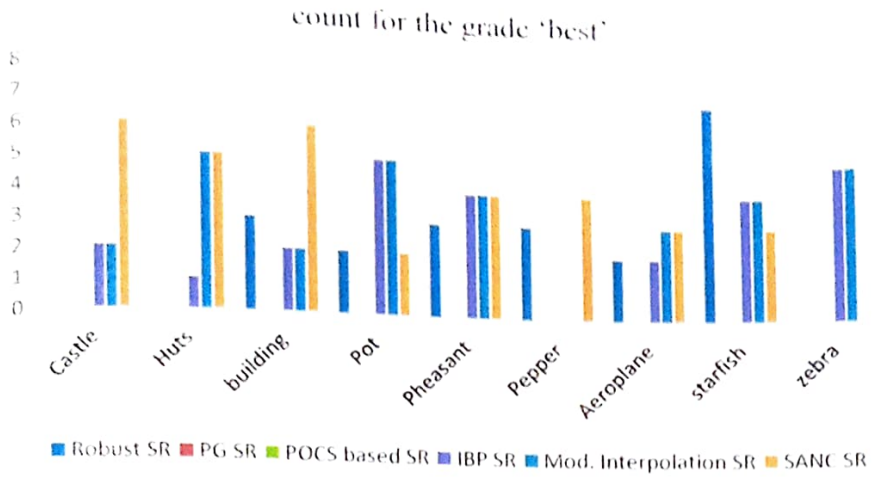

Figure No. 4.46 Plot of voting count for the grade 'best'

From the above result it is concluded that the SA-NC SR reconstruction algorithm results are slightly better than all other algorithms, as processed resultant image has observable minute details and reduced ringing effect. Hence in this research work the SANC SR reconstruction algorithm is proposed for considerable quality of SR image. Further it is also observed that the quality of image is poor for low intensity variations and this problem may be improved in proposed PSO based multi-image SR algorithm.

4.3 Reconstruction of SR algorithm using PSO with Multiple LR Images:

Reconstruction of SR algorithm Using PSO for Multiple LR Images is tested for large number of cases with variety of images and their comparison with results of bicubic interpolation technique. The results are shown in the Table 4.21, where measuring parameters used are PSNR, SNR and MSE.

Table 4.21 PSNR, SNR and MSE of Bicubic and Proposed Approach of Reconstruction of SR Using PSO

Image	Bicubic			proposed		
	PSNR	SNR	MSE	PSNR	SNR	MSE
Lenna	18.207128	6.436324	982.579289	29.880554	12.272876	66.838233
Areoplane	18.145547	7.295102	530.238472	34.75432	16.017055	9.557437
pot	19.686405	7.383778	451.717824	30.77529	13.172102	31.482878
baby	16.849926	6.315659	1343.03626	32.019729	13.905162	40.842046
butterfly	12.668261	3.583611	3517.6635	25.522888	9.996932	182.302038
women	15.451666	5.253293	1853.16363	28.740956	11.918421	84.860474
Snake	18.837137	7.008158	632.603569	25.012655	10.278427	140.378125
Zebra	15.884642	4.408581	1677.32093	21.231778	7.085779	489.668947
River	14.566627	5.490817	2272.04904	23.320199	9.870589	302.733511
pepper	17.517203	5.790305	1151.75477	28.554053	11.435796	85.802138
zebra	13.471959	3.869621	2923.37482	25.697744	9.980091	175.107978
img_001	16.926543	4.902713	1319.55053	25.660568	9.271385	176.613358
img_025	18.731241	6.467194	870.87595	29.731605	11.961524	69.170335
Elephant	19.054605	5.774423	795.757184	29.678859	11.104532	68.377804
Cassel	16.737816	5.509114	1378.15721	24.93501	9.616822	208.727348
Mushroom	18.729087	5.024129	871.307917	27.027059	9.172052	128.936074
Tree	19.255003	6.430693	548.752599	25.032117	9.612954	126.817865
Bird	19.100395	6.151192	799.909422	28.788992	11.000377	85.937196
baboon	16.122947	4.719744	1587.76294	20.586373	6.957598	563.676721
Barbara	17.369971	5.508493	1182.14377	24.092429	8.887633	247.490328
face	21.400304	6.52468	471.031531	29.788595	10.763854	68.268575
monarch	16.939688	5.08108	1315.5628	30.134984	11.672179	63.035032
comic	12.93943	4.289935	3304.74022	21.451224	8.549375	465.541077

These results are graphically presents in the following Figures. It is important characteristic of the proposed algorithm is that it is been implemented using multiple LR images whereas the bicubic interpolation technique implemented over single LR reference image. The Comparison is shown graphically with respect to performance measuring parameters PSNR, SNR and MSE in the Figure No. 4.47, Figure No. 4.48 and Figure No. 4.49 respectively.

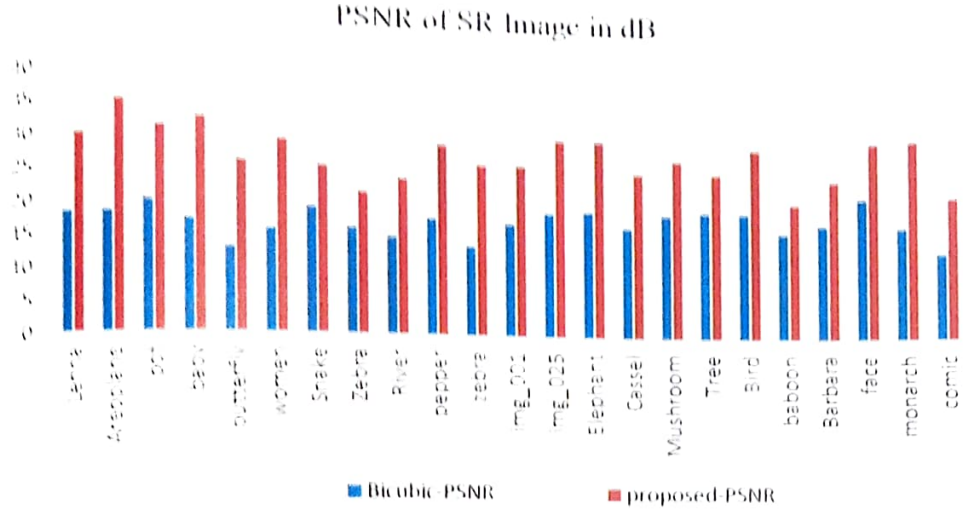

Figure No. 4.47 Comparison of PSNR in dB for Bicubic and Proposed Reconstruction of SR Using PSO with Multiple LR Images

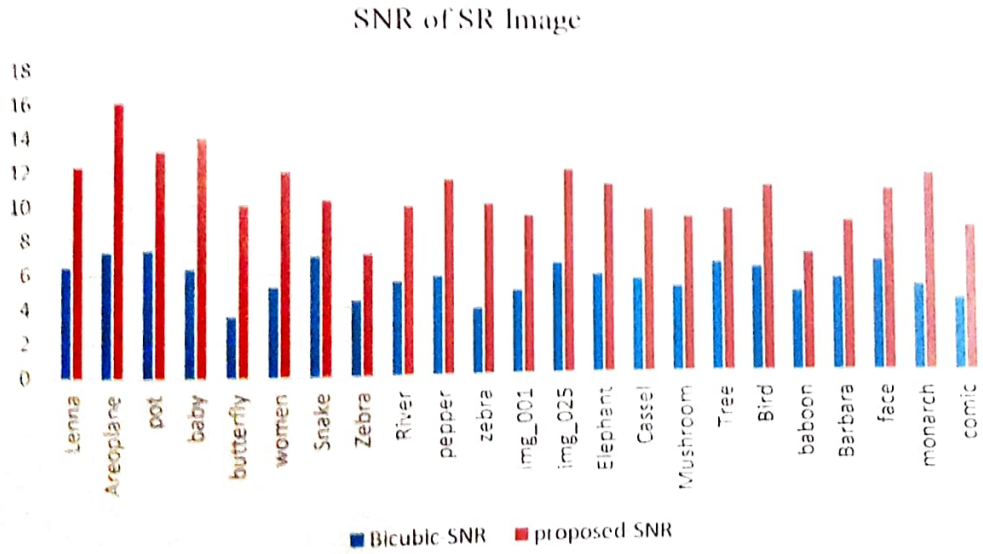

Figure No. 4.48 Comparison of SNR for Bicubic and Proposed Reconstruction of SR Using PSO with Multiple LR Images

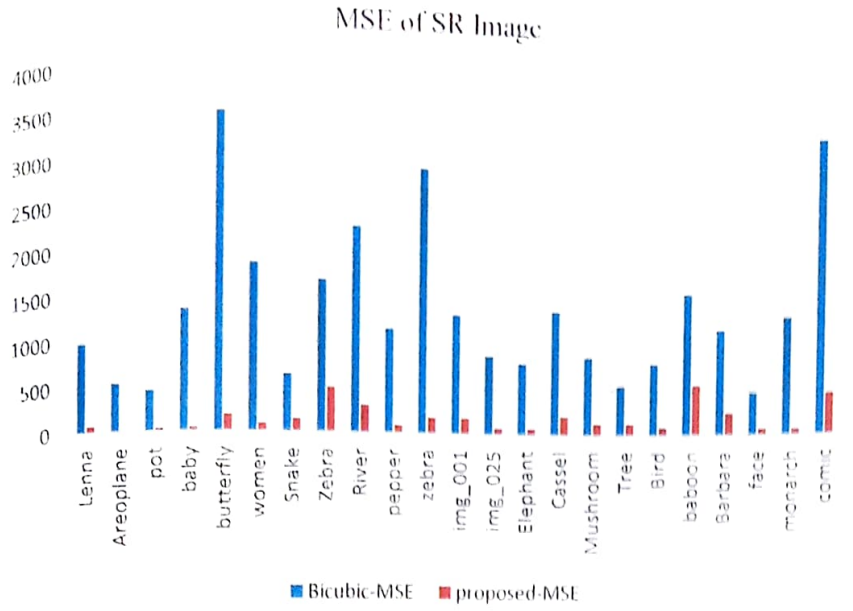

Figure No. 4.49 Comparison of MSE for Bicubic and Proposed Reconstruction Of SR Using PSO with Multiple LR Images

Few test results are shown in the subsequent pages consist of Low Resolution reference image, Low Resolution images with different orientations, resultant SR image obtained by using bicubic interpolation and proposed Reconstruction algorithm using PSO with multiple LR images.

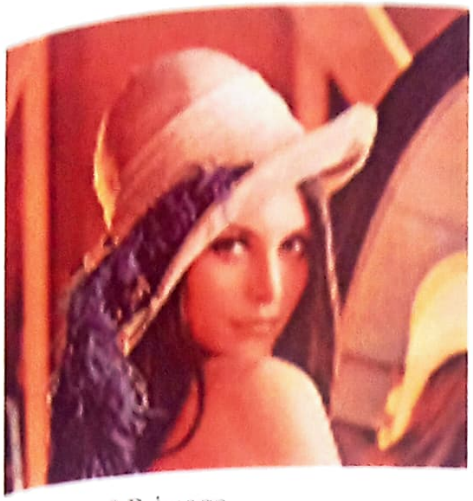

Reference LR image

LR2 image(θ=0.2, shift x=0.05,shift y=-0.08)

LR3 image(θ=0.1, shift x=-0.3,shift y=0.065)

LR4 image(θ=0.3, shift x=0.05,shift y=-0.3)

Result of Bicubic interpolation

Result of proposed technique

Figure No. 4.50 :Result of 'Lenna' image

To verify the visual quality of image obtained using the bicubic interpolation and by proposed technique, the specific region of the resultant image has been considered and shown in Figure No. 4.51.

Result of Bicubic interpolation

Result of proposed technique

Figure No 4.51 : Selected region of ' Lenna' image

Reference LR image

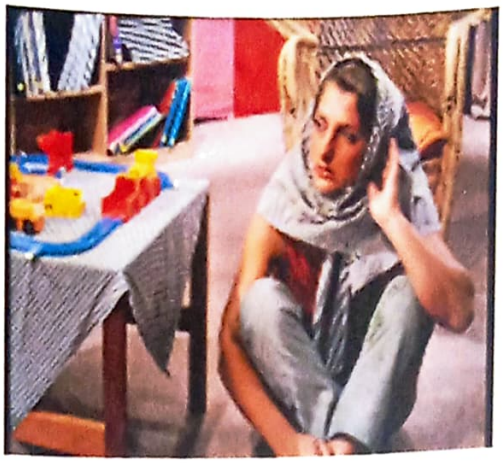

LR2 image(θ=0.025, shift x=0.05,shift y=0.025)

LR3image(θ=0.035,shift x=0.06,shift y=-0.045)

LR4 image(θ=0.03, shift x=0.1,shift y=-0.075)

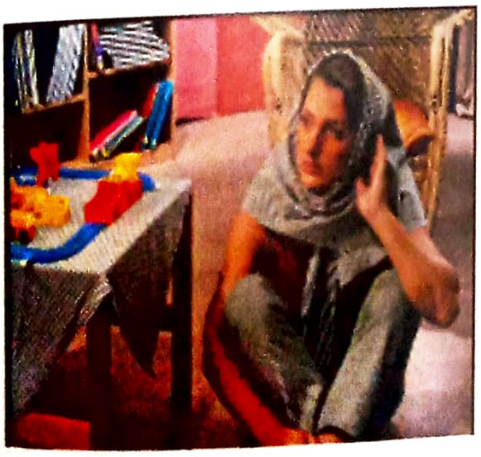

Result of Bicubic interpolation

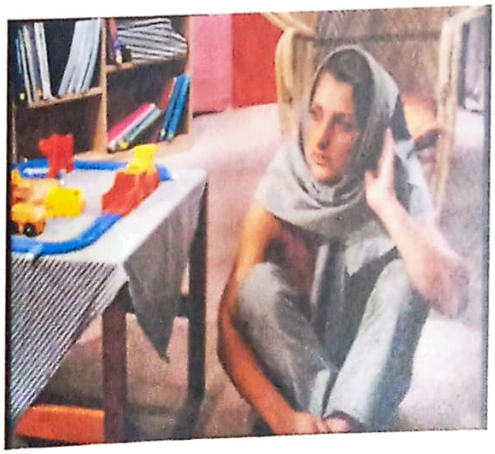

Result of proposed technique

Figure No. 4.52 :Result of 'Barbara' image

To verify the visual quality of image obtained using the bicubic interpolation and by proposed technique, the specific region of the resultant image has been considered and shown in Figure No. 4.53.

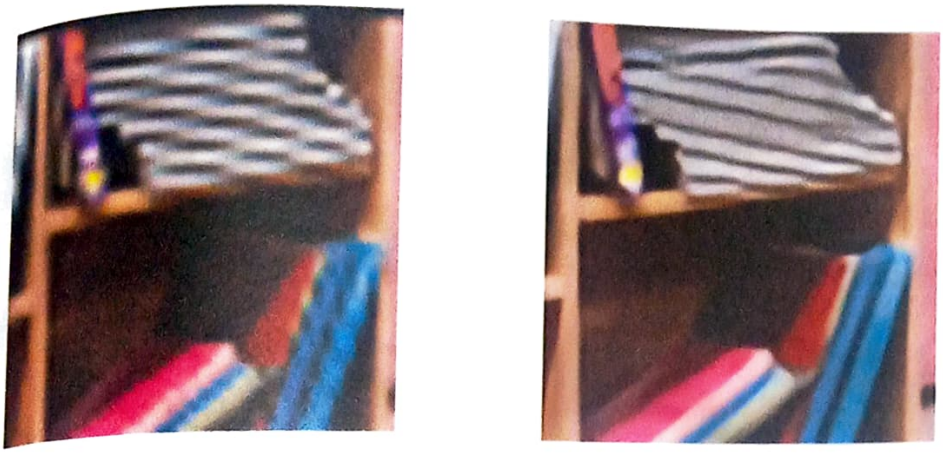

Result of Bicubic interpolation Result of proposed technique

Figure No 4.53 : Selected region of 'Barbara' image

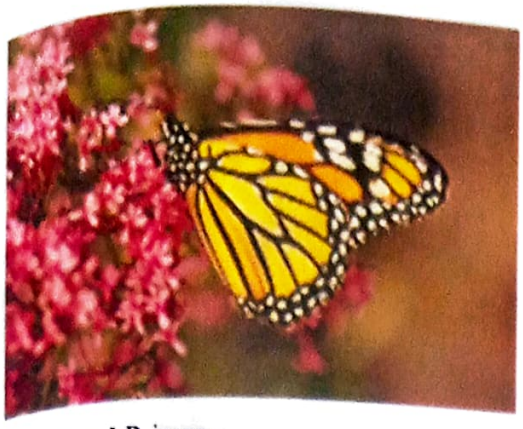

Reference LR image

LR2 image(θ=0.1, shift x=0.05,shift y=-0.08)

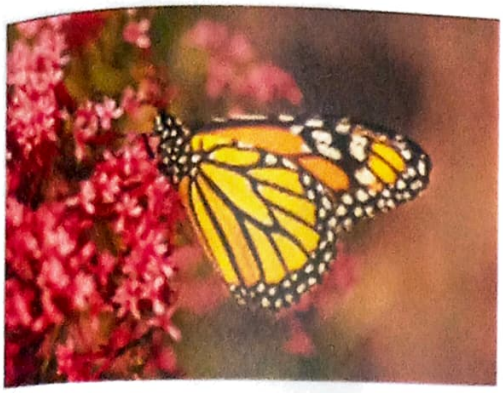

LR3 image(θ=0.4, shift x=0.05,shift y=-0.04)

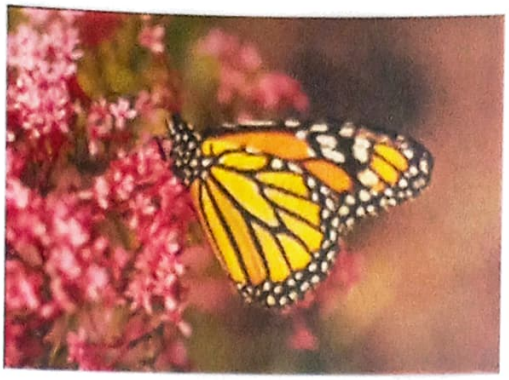

LR4 image(θ=0.3, shift x=0.05,shift y=-0.2)

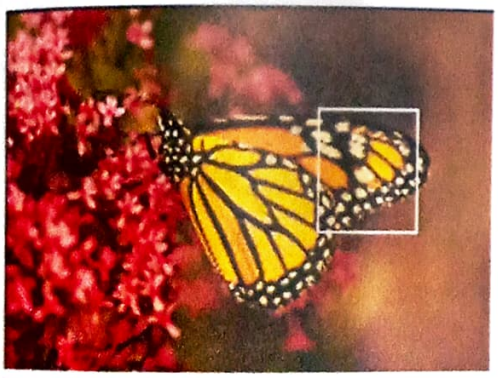

Result of Bicubic interpolation

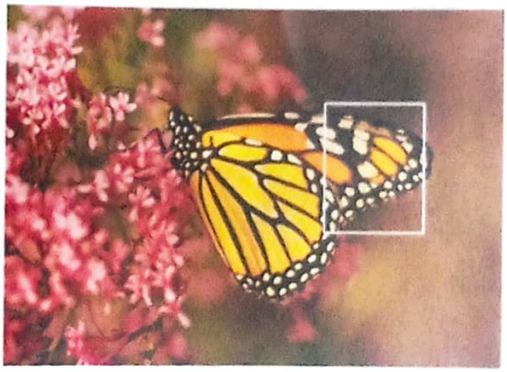

Result of proposed technique

Figure No. 4.54 :Result of 'monarch' image

To verify the visual quality of image obtained using the bicubic interpolation and by proposed technique, the specific region of the resultant image has been considered and shown in Figure No. 4.55

Result of Bicubic interpolation

Result of proposed technique

Figure No 4.55 : Selected region of 'monarch' image

Reference LR image

LR2 image(θ=0.1, shift x=0.36 shift y=-0.025)

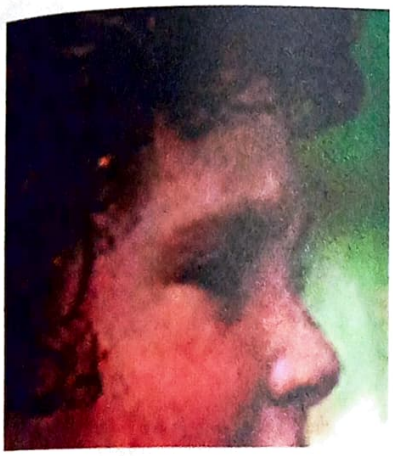

LR3 image(θ=0.25, shift x=0.24,shift y=0.02)

LR4 image(θ=-0.08, shift x=0.02,shift y=-0.3)

Result of Bicubic interpolation

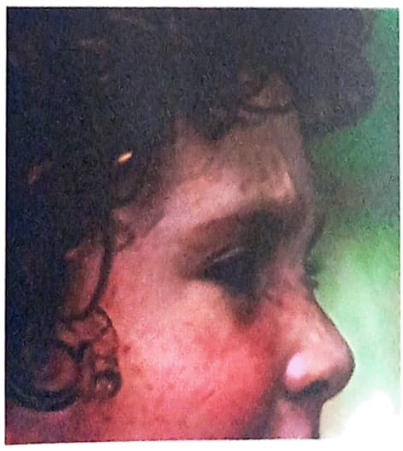

Result of proposed technique

Figure No. 4.56 :Result of 'face' image

Reference LR image

LR2 image(θ=0, shift x=0.25,shift y=0.6)

LR3 image(θ=0.3, shift x=0.3,shift y=0.015)

LR4 image(θ=0.05, shift x=0.06,shift y=0.5)

Result of Bicubic interpolation

Result of proposed technique

Figure No. 4.57 :Result of 'img_001' image

To verify the visual quality of image obtained using the bicubic interpolation and by proposed technique, the specific region of the resultant image has been considered and shown in Figure No. 4.58.

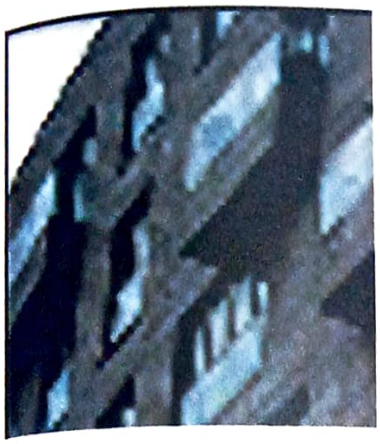

Result of Bicubic interpolation

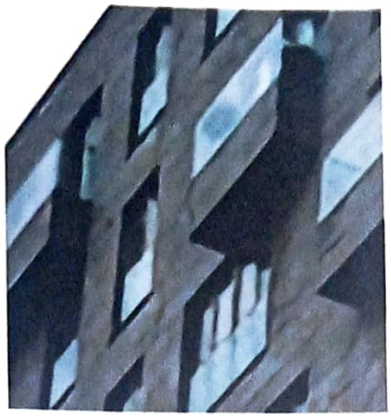

Result of proposed technique

Figure No 4.58 : Selected region of 'img_001' image

Reference LR image

LR2 image(θ=-0.002, shift x=0.015, shift y=-0.008)

LR3 image(θ=0.015, shift x=-0.0045, shift y=0.0065)

LR4 image(θ=0.0045, shift x=-0.02, shift y=0.023)

Result of Bicubic interpolation

Result of proposed technique

Figure No. 4.59 :Result of 'Aeroplane' image

To verify the visual quality of image obtained using the bicubic interpolation and by proposed technique, the specific region of the resultant image has been considered and shown in Figure No. 4.60.

Result of Bicubic interpolation

Result of proposed technique

Figure No 4.60 : Selected region of 'Aeroplane' image

Reference LR image

LR2 image(θ=-0.04, shift x=0.005, shift y=0.02)

LR3 image(θ=0.03, shift x=0.025, shift y=0.008)

LR4 image(θ=0.05, shift x=0.03, shift y=-0.05)

Result of Bicubic interpolation

Result of proposed technique

Figure No. 4.61 :Result of 'River' image

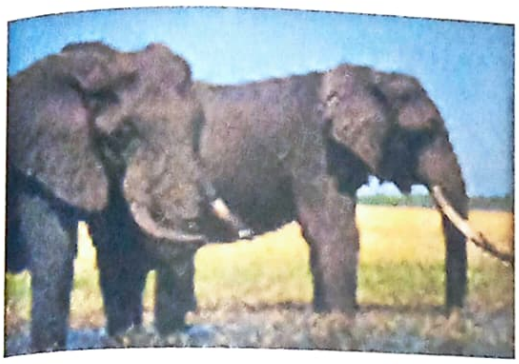

Reference LR image

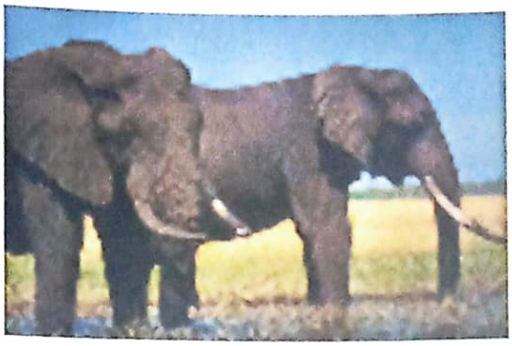

LR2 image(θ=0.06, shift x=0.02 ,shift y=-0.04)

LR3 image(θ=0.04, shift x=0.04, shift y=-0.06)

LR4 image(θ=0.02, shift x=0.06, shift y=0.25)

Result of Bicubic interpolation

Result of proposed technique

Figure No. 4.62 :Result of 'elephant' image

To verify the visual quality of image obtained using the bicubic interpolation and by proposed technique, the specific region of the resultant image has been considered and shown in Figure No. 4.63.

Result of Bicubic interpolation

Result of proposed technique

Figure No 4.63 : Selected region of 'elephant' image

From the Table No 4.21, it is concluded that the result of proposed techniques are improved and PSNR is improved by average value of 8-10 dB and The SNR is almost doubled or in some case tripled as compare to bicubic interpolation. The MSE (mean square error) is minimized to the great extend and it is 15-20 times less as compare to interpolation approach under consideration.

The visual quality of the SR images obtained using proposed algorithm is good and comparable to original HR image.

For better qualitative view the small section of resultant images are shown where in the magnified region it is clearly observed that the significant aliasing effect which is present in interpolation technique is not present in proposed technique.

4.4 Comparison of Reconstruction Results of SANC SR Algorithm and SR Algorithm using PSO with Multiple LR Images

Table 4.22 shows the reconstruction results of SANC SR algorithm and SR algorithm Using PSO with Multiple LR Images, where measuring parameters used are PSNR, SNR and MSE.

Table 4.22 Reconstruction Results of SANC SR Algorithm and SR Algorithm using PSO with Multiple LR Images

Image	SANC SR			PSO based SR		
	PSNR	SNR	MSE	PSNR	SNR	MSE
Areoplane	30.52126	13.1461	35.831594	34.75432	16.017055	9.557437
River	18.782342	7.59867	860.688845	23.320199	9.870589	302.733511
img_001	24.97156	8.92688	206.978106	25.660568	9.271385	176.613358
Elephant	21.926476	7.17616	417.285031	29.678859	11.104532	68.377804
Barbara	23.305306	8.44268	303.773419	24.092429	8.887633	247.490328
face	27.649392	9.69425	111.722638	29.788595	10.763854	68.268575
monarch	25.194103	9.20174	196.639193	30.134984	11.672179	63.035032

The Comparison is shown graphically with respect to performance measuring parameters: PSNR, SNR and MSE in the Figure No. 4.64, Figure No. 4.65 and Figure No. 4.66 respectively.

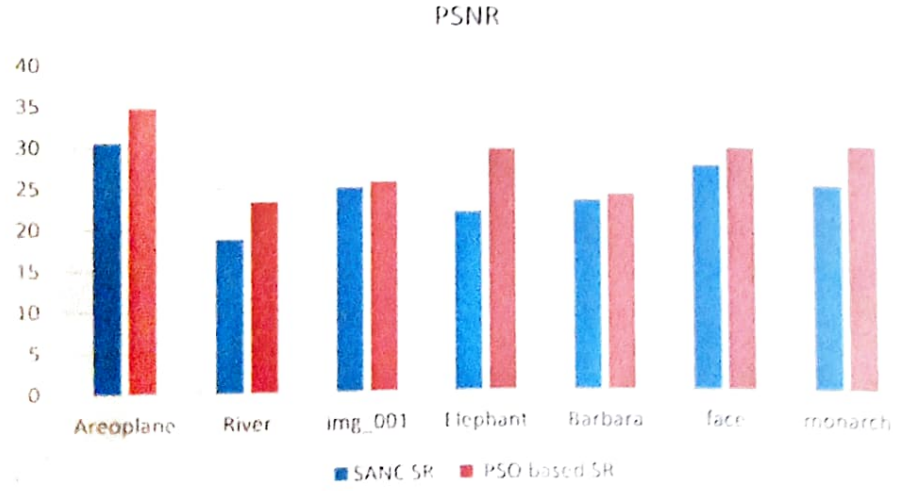

Figure No. 4.64 Comparison of PSNR in dB for SANC SR and SR using PSO with Multiple LR Images

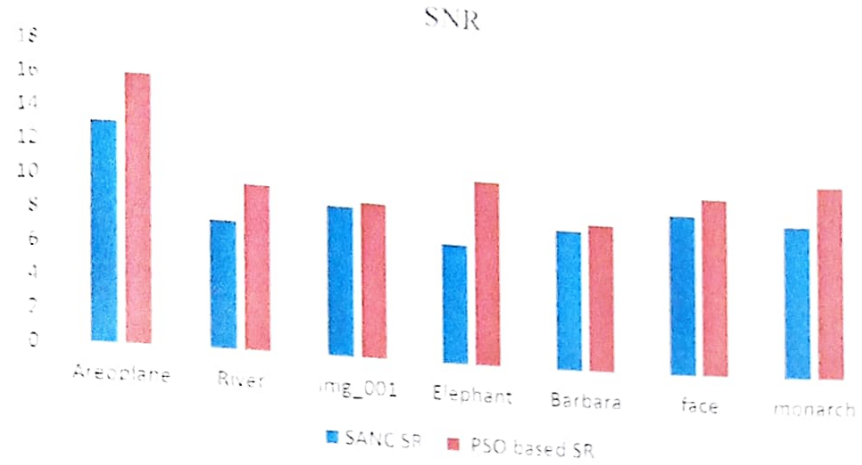

Figure No. 4.65 Comparison of SNR for SANC SR and SR using PSO with Multiple LR Images

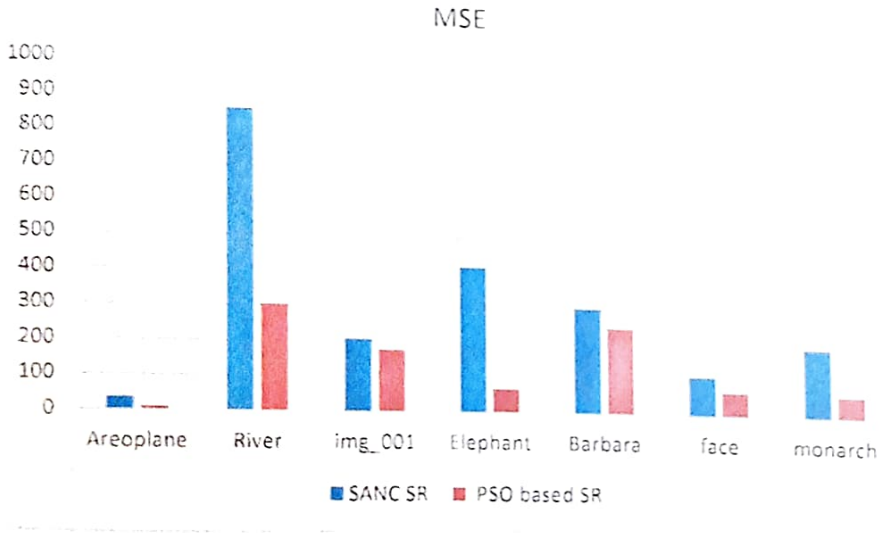

Figure No. 4.66 Comparison of MSE for SANC SR and SR using PSO with Multiple LR Images

For visual comparison sample resultant images of SANC SR and SR Using PSO with multiple LR images are shown in Figure No. 4.67 to Figure No. 4.73.

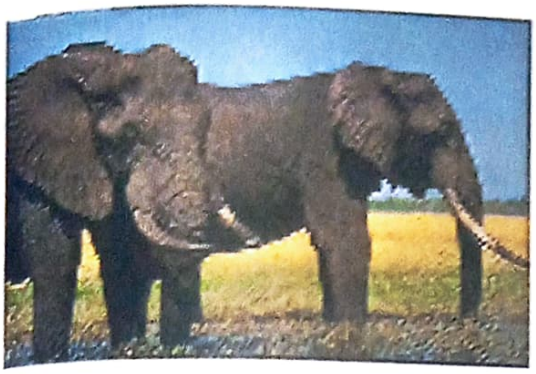

Result of SANC SR

Result of PSO based SR

Figure No 4.67 : Result of 'elephant' image

Result of SANC SR

Result of PSO based SR

Figure No 4.68 : Result of 'Areoplane' image

Result of SANC SR

Result of PSO based SR

Figure No 4.69 : Result of 'River' image

Result of SANC SR

Result of PSO based SR

Figure No 4.70 : Result of 'img_001' image

Result of SANC SR

Result of PSO based SR

Figure No 4.71 : Result of 'face' image

Result of SANC SR

Result of PSO based SR

Figure No 4.72: Result of 'monarch' image

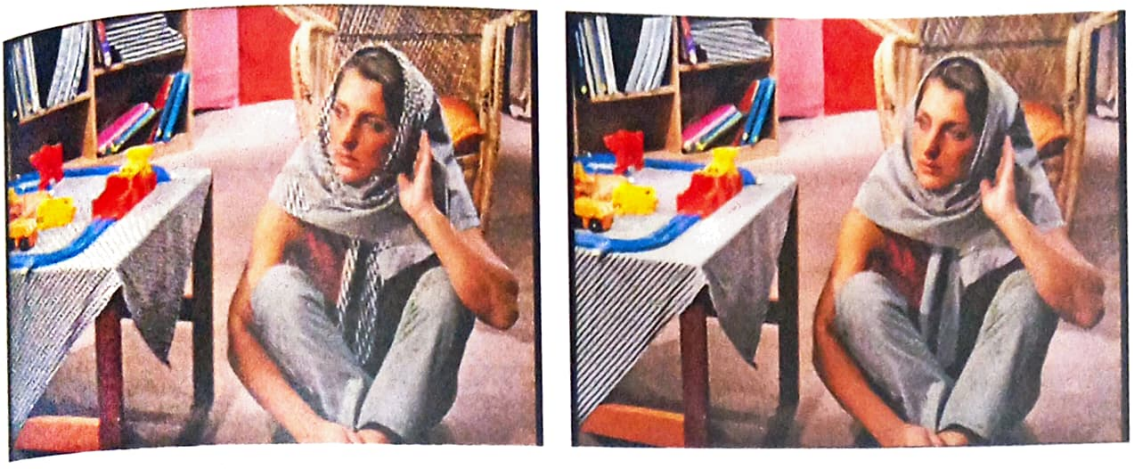

Result of SANC SR Result of PSO based SR

Figure No 4.73 : Result of 'Barbara' image

From the comparative results of SANC SR and SR Using PSO with multiple LR images it is concluded that the PSNR of PSO based algorithm is improved by 2dB, SNR is improved and MSE is decreased by a factor 5 to 6 as compared to SANC SR algorithm. The curved edges in SANC SR has ringing or step edges artifacts and for region with low intensity variation salt and pepper noise is observed.

From the above result it is concluded that the PSO based reconstruction of SR using multiple LR images results are good as compared to other approaches. The processed resultant image is sharper and has observable minute details. Hence in this research work the reconstruction of SR using PSO with multiple LR images algorithm is strongly proposed for quality of SR image reconstruction.

Chapter 5

Conclusion and Future Scope

This chapter presents summary of research work. The objective of the chapter is to present the conclusions drawn from the implemented algorithms and their results. It ends with future scope that identifies some future research directions.

5.1 Conclusions

To overcome the limitations of image capturing device, the concept of super resolution is proposed by the different researchers. After thorough review it is found that number of researchers worked in same area and proposed the results but there was always the room for improvement. Considering the need of SR image in various applications where the minute details play the important role in concluding the inferences, this area is finalized for the research.

In a super resolution technique the multiple images with different orientation capture the varying details are used. The objective of super resolution is to reconstruct the high resolution image by selecting varying details from set of images. To reconstruct the original image by using the varying details of captured low resolution images it is crucial to map the captured information at a right place otherwise the problems of aliasing, blurring, ringing are observed. The mapping of captured information is known as process of registration and reconstruction of image. In a registration process the motion parameters between the reference image and every different orientation image has been calculated which is used in process of reconstruction.

In this research work three algorithms of registration have been implemented namely Vandewalle's frequency domain registration, Marcel frequency domain registration and Hybrid approach using L-P FFT , and six

algorithms of reconstruction have been implemented namely Robust super resolution reconstruction algorithm, Popoulis-Gerchberg (PG) SR reconstruction algorithm. POCS based SR reconstruction algorithm, Iterative Back Projection (IBP) SR reconstruction algorithm, Modified Interpolation SR reconstruction algorithm and Structure-adaptive Normalized Convolution (SA-NC) SR reconstruction algorithm.

The measure the quantitative performance of reconstructed image the performance measure are used such as SSI, MSE, SNR, PSNR and Entropy. And finally subjective analysis is used to measure the visual quality which is classified into five grades: worst, bad, average, good and best.

The results of registration algorithms are presented and their comparison has been carried out to and finalize the registration algorithm is a process of super resolution i.e. hybrid approach using L-P FFT.

The results of all implemented registration algorithms are presented and their comparative analysis has been carried out. It is found that the results of Structure-adaptive Normalized Convolution (SA-NC) SR reconstruction algorithm are better than other implemented algorithms.

Finally the Reconstruction of SR algorithm Using PSO for Multiple LR Images is implemented, their results have been compared with bicubic interpolation and Structure-adaptive Normalized Convolution (SA-NC) SR reconstruction algorithm. It is observed that the PSNR of result of Reconstruction of SR algorithm Using PSO for Multiple LR Images is improved by 8-10 dB in an average as compare to Bicubic interpolation approach, the SNR is almost doubled or in some case tripled as compare to Bicubic interpolation and the MSE is minimized to the great extent and it is 15-20 times less as compare to interpolation approach under consideration.

The visual quality of the SR images obtained using Reconstruction of SR algorithm Using PSO for Multiple LR Images is good and comparable to original HR image, and the aliasing effect which is present in interpolation technique is not observed.

From the comparative results of SANC SR and SR Using PSO with multiple LR images, it is found that the PSNR of PSO based algorithm is improved by 2 to 5 dB, SNR is slightly improved and MSE is decreased by a factor 5 to 6.

Finally, the reconstruction of SR using PSO with multiple LR images algorithm is strongly proposed for quality of SR image reconstruction.

5.2 Future Scope

With reference to current research domain following are the few research directions,

- The technique presented in this research work uses PSO with multiple LR images with selected few investigation parameters of PSO there is a scope to use the same algorithm with additional investigation parameters.
- This algorithm with modification can be applied for video signal.
- To minimize the time complexity of algorithm penalization can be applied to certain code area to be implemented on parallel systems.

References

[1]. Andrey Krokhin, "Super-Resolution in Image Sequences," A Thesis at Department of Electrical and Computer Engineering Northeastern University Boston, Massachusetts September 2005.

[2]. Sina Farsiu, Dirk Robinson, Michael Elad, Peyman Milanfar,"Advances and Challenges in Super-Resolution", J. Imag. Syst. Technol., Wiley Periodicals, Inc. vol. 14, no. 2, pp. 47–57, Oct. 2004.

[3]. Sean Borman and Robert Stevenson,"Spatial Resolution Enhancement of Low-Resolution Image Sequences A Comprehensive Review with Directions for Future Research,"University of Notre Dame, Notre, IN 46556- July 8, 1998.

[4]. R. Y. Tsai and T. S. Huang, "Multiframe image restoration and registration," in Advances in Computer Vision and Image Processing, vol. 1, chapter 7, pp. 317–339, JAI Press, Greenwich, Conn, USA, 1984.

[5]. A. K. Jain, "Fundamentals of Digital Image Processing" Pearson Education, ISBN 81-297-0083-2, First Indian reprint 2003.

[6]. A. M. Tekalp, M. K. Ozkan, and M. I. Sezan, "High-Resolution Image Reconstruction from Lower-Resolution Image Sequences and Space-Varying Image Restoration," Proceedings of the IEEE International Conference on Acoustics, Speech and Signal Processing, San Francisco, CA, vol. III, pp. 169–172, 1992.

[7]. Mahesh Chappalli and N K Bose, "Simultaneous Noise Filtering and Super Resolution with Second Generation Wavelets", IEEE Signal Processing letters, vol 12, n0 11, Nov 2005, pp- 772-775.

[8]. Turgay Celik and Tardi Tjahjadi, "Image Resolution Enhancement using Dual-Tree Complex Wavelet Transform," IEEE Geoscience and Remote Sensing Letters, Vol. 7, No. 3, July 2010

[9]. Prakash P. Gajjar and Manjunath V. Joshi, "New Learning Based Super-Resolution:Use of DWT and IGMRF Prior,"IEEE Transactions on Image Processing, Vol. 19, No. 5, May 2010.

[10]. Hasan Demirel and Gholamreza Anbarjafari, "Image Resolution Enhancement by Using Discrete and Stationary Wavelet Decomposition," IEEE Transactions on Image Processing, Vol. 20, No. 5, May 2011.

[11]. M. Dirk Robinson, Cynthia A. Toth, Joseph Y. Lo and Sina Farsiu, "Efficient Fourier-Wavelet Super-Resolution," IEEE Transactions on Image Processing, Vol. 19, No. 10, October 2010.

[12]. HuiJi and Cornelia Fermuller, "Robust Wavelet-Based Super-Resolution Reconstruction: Theory and Algorithm," IEEE Transactions on Pattern Analysis and Machine Intelligence, Vol. 31, No. 4, April 2009.

[13]. Sina Farsiu, M. Dirk Robinson, Michael Elad, and Peyman Milanfar, "Fast and Robust Multiframe Super Resolution,"IEEE Transactions on Image Processing, Vol. 13, No. 10, October 2004.

[14]. Sina Farsiu, Michael Elad, and Peyman Milanfar, "Multiframe Demosaicing and Super-Resolution of Color Images," IEEE Transactions on Image Processing, Vol. 15, No. 1, January 2006.

[15]. Nathan A. Woods, Nikolas P. Galatsanos, and Aggelos K. Katsaggelos, "Stochastic Methods for Joint Registration, Restoration, and Interpolation of Multiple Under Sampled Images,"IEEE Transactions on Image Processing, Vol. 15, No. 1, January 2006.

[16]. Giannis K. Chantas, Nikolaos P. Galatsanos and Nathan A. Woods, "Super-Resolution Based on Fast Registration and Maximum a Posteriori Reconstruction," IEEE Transactions on Image Processing, Vol. 16, No. 7, July 2007.

[17]. Russell Hardie, "A Fast Image Super-Resolution Algorithm Using an Adaptive Wiener Filter,"IEEE Transactions on Image Processing, Vol. 16, No. 12, December 2007

[18]. Yu He, Kim-Hui Yap, Li Chen and Lap-PuiChau, "A Nonlinear Least Square Technique for Simultaneous Image Registration and Super-Resolution," IEEE Transactions on Image Processing, Vol. 16, No. 11, November 2007.

[19]. Uma Mudenagudi, Subhashis Banerjee, and Prem Kumar Kalra, "Space-Time Super-Resolution using Graph-Cut Optimization," IEEE Transactions on Pattern Analysis and Machine Intelligence, Vol. 33, No. 5, May 2011.

[20]. S. DerinBabacan, Rafael Molina, and Aggelos K. Katsaggelos, "Variational Bayesian Super Resolution," IEEE Transactions on Image Processing, Vol. 20, No. 4, April 2011.

[21]. XinboGao, Qian Wang, Xuelong Li, Dacheng Tao, and Kaibing Zhang, "Zernike-Moment-Based Image Super Resolution," IEEE Transactions on Image Processing, Vol. 20, No. 10, October 2011.

[22]. Esmaeil Faramarzi, Dinesh Rajan, and Marc P. Christensen, "Unified Blind Method for Multi-Image Super-Resolution and Single/Multi-Image Blur Deconvolution," IEEE Transactions on Image Processing, Vol. 22, No. 6, June 2013.

[23]. Feng Li, XiupingJia, Donald Fraser, and Andrew Lambert, "Super Resolution for Remote Sensing Images Based on a Universal Hidden Markov Tree Model," IEEE Transactions on Geoscience and Remote Sensing, Vol. 48, No. 3, March 2010.

[24]. Kwang In Kim and Younghee Kwon, "Single-Image Super-Resolution using Sparse Regression and Natural Image Prior," IEEE Transactions on Pattern Analysis and Machine Intelligence, Vol. 32, No. 6, June 2010.

[25]. Young Cheul Wee and Hyun Joon Shin, "A Novel Fast Fractal Super Resolution Technique," IEEE Transactions on Consumer Electronics, Vol. 56, No. 3, August 2010.

[26]. Jianchao Yang, John Wright, Thomas S. Huang, and Yi Ma, "Image Super-Resolution Via Sparse Representation," IEEE Transactions on Image Processing, Vol. 19, No. 11, November 2010.

[27]. Jian Sun, ZongbenXu, and Heung-Yeung Shum, "Gradient Profile Prior and Its Applications in Image Super-Resolution and Enhancement," IEEE Transactions on Image Processing, Vol. 20, No. 6, June 2011.

[28]. XinboGao, Kaibing Zhang, Dacheng Tao and Xuelong Li, "Joint Learning for Single-Image Super-Resolution via a Coupled Constraint," IEEE Transactions on Image Processing, Vol. 21, No. 2, February 2012.

[29]. Fei Zhou, Wenming Yang and Qingmin Liao, "Single Image Super-Resolution Using Incoherent Sub-dictionaries Learning," IEEE Transactions on Consumer Electronics, Vol. 58, No. 3, August 2012.

[30]. Kaibing Zhang, XinboGao, Xuelong Li, and Dacheng Tao, "Partially Supervised Neighbor Embedding for Example-Based Image Super-Resolution," IEEE Journal of Selected Topics in Signal Processing, Vol. 5, No. 2, April 2011.

[31]. Kaibing Zhang, XinboGao, Dacheng Tao, and Xuelong Li., "Single Image Super-Resolution with Multiscale Similarity Learning" IEEE Transactions on Neural Networks And Learning Systems, Vol. 24, No. 10, October 2013.

[32]. Min-Chun Yang and Yu-Chiang Frank Wang, "A Self-Learning Approach to Single Image Super-Resolution," IEEE Transactions on Multimedia, Vol. 15, No. 3, April 2013.

[33]. Shuyuan Yang, Min Wang, Yiguang Chen, and Yaxin Sun, "Single-Image Super-Resolution Reconstruction via Learned Geometric Dictionaries and Clustered Sparse Coding," IEEE Transactions on Image Processing, Vol. 21, No. 9, September 2012.

[34]. Xiaoqiang Lu, Yuan Yuan, and Pingkun Yan, "Image Super-Resolution via Double Sparsity Regularized Manifold Learning," IEEE Transactions on Circuits and Systems for Video Technology, Vol. 23, No. 12, December 2013.

[35]. Haichao Zhang, Yanning Zhang, HaisenLi, and Thomas S. Huang, "Generative Bayesian Image Super Resolution with Natural Image Prior," IEEE Transactions on Image Processing, Vol. 21, No. 9, September 2012.

[36]. Lingfeng Wang, Shiming Xiang, GaofengMeng, Huaiyu Wu, and Chunhong Pan, "Edge-Directed Single-Image Super-Resolution via Adaptive Gradient Magnitude Self-Interpolation," IEEE Transactions on Circuits and Systems for Video Technology, Vol. 23, No. 8, August 2013.

[37]. HongtengXu, GuangtaoZhai, and Xiaokang Yang, "Single Image Super-Resolution with Detail Enhancement Based on Local Fractal Analysis of Gradient," IEEE Transactions on Circuits and Systems for Video Technology, Vol. 23, No. 10, October 2013.

[38]. T. Komatsu, K. Aizawa, T. Igarashi, and T. Saito, "Signal-processing based method for acquiring very high resolution image with multiple cameras and its theoretical analysis," Proc. Inst. Elec. Eng., vol. 140, no. 1, pt. I, pp.19-25, Feb. 1993.

[39]. Michel Irani and Shmuel Peleg "Improving Resolution by Image Registration" CVGIP Graphics Model and Image Processing Vol. 53 No. 3 May PP 231-239.

[40]. M. Irani and S. Peleg, "Motion analysis for image enhancement: resolution, occlusion, and transparency" , Journal of Visual Communication and Image Representation, vol. 4, no. 4, pp. 324–335, 1993.

[41]. H. Ur, D. Gross, "Improved resolution from sub-pixel shifted pictures", CVGIP: Graph. Models Image Process. 54 (1992) pp181–186.

[42]. P. Vandewalle, Sbaiz, Vetterlia and Susstruk, "Super Resolution from Highly Under Sampled Images", IEEE Digital Library Conf. Proceeding.

[43]. Patrick Vandewalle, Luciano Sbaiz, JoosVandewalle, and Martin Vetterli, "Super-Resolution From Unregistered and Totally Aliased Signals Using Subspace Methods" IEEE Transactions On Signal Processing, Vol. 55, No. 7, July 2007

[44]. Cheol Park, Min Kyu Park, and Moon Gi Kang, "Super-Resolution Image Reconstruction: A Technical Overview", IEEE Signal Processing Magazine, May 2003; a special issue on Super Resolution Imaging. pp 21-36.

[45]. Maria Teresa Merino and Jorge Nunez, "Super-Resolution of Remotely Sensed Images With Variable-Pixel Linear Reconstruction" IEEE Transactions On Geoscience And

Remote Sensing, VOL. 45, NO. 5, MAY 2007, pp-1446 -1457.

[46]. Patrick Vandewalle, Sabine Susstrunk and Martin Vetterli, "A Frequency Domain Approach to Registration of Aliased Images with Application to Super-resolution", Hindawi Publishing Corporation EURASIP Journal on Applied Signal Processing Volume 2006, Article ID 71459, Pages 1–14 DOI 10.1155/ASP/2006/71459

[47]. Manjunath V. Joshi a, Subhasis Chaudhuri, "Simultaneous estimation of super-resolved depth map and intensity field using photometric cue", Elsevier Inc., Computer Vision and Image Understanding 101, Oct 2005, PP- 31–44

[48]. D. Rajan and S. Chaudhuri, "Simultaneous estimation of super-resolved scene and depth map from low resolution defocused observations," IEEE Transactions on Pattern Analysis and Machine Intelligence, vol. 25, no. 9, pp. 1102–1117, 2003.

[49]. M. Elad and A. Feuer, "Restoration of a single super-resolution image from several blurred, noisy and under sampled measured images", IEEE Transactions on Image Processing, vol. 6, no. 12, pp. 1646–1658, 1997.

[50]. Bahedir Gunturk & Gevrekci in letter "High Resolution Image Reconstruction from Multiple Differently Exposed Images", IEEE Digital Library Conf. Proceeding

[51]. M.V.W. Zibetti and J Mayer, "Outlier Robust and Edge Preserving Simultaneous Super resolution", IEEE, 2006, PP-1741 -1744

[52]. Guilherme Holsbach Costa, and José Carlos Moreira Bermudez, "Statistical Analysis of the LMS Algorithm Applied to Super-Resolution Image Reconstruction", IEEE Transactions On Signal Processing, VOL. 55, NO. 5, MAY 2007

[53]. Wenze Shao, Zhihui Wei, "Efficient Image Magnification and Applications to Super Resolution Reconstruction", Proc. of ICMA06, IEEE, pp-2372-2376.

[54]. N.Nguyen, P.Milanfar, and G. Golub, "A computationally efficient super-resolution image reconstruction algorithm," IEEE Transactions on Image Processing, vol. 10, no. 4, pp. 573–583, 2001.

[55]. Huanfeng Shen, Liangpei Zhang, Bo Huang and Pingxiang, " A MAP Approach for Joint Motion Estimation, Segmentation & Super resolution", IEEE Transaction on Image Processing, Vol 16, No 2 Feb 2007 pp-479-489

[56]. Tuan Pham, Vliet & Schutte, "Robust Fusion of Irregularly sampled Data Using Adaptive Normalized Convolution", Hindawi Publishing Corporation EURASIP Journal on Applied Signal Processing Volume 2006, Article ID 71459, Pages 1–12 DOI 10.1155/ASP/2006/83268

[57]. Bo-Won Jean, Park & Yang, "Resolution Enhancement by Prediction of High Frequency Image Based on the Laplacian Pyramid", Hindawi Publishing Corporation EURASIP Journal on Applied Signal Processing Volume 2006, Article ID 71459, Pages 1–12 DOI 10.1155/ASP/2006/72520

[58]. F. Sroubek& J Flusser "Resolution Enhancement via Probabilistic Deconvolution of Multiple Degraded Images", Pattern Recognition Letters 27 (2006), Elsevier, PP-287-293.

[59]. Y. He, K. Yap, L. Chen & L. Chau, "Joint Image Registration and Super Resolution Using Nonlinear Least Squares Method", 2007, Proceeding of International Conf. on ICASSP 2007, pp-I 561-564

[60]. Cohen, Avrin and Dinstein, "Poly phase Back Projection Filtering for Resolution Enhancement of Image Sequences", 2000, Proceeding of International Conf. on pp- 2171-2174

[61]. Balaji N, Kenneth E, " A Computationally Efficient Super Resolution Algorithm for Video Processing using Partition Filters", IEEE Trans on circuits & systems for Video Tech., Vol. 17, No5, May 2007, pp-621-634

[62]. Frank M. Candocia, and Jose C. Principe, "Super-Resolution of Images Based on Local Correlations" IEEE Transactions On Neural Networks, Vol. 10, No. 2, March 1999 pp 372-380

[63]. Olcay Kursun and Oleg Favorov, "Single frame super resolution by a Cortex based mechanism using high level visual features in natural images", Proc. Of IEEE ICWACV 2002.

[64]. W. T. Freeman, T. R. Jones, and E. C. Pasztor, "Example-based super-resolution", IEEE Computer Graphics and Applications, vol. 22, no. 2, pp. 56–65, 2002.

[65]. C V Jijji, and S. Choudhari, " Single Frame Image Super Resolution Through

Contourlet Learning", "Super-Resolution-Imaging: Analysis, Algorithms, and Applications", EURASIP Journal on Applied Signal Processing, 2006 DOI 10.1155/ASP/2006/73767,PP-1-11

[66]. C. V. Jiji, M. V. Joshi, and S. Chaudhuri, "Single-frame image super-resolution using learned wavelet coefficients," International Journal of Imaging Systems and Technology, vol. 14, no. 3, pp. 105–112, 2004.

[67]. Hong Chang, Dit Yan Yeng, "Super Resolution through Neighbor Embedding", proc. Of IEEE conf. CVPR 2004.

[68]. Liming Zhang and Fengzhi Pan, "A New Method of Images Super Resolution Restoration by Neural Network", Proc. ICONIP02 pp-2414-2418

[69]. David Chapel and Zisserman, "Super Resolution from Multiple Views Using Learnt image models", Proc. of International Conference on 2001, PP- II 627-633

[70]. Min Cheng Pan, "Improving a Single Down-sampled Image Using Probability Filtering Based Interpolation and Improved Poisson Maximum a Posteriori Super Resolution", Hindawi Publishing Corporation EURASIP Journal on Applied Signal Processing Volume 2006, Article ID 71459, Pages 1–11 DOI 10.1155/ASP/2006/97492

[71]. Rajaram, Gupta, Petrovic and Huang, "Learning Based Nonparametric Image SR" Hindawi Publishing Corporation EURASIP Journal on Applied Signal Processing Volume 2006, Article ID 71459, Pages 1–11 DOI 10.1155/ASP/2006/51306

[72]. Manjunath Joshi, S. Choudhari and R. Panuganti, "A Learning Based Method for Image Super Resolution From zoomed Observations", IEEE Transaction On Systems, Man and Cybernetics Vol 35, No 3, June 2005, PP-527-537

[73]. Guilherme Holsbach Costa and José Carlos Moreira Bermudez, "Informed Choice of the LMS parameters in Super Resolution Video Reconstruction Applications", IEEE Tranc. On Signal Processing, vol 56, no 2, Feb 2008 pp555-564

[74]. Heng Lain, " Variational Local Structure Estimation For Image Super Resolution", IEEE, 2006, pp 1721-1724

[75]. Dirk Robinson & Milanfar in "Statistical Performance Analysis of Super Resolution", IEEE Tranc. On Image Processing, vol 16, no 6, June 2007 pp- 1596-1610

[76]. Deepu Ranjan, S Chaudhari, M Joshi, "Multi-Objective Super Resolution: Concept and Examples", IEEE Signal Processing Magazine, May 2003; a special issue on Super Resolution Imaging. pp 49-61

[77]. S. Baker and T. Kanade, "Limits on super-resolution and how to break them," IEEE Transactions on Pattern Analysis and Machine Intelligence, vol. 24, no. 9, pp. 1167–1183, 2002.

[78]. Choong boon, Onur Guleryuz, Toshiro and Y Suzuki, " Sparse Super resolution reconstruction of video from mobile devices in digital TV broadcast applications PS-2006-0117", Research Laboratories, NTT DoCoMo Inc, Japan.

[79]. Tuan Pham, Lucas J, Van Vliet and Klamer S, "Influence of Signal to Noise Ratio and Point Spread Function on Limits of Super-Resolution", Proc. Of SPIE-IS&T Electronic Imaging, SPIE Vol 5672© 2005, pp 169-180

[80]. Zhouchenlin, Heng-Yeung shum, "On the Fundamental Limits of reconstruction Based Super Resolution Algorithms", IEEE Digital Library Conf. Proceeding pp- I-1171-1176

[81]. Minminshen, Ci Wang, Ping Xue and Weisilin," Initial Selection and Its Influence on Super Resolution Reconstruction", Proc of SiPS 2007, pp- 86-89

[82]. Barbara Zitova, Jan Flusser, " Image Registration Methods : a survey", Image and Vision Computing 21, Elsevier, 2003 PP- 977-1000

[83]. Isabelle Begin and Frank Ferrie, " Training Database Adequacy Analysis for Learning Based Super Resolution", Proc of 4th Canadian Conf. on Computer and Robot Vision 2007, pp 1-6

[84]. Kevin Su, Qi Tian, Quing, Nicu, Jingsher, "Neighborhood Issue in Single Frame Image Super resolution", IEEE Digital Library Conf. Proceeding. pp 1-6

[85]. I I Ibrahim, M K Ahemad, Noissiar, Allam, "Comparative Study on Super Resolution of Images", IEEE Digital Library Conf. Proceeding,pp-220-225

[86]. Isabelle Begin and Frank Ferrie, "Comparison of Super Resolution Algorithms Using Image Quality Measures", Proc of 4th Canadian Conf. on Computer and Robot Vision 2007, pp 1-6

[87]. Thomas M Lehman, Claudia and Klaus, " Survey: Interpolation Methods in Medical Image Processing", IEEE Transaction on Medical Imaging Vol 18, No 11, Nov 1999, pp 1049-1075

[88]. Einar Maeland, " On the Comparison of Interpolation Methods", IEEE Transaction on Medical Imaging, Vol 7, No 3, Sept 1998, pp-213-217

[89]. Erik Meijering, " A Chronology of Interpolation", Proceedings of IEEE, Vol 90, no.3, March 2002, pp- 319-342

[90]. W.T. Freeman and E.C. Pasztor, "Learning to Estimate Scenes from Images," Adv. Neural Information Processing Systems, M.S. Kearns, S.A. Solla, and D.A. Cohn, eds., vol.11, MIT Press, Cambridge, Mass., 1999, pp. 775-781.

[91]. W.T. Freeman and E.C. Pasztor, "Markov Networks for Super resolution," Proc. 34th Ann. Conf. Information Sciences and Systems (CISS 2000), Dept. Electrical Eng., Princeton Univ., 2000.

[92]. A. Papoulis, "Generalized sampling theorem," IEEE Trans. Circuits Syst. vol. 24, pp. 652-654, Nov. 1977.

[93]. J.L. Brown, "Multi-channel sampling of low pass signals," IEEE Trans. Circuits Syst., vol. CAS-28, pp. 101-106, Feb. 1981.

[94]. ITU, "Methodology for the Subjective Assessment of the Quality of Television Pictures", ITU-R rec BT, 500-9 (1998)

[95]. Sonja Grgic, MislavGrgic, Marta Mrak, "Reliability of Objective Picture Quality Measures", Journal of Electrical Engineering, vol 55, no 1-2, 2004, pp 3-10

[96]. Ismail A, Bulent Sankar, Khalid Sayood, "Statistical evaluation of image quality measures", Journal of Electronic Imaging 11(2), April 2002, pp 206-223

[97]. Zhou Wang, Alan C. Bovik, Haqmid Rahim Sheikh and Eero P. Simonelli "Image Quality Assessment: From Error Visibility to Structural Similarity" IEEE Transactions on image Processing Vol. 13. No. 4. April-2004.

[98]. Martin Bernas " Image Quality Evaluation" VIPromCom-2002, 4th EURISP-IEEE Region 8th International Symposium on video/Image Processing and Multimedia

Communication, 16-19 June 2002, Zadar, Croatia.

[99]. Rafael C. Gonzalez, Richard E. Woods," Digital Image Processing", Pearson Education. ISBN 81-7808-629-8, First Indian reprint 2002.

[100]. C. Wayne Brown and Barry J. Shepherd, " Graphics File Formats", reference and guide, ISBN-884777-00-7, Printed in the United State of America.

[101]. Dirk Robinson, Peyman Milanfar, "Fundamental Performance Limits in Image Registration", IEEE Tranc. On Image Processing, vol 13, No 9, Sept 2004.

[102]. Peter N. Crabtree, Collin Seanor, Jeremy Murray-Krezan, and Patrick J. McNicholl Air Force Research Laboratory, Space Vehicles Directorate 3550 Aberdeen Ave. SE, Kirtland AFB, NM USA "Robust global image registration based on a hybrid algorithm combining Fourier and spatial domain techniques".

[103]. Luca Lucchese and Guido Maria Cortelazzo "A Noise-Robust Frequency Domain Technique forEstimating Planar Roto-Translations" IEEE Transactions On Signal Processing, Vol. 48, No. 6, June 2000-PP 1769-1786

[104]. Kamran, M., Suhail, S.; Farooq, M., "A robust, distortion minimizing technique for watermarking relational databases using once-for-all usability constraints," IEEE Transactions on Knowledge and Data Engineering, on , vol.PP, no.99, pp.1-1, Dec 2013.

[105]. M. Shehab, E. Bertino, and A. Ghafoor, Watermarking Relational Databases Using Optimization-Based Techniques, IEEE Trans. Knowledge and Data Eng., vol. 20, no. 1, pp. 116-129, Jan. 2008.

[106]. R. Agrawal, P. Haas, and J. Kiernan, Watermarking Relational Data: Framework, Algorithms and Analysis, The VLDB J., vol. 12, no. 2, pp. 157-169, 2003.

[107]. R. Halder and A. Cortesi, A Persistent Public Watermarking of Relational Databases, Proc. Intl Conf. Information Systems Security, pp. 216-230, 2011.

[108]. R. Halder, S. Pal, and A. Cortesi, Watermarking Techniques for Relational Databases: Survey, Classification and Comparison,J. Universal Computer Science, vol. 16, no. 21, pp. 3164-3190, 2010.

[109]. Y. Wang, Z. Zhu, F. Liang, and G. Jiang, Watermarking Relational Data Based onAdaptive Mechanism, Proc. Intl Conf. Information and Automation (ICIA 08), pp.131-134, 2008.

[110]. Ali Ajdari Rad, Laurence Meylan, Patrick Vandewalle and Sabine Susstrunk Ecole Polytechnique 1015 Lausanne, Switzerland "Multidimensional Image Enhancement from a Set of Unregistered and Directly Exposed Images"

[111]. Jianchao Yang, Thomas Huang University of Illinois at Urbana-Champaign A book on "Image super-resolution: Historical overview and future challenges" chapter one.

[112]. S.A. Mohamed, A.K. Helmi, M.A. Fkirin, , S.M. Badwai "Subpixel Accuracy Analysis of Phase Correlation Shift Measurement Methods Applied to Satellite Imagery" (IJACSA) International Journal of Advanced Computer Science and Applications. Vol. 3, No. 12, 2012

[113]. Priyam Chatterjee, Sujata Mukherjee, Subhasis Chaudhuri and Guna Seetharaman "Application of Papoulis-Gerchberg Method in Image Super-resolution and Inpainting" The Author 2005. Published by Oxford University Press on behalf of The British Computer Society. The Computer Journal Vol. 00 No. 0, 2007.

[114]. Luca Lucchese, , Gianfranco Doretto, Guido Maria Cortelazzo "A Frequency Domain Technique for Range Data Registration" IEEE Transactions On Pattern Analysis And Machine Intelligence, Vol. 24, No. 11, November 2002

[115]. AssafZomet, Alex Rav-Acha and ShmuelPeleg " Robust Image Superresolution"

[116]. Patrick Vandewalle "Super-Resolution from Unregistered Aliased Images" Thesis No 3591 (2006) École Polytechnique Fédérale De Lausanne Présentée Le 21 Juillet 2006.

[117]. Budi Setiyono, Mochamad Hariadi, Mauridhi Hery Purnomo "Superresolution Using Papoulis-Gerchberg Algorithm Based Phase Based Image Matching" JurnalIlmiah KURSOR Vol. 6, No. 3, Januari 2012, hlm.159-166.

[118]. Sony Corporation, Super HAD CCD. http://www.sony.net/product/SC-Hp/sys/ccd/sensor/super_had.html

[119]. Karl S. Ni and Truong Q. Nguyen in "Image Super resolution Using Support Vector Regression", IEEE Tranc. On Image Processing, vol 16, no 6, June 2007 pp- 1596-1610

[120]. Rafael C. Gonzales, Richard Woods, and Steven L. Eddins "Digital Image Processing Using MATLAB" Tata McGraw-Hill Education publishing.

[121]. Rafael C. Gonzales, Richard Woods, and Steven L. Eddins "Digital Image Processing Using MATLAB, 2e" Gatesmark Publishing, 2009, ISBN: 978-0-9820854-0-0

[122]. MATLAB Documentation Reference Manual "Image Processing Toolbox 6.5" R2015a.

[123]. Michel E Tipping and Christopher M. Bishop, Microsoft Research, Cambridge CB3 OFB U.K." Bayesian Image Super-resolution"